CELLULAR AUTOMATA MODELS FOR TRAFFIC FLOW IN URBAN NETWORKS

by

Abdelhakeem A. Hammad, B.Sc. M.Sc.

A thesis submitted in fulfilment of the
requirements for the degree of

Ph.D. m Computer Applications

School of Computer Applications
Dublin City University
Dublin 9, Ireland

Supervisors

Dr. Heather Ruskin and Dr.Micheal O'hEigeartaigh

CELLULAR AUTOMATA MODELS FOR TRAFFIC FLOW IN URBAN NETWORKS

Abstract

Recently, traffic problems have attracted considerable attention Numerical simulations, hydrodynamics models, and queueing theory are a few of the basic theoretical tools used to describe car traffic on highways
Computationally, Cellular Automaton models are simple and flexible and are increasingly used in simulations of complex systems, providing considerable insight on traffic behaviour A particular strength of these models is fast "minimal" microscopic simulation, which nevertheless can reproduce important macroscopic features

This methodology requires streets to be divided into sites (cells), with sites linked into road segments and forming networks, punctuated by junctions, traffic signals and so on Car movements are represented by "jumps", where each jump represents the current car speed

Much previous work has concentrated on flow of cars under highway conditions, but less effort has been concerned with urban networks and the constraints, which apply in this context The research reported here, uses Cellular Automaton methodology to examine traffic patterns in urban and inter-urban areas A three state deterministic Cellular Automata Model is defined for the dynamic process and networks of various sizes are investigated, with all nodes controlled and diverse traffic conditions considered at each intersection Both transient movements of cars through the network and temporary lost to flow, through off-street parking, are examined for impact on traffic parameters

A stochastic feeding mechanism, in which car arrivals follow a Poisson process, has been implemented throughout the simulation for different arrival rates Lane-changing rules for simulation of two-lane traffic are also discussed and, finally, a Stochastic Cellular Automata Model for inter-urban areas is presented Key features of traffic behaviour under the various network conditions are analysed and comparisons with highway flow
Suggestions and future improvements on model realism are also given

Acknowledgements

I take this opportunity to thank my advisors, Dr Heather Ruskin and Dr Micheal O'hEigeartaigh, for their invaluable advice and guidance throughout my research study Their constant support, encouragement and friendship made my stay at DCU an enjoyable

I would like to thank Prof Michal Ryan and the School of Computer Applications in general for providing me with the opportunity and the necessary funding to undertake this research

Many thanks to Rory Boland, the director of the traffic section in Dublin, and to all people in the traffic control room for helping me to conduct my survey

I also thank Prof Duarte for helpful discussions at an early stage and for pointing me to some important references

Thanks for Mostafa Abou_Shaban for helping me with the code used to plot the space-time diagrams

Finally, I wish to express my heartfelt thanks to my wife, for her understanding and her constant support, and to my parents for their affection and encouragement

Declaration

I hereby certify that this material, which I now submit for assessment on the programme of study leading to the award of Ph.D. is entirely my own work and has not been taken from the work of others save and to the extent that such work has been cited and acknowledged within the text of my work.

Signed A. Hammond Date 27-09-1998

Table of Contents

List of Figures

List of Tables

Chapter 1

"Introduction"

1.0 Introduction

The modelling of traffic flow has never been an easy task in view of the high complexity of social networks Unlike physical networks, there are no underlying dynamics in traffic but rather dynamical consequences that appear as the result of the interaction of various vehicle-driver units, with one another, with the road and with control networks

External parameters such as weather conditions, different road conditions, different motivations for the drivers have a great impact on traffic performance These external parameters are changeable from one location to another, and even for an individual stretch of the road these conditions vary over time

The initial development of traffic models was started in the 1950s in order to study the theoretical description of traffic flow These models are based on a set of mathematical equations or on an analogy to other physical systems

Traffic flow models, which have been developed recently, may be classified into two classes

- Models which attempt to explain traffic phenomena on the basis of the behaviour of the individual elements, (single vehicles), are called Microscopic Models In microscopic models each vehicle in the road network may be described by its position, its actual velocity, its desired velocity, its origin-destination route, its tendency to overtake other vehicles and other characteristics of the driver's behaviour and the vehicle
- In contrast, where traffic flow phenomena are described through

parameters, which characterise the aggregate traffic properties, the resulting models are called Macroscopic models

1.1 Literature Review

1.1.1 Microscopic Traffic Flow Models

These models are based on a mechanism, which describes the process of one car following the other Microscopic models are also known as " Headway Models" because they relate the headway between two cars to the speed

Models of this kind allow for the characteristics and behaviour of individual cars to be distinct They are well suited for simulation studies in which stochastic behaviour can be represented by using probabilistic techniques

In the transportation field this approach to modelling has been applied to queueing and gap acceptance process (Berilon, 1988, 1991), car following and lane changing models (Gipps, 1981, 1986) and models of travel, route and departure time (Macket, 1990)

Microscopic models consist basically of two main components

a) An accurate description of the road network geometry, including traffic facilities such as traffic lights, traffic detectors, variable message sign panels, etc

b) A very detailed model of traffic behaviour, which reproduces the dynamics of each individual car, distinguishing between different types of cars, with the possibility of taking into account behavioural aspects of vehicles drivers

Microscopic models are close to reality in that they reproduce the traffic systems well They open up a wide range of traffic scenarios in which precise description of traffic control and traffic management schemes can be explicitly included Before we discuss microscopic models in detail one might ask for the reasons behind microscopic simulations? To answer this question we need to know their advantages and the disadvantages

Microscopic advantages

Firstly, as a great many parameters can be used to describe the individual features of driver behaviour it is easy to investigate very subtle changes that may be induced through, for example, changes in the driver education

Secondly, the simulation outputs are capable of describing the motion of an individual car which, in turn, allow us to study and interpret certain aspects of the traffic dynamics

Microscopic disadvantages

Against these advantages of microscopic simulations one should consider the effort in model specification, data requirements, statistical analysis and computational requirements (time and memory)

Brackstone and McDonald(1995) have mentioned other important factors which may limit the use of microscopic simulations in the inter-urban area In this case, cars have plenty of opportunity to interact with each other, which gives the chance for a shock wave to form and propagate if the flow is high enough, which in turn leads to flow breakdown

The *first factor* is the *lack of appropriate data*, which can be demonstrated as follows, the validity of any microscopic simulation model has to be maintained at two levels

i A macroscopic level,(validation), to ensure the general performance of the model gives a good approximations to the observed traffic

ii A microscopic level,(calibration), with respect to interaction between vehicles

The macroscopic data can be obtained by recording the traffic parameters, flow and average velocity, at regular specific time intervals In contrast, microscopic data is not easy to obtain and investigate as most of the parameters required relate to " the leader" car and hence cannot be sampled sufficiently at regular time intervals by a method which uses only one set point for observations

The *second factor* is the *lack of knowledge* of the sensitivity of the models Since microscopic models are evaluated according to their ability to reproduce traffic jams and the flow density relations, the following question arises

Can we find a "perfect set of parameters" to obtain the "best fit" data using different combinations of changes in parameters?

The reasons behind our inability to find the "perfect set of parameters" are

1 a lack of appropriate data

2 inability to optimise a system with large number of degrees of freedom per car

For example, it is not possible to define how changes in one parameter will affect the system performance both macroscopically

and microscopically, following interactions between a large number of cars over a long period of time

The *stability of the traffic model* is our *third factor* If we assume that the other problems are solved, there is still this further problem namely, the variability of data due to different traffic patterns For example, if we measure the flow-density relation for a certain number of days, we find different breakdown points of the flow, despite the fact that all the measurements were done under the same conditions This is due to different configurations of the traffic stream and also to different events occurring and these will have almost unpredictable chain reactions, within the traffic stream, that will cause the speed of successive cars to vary in a differing order in both space and time

1.1.1.1 Car following theory

The process in which one car in a stream of traffic reacts to the behaviour of the preceding car is called "*car following theory*" and it is based on a cycle of stimulus and response

"Car following models" are used to describe the behaviour of the driver-car system in a stream of interacting particles,(the cars), and to provide the basic components of microscopic traffic simulation models Car-following models (Gazis, 1974, Gabord, 1991) consist of a differential difference equation, which is used to model continuous-time systems with inputs and outputs, which produces the acceleration at time instant (t+T) from

- car speed
- The relative distance, speed of the car ahead

At time instant t, the general form of the car following models can be written as

response (t+T) = sensitivity * stimulus (t)

The nature of the response is acceleration or deceleration of the following car, and the stimulus is the difference in velocity between the lead car and the follower

The most common model was introduced by Gazis *et al* (1961)

$$a_n(t+T) = \alpha \frac{v_n^m(t)\ \Delta v(t)}{(\Delta x)^l(t)} \qquad (1\ 1)$$

where

$$\Delta v(t) = v_{n-1}(t) - v_n(t)$$

$$\Delta x(t) = x_{n-1}(t) - x_n(t)$$

Here the reaction time T tries to model the delay between stimulus and reaction The parameters α, m and l must be evaluated from observations and $\Delta v(t)$, $\Delta x(t)$ are the changes in both the speed and the space

Simple "*car–following models*" resembles a feedback control process in which oscillations may occur This leads to various kinds of instabilities in the traffic flow, which in turn can lead to collisions

There are two types of instability

1 Local instability, which can be observed in situations in which disturbance, (e g a change in a distance-headway resulting from the change in speed of the leading car), does not die out but rather increases with time

ii Asymptotic instability, defined as the situation in which a disturbance grows in magnitude as it propagates from car to car

In contrast, stability of the traffic flow model means that changes in the velocity by the lead car of a traffic stream will not be amplified by successive cars in the stream (until a collision occurs) Also there are two types of stability

i Local stability, which considers the response of a car to the change in motion of the car immediately ahead

ii Asymptotic stability, which deals with the propagation of a fluctuation through a platoon of cars

Recently (Gipps, 1981, 1986) proposed a new car-following model, which was designed to possess the following features

i The parameters in the model, α, m, and l should correspond to obvious characteristics of drivers and cars

ii The model should be well behaved when the interval between successive recalculations of speed and position is the same as the reaction time

This model is based on the assumption that the driver of the following car selects limits to his desired braking and acceleration rates For acceleration

$$v_{n(t+T)} \leq v_n(t) + 2.5\, a_n\, T \left[1 - \frac{v_n(t)}{V_n}\right] * \left(0.025 + \frac{v_n(t)}{V_n}\right)^{\frac{1}{2}} \qquad (1.2)$$

where

$v_n(t+T)$ is the maximum speed to which car n can accelerate during the time interval(t, t+T)

V_n is the desired speed for car n and a_n is the maximum acceleration for car n

For braking

$$v_n(t+T) \le b_n T + \left(b_n{}^2 T^2 - b_n\left(2[x_{n-1}(t) - s_{n-1} - x_n(t)] - v_n(t)T - v_{n-1}{}^2(t)/B\right)\right)^{\frac{1}{2}} \quad (1\,3)$$

where

$v_n(t+T)$ is the maximum speed for a car n with respect to car n-1

b_n is the most severe braking that the driver of car n wishes to undertake,$(b_n \le 0)$

s_n is the effective size of car n,(i e , the physical length plus a margin into which the following car is not willing to intrude), even at rest

B is the estimate of b_{n-1} used by the driver of car n

If it is assumed that the driver travels as fast as safety and the limitation of the car permit, the mean speed is given by combining these equations, as follows

$$v_n(t+T) = \min(\text{acceleration, braking}) \quad (1\,4)$$

The model has been used to simulate vehicular traffic in multi-lane arterial roads with special attention devoted to the structure of the lane changing decisions

More recently (Bando *et al*, 1994, 1995) the following equation has been used for calculating the acceleration

$$a(t) = \frac{1}{t}\left[V(gap(t)) - v(t)\right] \quad (1\,5)$$

Where V is the desired velocity function, which has approximately a linear relationship with gap and also depends on some other variables such as road conditions

1.1.1.2 Psychological-Physiological Spacing models

Car following equations assume that the driver of the following car reacts, to arbitrary small changes in the relative speed, even at a very large differences in distances to the front car Therefore, car following equations assume that there is no response as soon as speed differences disappear, which is not very realistic

A significant new approach was developed by Wiedmann(1974) based on knowledge about human perception and reaction behaviour and which used different perceptual thresholds Only when these thresholds are reached will the driver of the following car be able to perceive the change in the apparent size of the leading car and, subsequently, be able to react to the changes of acceleration or deceleration

Such thresholds are presented as parabolas in the relative distance vs relative speed relation in Fig (1 1) It can also be seen from this picture how car following proceeds A vehicle with speed v(n+1), which is larger than the speed v(n) of the preceding vehicle will catch up with constant relative speed Δv Upon reaching the threshold, the driver reacts by reducing his speed One such example of relative motion with constant deceleration appears as a parabola The minimum of the parabola lies on the Δx-axis The driver tries to decelerate so as to reach a point at which $\Delta v = 0$ He is not able to do this

accurately because, firstly, he is not able to perceive small speed differences and, secondly, he is not able to control his speed sufficiently well

The result is that the spacing will again increase When the driver initially reaches the opposite threshold he accelerates and tries again to achieve the desired spacing (indicating in Fig (1 1) by the upper part of the loop)

If one assumes that the relationship of the perceptual thresholds for spacing are the same for both positive and negative changes in relative speed, then the resulting spacing behaviour resembles a symmetrical pendulum about its equilibrium point

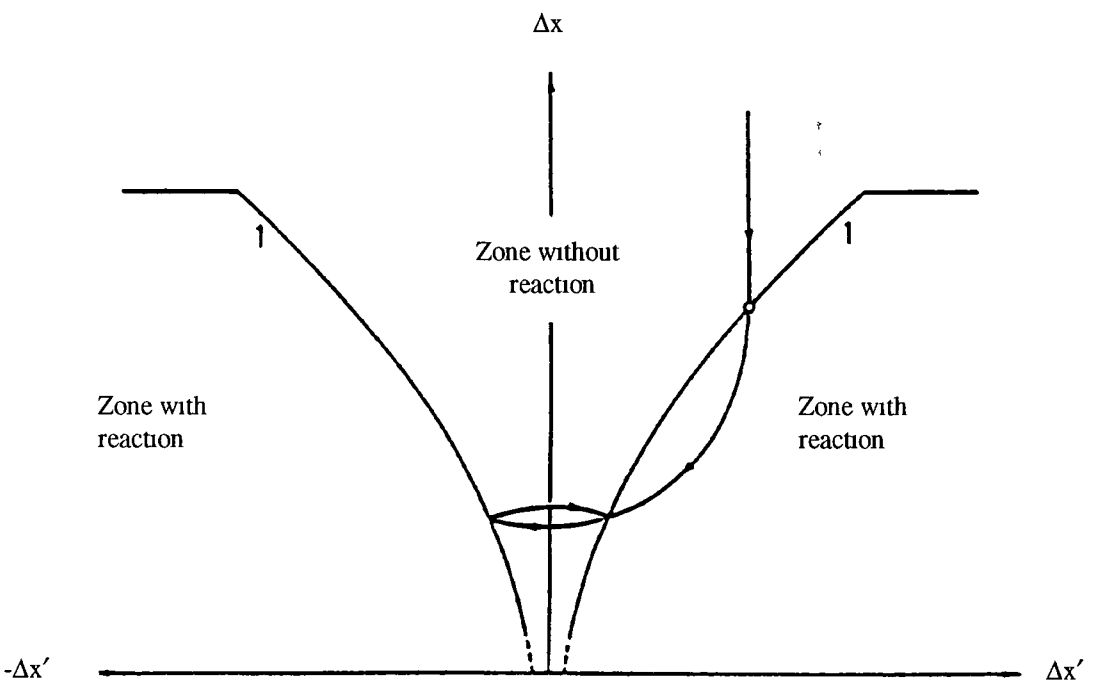

1 perceptual threshold

Fig(1 1) Perceptual thresholds in car-following behaviour, Source Wiedemann (1974)

1.1.2 Macroscopic Models

Macroscopic traffic flow models (Lighthill and Whitham, 1955, Gazis, 1974) treat the traffic system as a continuous fluid They are concerned only with the behaviour of groups of cars, ignoring the behaviour of the individual transportation units

Before we classify macroscopic models, we mention some of their advantages and disadvantages

Macroscopic advantages

i They are useful in studying traffic behaviour under heavy traffic conditions

ii Due to the use of the aggregate traffic variables, flow, density, and mean speed, the computational requirements are much less than with microscopic variables, allowing real time simulation of traffic flow in large networks

Macroscopic weaknesses

i Do not incorporate driver, car, and roadway parameters in an explicit way

ii Macroscopic models are not able to provide information about fuel consumption or route choice for individual cars and sometimes show poor results in the event of microscopic phenomena occurring e g like queueing at traffic light, on-ramps, and others

In the next section we classify macroscopic models, giving a brief description of each

1.1.2.1 Continuum Models

The first contribution to the continuum models are due to Lighthill and Whitham (1955), who proposed that certain traffic phenomena of dense highway traffic can be described in terms of continuum variables, traffic flow, density, and mean speed

The assumption of the theory is that

At any point of the road the flow is a function of the concentration of cars

This assumption implies that simple changes in the flow rate are propagated backwards through the traffic stream along a kinematic wave whose velocity relative to the road is the slope of the flow-density curve

The flow q and the concentration k have no significance except as means The purpose of the theory is to determine how these mean values vary in space and time This is done by considering the speed with which changes in q and k are propagated along the roadway

A fixed observer sees a flow $q = \frac{N}{T} = uk$ where N is the number of vehicles passing him in time T, and u is the mean speed at which the N vehicles pass him Assuming that the observer moves upstream with uniform speed c, then he will pass additional vehicles say, c k which will be added to q so that

$$q + ck = \frac{N}{T}$$

and, if he moves down stream this becoms (1 6)

$$q - ck = \frac{N}{T}$$

N is the difference between the number of vehicles passing the observer and those, which he passes If he moves at the mean speed of the stream, then N = 0 and $c = u$

Consider now two observers moving at a uniform speed c, the second starting at time T and remaining behind the first Suppose that the flow and concentration are changing with time, but that the observers jointly adjust their speed c so that the number of vehicles which pass them minus the number which they pass, is, on the average, the same for each observer during a time interval T This is illustrated in Fig (1 2) By (1 6) the result of their observation would be

$$q1 - ck1 = \frac{N}{T} = q2 - ck2 \tag{1 7}$$

if they were moving downstream in the positive direction of flow

Solving for c, we find that

$$c = \frac{q2 - q1}{k2 - k1} \tag{1 8}$$

If the changes in flow and concentration are small, then

$$c = \frac{\Delta q}{\Delta k} \tag{1 9}$$

Thus, when the difference in flow and concentration are small, they propagate at a speed given by the tangent $\frac{\Delta q}{\Delta k}$ to the flow-concentration diagram

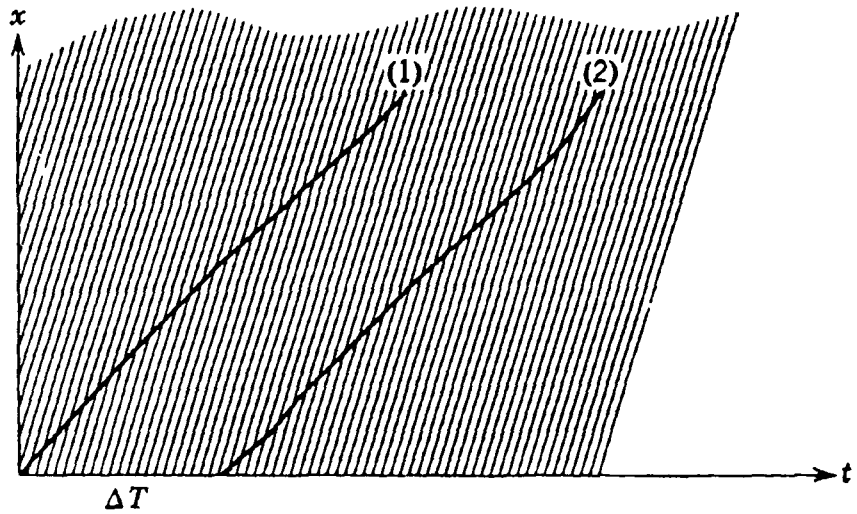

Fig(1 2) Vehicles passed by two moving observers,

Source D Gazis (1974)

1.1.2.1.1 Simple continuum models

Continuum traffic flow models are based on a fluid flow analogy which regards traffic flow as a particular fluid process, with states characterised by aggregate variables such as density (in Veh/km), flow (in Veh/h) and mean speed (in km/h)

In fluid flow analogy, the traffic stream is treated as a one-dimensional compressible fluid This leads us to describe the dynamic evolution of macroscopic traffic parameters by means of a

i Conservation or continuity equation

ii One-to-one relationship between speed and density or between flow and density, which is known as the fundamental diagram of traffic engineering

The simple continuum model consists of the continuity equation and the equation of state:

flow = density * mean speed.

If these equations (1.10.a and b) are solved together, then we can obtain speed, flow, and density at any time and point of the roadway:

$$q = uk \tag{1.10.a}$$

$$\frac{\partial q}{\partial x} + \frac{\partial k}{\partial t} = 0 \tag{1.10.b}$$

By knowing these traffic variables, we know the state of the traffic stream and can derive measures of effectiveness, such as delay stops, total travel time and others that help engineers to evaluate the performance of the traffic systems.

Equation of continuity

Equation (1.10.b) expresses the law of conservation of a traffic stream (cars) and is known as the conservation or continuity equation. It has the same form as in fluid flow.

If entries/exits exist within the stretch of the roadway, then the equation takes the form

$$\frac{\partial q}{\partial x} + \frac{\partial k}{\partial t} = g(x,t) \tag{1.11}$$

Where $k(x,t)$ and $q(x,t)$ are the traffic density and flow ,respectively, at the space-time point(x,t). The generation term $g(x,t)$ represents the number of cars entering or leaving the traffic flow in a roadway section with entries/exits. The equation of continuity relates two fundamental variables, density and flow rate with two independent ones (space and time).

The solution of equation (1 10 b) is impossible without an additional equation The first possibility considers the momentum equation described later The second option uses the fundamental diagram

Fundamental diagram

The macroscopic parameters of the traffic flow are related by equation (1 10 a) where the equilibrium speed $u(x,t) = u(k)$ must be provided by a theoretical or empirical equation of state, that can take the form

$$u_e = u_f \left[1 - \left(\frac{k}{k_{jam}} \right)^a \right] \qquad (1\ 12)$$

Where U_e is the equilibrium speed, U_f is free flow speed

Equation (1 10 b) simply states that flow, q, is a function of density, k, i e $q = f(k)$ Using this relation one can also obtain the relation, which relates the mean speed and the density i e $u = f(k)$ This, however, is only valid at equilibrium Equilibrium can hardly be observed in practice, so that obtaining a satisfactory speed-density relationship is a task that is hard to achieve and is always assumed theoretically

The flow-density relation presented in Fig (1 3) reveals two extreme points

$$K = 0 \qquad \Rightarrow \qquad q = 0$$

$$K = k_{max} \qquad \Rightarrow \qquad u = 0 \qquad \Rightarrow \qquad q = 0$$

The cloud of points between these two extremes is based on measurements performed over specific time intervals This cloud of points represents an area of maximum flow, which is considered to be an important feature of the road section under concern

The fundamental diagram can be divided into two regions

i The free flow area, in which all cars are moving with their desired speed

ii The dense traffic area, in which all cars are almost stopped

According to Hall (1993) the fundamental diagram can be characterised by the following

a) Free flow traffic area, which can be represented by sections of linear approximations

b) the dense traffic regime

c) Measurement points found outside these two areas of traffic conditions represent transition situations, such as traffic leaving the head of a queue This traffic flow cannot be larger than the capacity of the congested area, but it can be faster than the congested flow

The solution of the simple continuum model leads to the formation of shock waves as illustrated in Fig (1 4) The shock wave is shown as a heavy line on the space-time diagram, ahead of it the flow is denser and the waves are drawn parallel to the tangent to the flow-density curve at A, which represents a situation where traffic flows at near capacity implying that speed is well below the free-flow speed

Behind it the concentration is less and the waves travel faster, they are drawn parallel to the tangent to the curve at B, which represents an uncongested condition where traffic flows at a higher speed because of the lower density

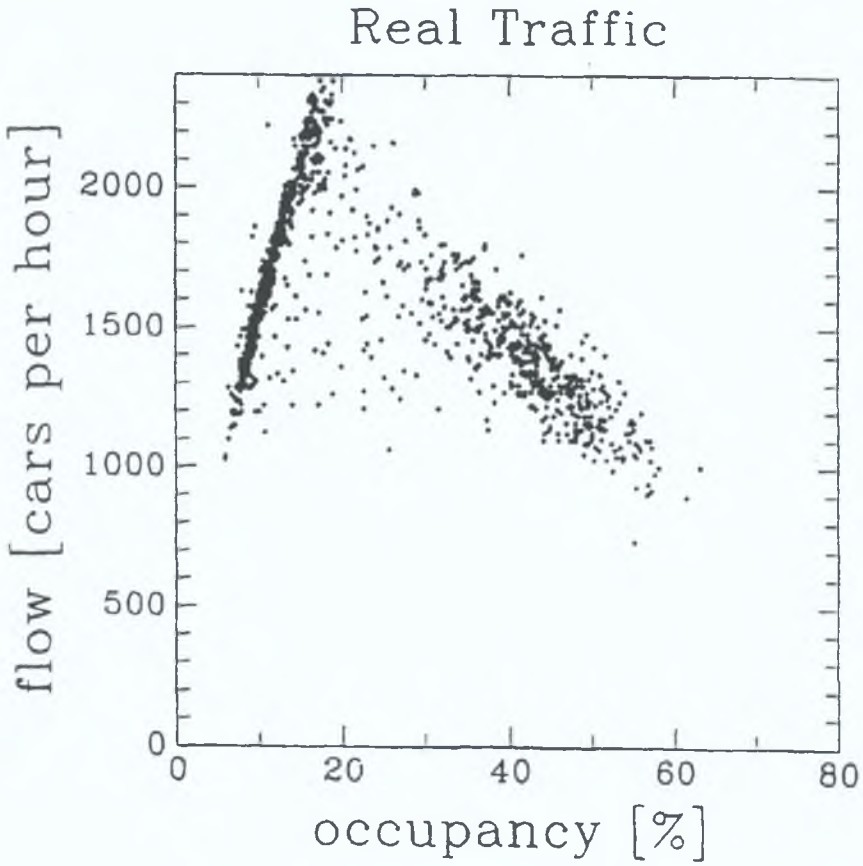

Fig.(1.3): Fundamental diagram obtained for real data; Source: Hall, L. *et al* (1986)

Lighthill and Whitham (1955) have used the flow-density curve to predict conditions near a shock wave.

Since the simple continuum models do not consider acceleration and inertia effects, they do not faithfully describe the non-equilibrium traffic flow dynamics. These are taken into account in the higher-order continuum models. These models add a momentum equation that accounts for the acceleration and inertia characteristics of the traffic mass. In this manner, shock waves are smoothed out and the equilibrium assumption is removed.

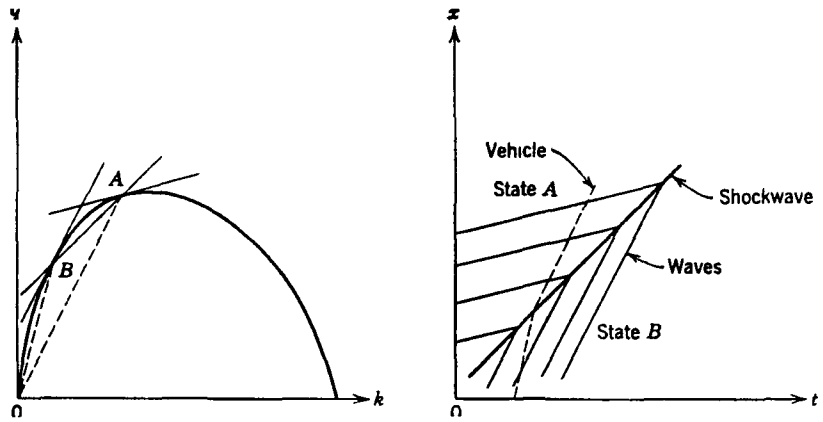

Fig (1 4) The use of the flow-density curve to predict the local conditions near a shock wave, source. Gazis(1974)

Disadvantages of simple continuum models

1- Kinematic models contain stationary speed-density relations (i e the mean speed should adjust instantaneously to traffic density) More realistically, it is adapted after a certain time delay and to reflect traffic conditions downstream.

2- Kinematic wave theory shows shock wave formation by steeping speed jumps (i e increases linearly) to infinite sharp jumps A macroscopic theory is based on values, which are average values from an aggregate of vehicles Averages are taken either over temporal or spatial extended areas Infinite jumps, therefore, are in contradiction to the basics of macroscopic description

3- Unstable traffic flow is characterised, under appropriate conditions, by regular stop-start waves with amplitude-dependent oscillation time

4- The dynamics of traffic flow result in the hysteresis phenomena This consists of generally retarded behaviour of vehicle platoons after emerging from a disturbance compared to the behaviour of the same vehicles approaching the disturbance Simple continuum models cannot describe such phenomena

5- Besides hysteresis, the crucial instability effect is bifurcation behaviour (i e , traffic flow becomes unstable beyond a certain critical traffic density) Above the critical density, the traffic flow becomes rapidly more congested without any obvious reason

1.1.2.1.2 Models with Momentum (inertia)

The extension of the simple continuum models, in order to explain the dynamic effects in the preceding section, was first pointed out by Whitham (1974) and Payne (1979)

The actual speed *u(x, t)* of a small ensemble of vehicles is obtained from the equilibrium speed-density relation, using a delay time τ, and from an anticipated location $x + \Delta x$

$$u(x,t+\tau) = U_e(k(x+\Delta x,t)) \qquad (1\ 13)$$

Muller and Eerden (1987) have studied this recursive equation in detail

Expanding, using Taylor series with respect to τ and Δx, assuming that both quantities can be kept small, yields the substantial acceleration of a platoon of vehicles

$$\frac{du}{dt} = \frac{1}{\tau}\left(U_e(k) - u\right) - c_o^2 \frac{1}{k}\frac{\partial k}{\partial x} \qquad (1\ 14\ a)$$

In a fixed co-ordinate system this transforms into

$$\frac{du}{dt} = \frac{du(x(t),t))}{dt} = u_x \frac{dx}{dt} + u_t = u_x u + u_t \qquad (1\ 14\ b)$$

And from equations (1 14 a) and (1 14 b) we get

$$\frac{\partial u}{\partial t} + u\frac{\partial u}{\partial x} = \frac{1}{\tau}\left[U_e - u\right] - c_o^2 \frac{1}{k}\frac{\partial k}{\partial x} \qquad (1\ 15)$$

where

τ is the relaxation time, the time in which a platoon of cars reacts to the speed alternations

U_e is the fundamental diagram

c_o^2 is constant, independent of density k, and is called the *anticipation term*

The L H S in equation (1 15) is decomposed into a *convention term*, the second term, indicating the acceleration due to spatial alternation of the streamlines and a local acceleration which is time dependent

The first term on the R H S is the equilibrium term, that is the effect of the drivers adjusting their speed to the fundamental diagram and the second term represents the anticipation on the downstream density (i e the effect of drivers reacting to the downstream traffic)

The continuity equation $\frac{\partial q}{\partial x} + \frac{\partial k}{\partial t} = 0$ from (1 10 b) and the momentum equation

$$\frac{\partial u}{\partial t} + u \frac{\partial u}{\partial x} = \frac{1}{T}\left[U_e - u\right] - c_o^2 \frac{1}{k} \frac{\partial k}{\partial x} \qquad (1\ 15)$$

form a set of first order, partial differential equations which describes the dynamic effects associated with the traffic flow, such as stop-start wave formation, bifurcation into unstable flow and transience, and behaviour at bottlenecks

To investigate these equations, the road section is discretised in time and space Numerical methods used in computational fluid dynamics can be applied to solve these equations

1.1.2.2 Two fluid theory

The two fluid theory of town traffic was proposed by Herrman and Prigogine (1979), Herrman and Arkekani (1984) Cars in a traffic stream can be viewed as two fluids, the first consisting of moving cars and the second of cars stopped due to congestion, traffic lights, stop signs, and obstructions resulting from constructions, accident and reasons other than parked cars, which are ignored since they are not components of the traffic

The two fluid theory provides a macroscopic measure of quality of traffic service in a street network which does not depend on the density

The two fluid model is based on the assumptions

i The average moving speed in a street network is proportional to the fraction of moving cars

ii The fraction of stopped time of a test car, circulating in a network, is equal to the average fraction of the cars stopped during the same period

The first assumption represents the relationship between the average speed of the moving cars and the fraction of moving cars which can be formulated as follows

$$V = V_m (1-f_s)^{n+1} \qquad (1\ 16)$$

where

V_m is the average maximum moving speed

n is an indication of the quality of traffic service in the network

V is the average speed, which can be written as $V = V_r f_r$

f_s is the fraction of stopped cars

The second assumption means that the network conditions can be represented by a single car appropriately sampling the network

Equation (1 16) can be written as

$$T = T_m\left(1 - f_s\right)^{-(n+1)} \tag{1 17}$$

$$f_s = \frac{T_s}{T} \tag{1 18}$$

Combining the Equations (1 17) and (1 18) we get

$$T_s = T - T_m^{\frac{1}{n+1}} \; T^{\frac{n}{n+1}} \tag{1 19}$$

which represents the two fluid formulation

Equation can be written as

$$T_s = T - T_r \tag{1 20}$$

where

$$T_r = T_m^{\frac{1}{n+1}} \; T^{\frac{n}{n+1}} \tag{1 21}$$

which represents the relation between the trip time per unit distance, T, and the running time per unit distance, T_r

Taking the natural logarithm of both sides in Equation (1 21) yields

$$\ln T_r = \frac{1}{n+1} \ln T_m + \frac{n}{n+1} \ln T \tag{1 22}$$

which provides a linear expression for the use of least squares analysis

1.1.3 Cellular Automata Models

Cellular automata (CA) are discrete dynamical systems, which are defined on a one-dimensional lattice (or multi-dimension grid) of k identical cells

The global behaviour of the system is determined by the evolution of the states of all cells as a result of multiple interactions

CA, which were developed to model simple mathematical systems, are increasingly used in the simulation of complex systems In this approach, the traffic system is regarded as an interacting particle system, which shows a transition between two phases

Low-density phase in which all cars move smoothly with maximum speed, and

High-density phase in which cars are almost stopped

The CA evolves in discrete time steps The state of each site at the next time step is determined from the state of the site itself and its nearest sites at the current time step

The CA models simulate the movement of each individual car according to a number of simple rules, essentially moving each forward by an integer number of increments at an integer speed

1.1.3.1 One-dimensional Cellular Automata Models

Very recently, Nagel and Shreckenberg (1992) have introduced a stochastic Cellular Automata model to simulate freeway traffic They found that there are two regions in the traffic flow

i Free-phase, which is dominant at low density

ii Congested traffic in which traffic jams appear at a high density

The model is defined over a lattice of k-identical sites, each of length 7 5 m representing the length of the car plus distance between cars in jam, and each site can be either empty or occupied by a single particle

Each particle can have an integer velocity between 0 and v_{max}, where $v_{max} = 5$ in general Given the configuration of the particles at time step t, the configuration at time step t+1 is computed by applying the following rules , which are done in parallel for all particles

- Calculate the headway distance(= gap)
- Deceleration

  If v> gap (the particle is running too fast), then slow down to

  v = gap (rule 1)
- Acceleration

  If v < gap and $v < v_{max}$ then accelerate by one

  $v = v + 1$ (rule 2)
- Randomisation

  If after these steps, the velocity v is greater than zero, then with probability p reduce v by one v = v-1 (rule 3)

- Car advance

  Each particle is advanced v sites ahead (rule 4)

Nagel and Schreckenberg (1992), showed that the start-stop waves, (traffic jams), appear in the congested traffic region Also, they obtained good agreement with realistic fundamental diagrams

Basically, they tried to model two properties of the road traffic

- Cars travel at some desired speed, unless they are forced to slow down in order to avoid collisions with other vehicles
- Interactions are short ranged and can be approximated by being restricted to nearest neighbours

Imperfections in the way drivers react is modelled as noise

The continuous limit of the CA model has been investigated by Krauß *et al* (1996), this is obtained by letting $v_{\max} \rightarrow \infty$ and $\rho_{\max} \rightarrow 0$

The generalised version of the CA model allows for continuous values of the velocities and spatial co-ordinates In the N-S model noise, is introduced by randomly decelerating car velocity by one with probability p_{break} This, however, is generalized to an equipartition between zero and the maximum acceleration in the generalized version

The CA rules for the intermediate model are defined as follows

$$v_{des} = \min(v(t) + a(t),\ v_{\max},\ gap(t)),$$

$$v(t+1) = \max(0,\ v_{des} - \sigma\ rand()), \qquad (1\ 23)$$

$$x(t+1) = x(t) + v(t+1)$$

Where *gap(t)* is the free headway distance, $a_{\max}$ is the maximum acceleration , *rand()* is a random number in the interval (0, 1) and σ is the maximum deceleration due to noise

Numerical simulations showed that the transition, leading from the free flow regime to the congested flow regime, bears strong similarities to a first order phase transition in equilibrium thermodynamics An additional advantage of the continuous model is that it is much easier to calibrate with real data, despite the slight decrease in the numerical efficiency

1.1.3.2 Two-dimension Cellular Automata Models

Two-dimensional problems, (city traffic), are more complicated compared to one-dimensional ones and in turn they are less realistic

Biham and Middleton (1992), have introduced a simple deterministic two-dimensional model Three variants of the model were investigated, the first two variants of the model use three-state Cellular Automata defined on a square lattice Each site contains either an arrow pointing upwards, an arrow pointing to the right, or is empty

In the first variant (Model I) the traffic dynamic is controlled by traffic lights, such that the right-arrows move only in even time steps and the up arrows move in odd time steps

On even time steps, each arrow moves one step to the right unless the site on its right-hand side is occupied by another arrow If it is blocked by another arrow it does not move, even if during the same time step the blocking arrow moves out of that site Similar rules apply to the up arrows, which move upwards

The model is defined on a square lattice of N x N sites with periodic boundary conditions

In model II, the traffic light is removed and all arrows move in all time steps (unless they are stopped) If both an up and a right arrow try to move to the same site, one of them will be chosen randomly, with equal probabilities Model II is considered to be the non-deterministic variant of the model

Extensive numerical simulation shows a sharp jamming transition which separates the low-density dynamical phase in which all cars move at maximal speed and the high-density jammed phase in which they are all stopped

The third variant of the model is a four-state C A defined on a square grid Each site contains either an arrow pointing upwards, an arrow pointing to the right, an arrow pointing left, or is empty In this four-state model all arrows try to move at every time step If both an up arrow and a right arrow try to move to an empty site at the same time step they both move in and overlap On the other hand no arrow can move into a site which is already occupied

The simulations of Biham and Middleton(1992) show that the model exhibits a continuous transition, which is qualitatively similar to the one-dimensional case

Nagatani (1993) has extended the CA model proposed by Biham and Middleton (1992) (the BML model), to investigate the effect of the two-level

crossing on the traffic jam in the original model The model, as in Fig (1 5), is defined on a disordered square lattice with two components

- The first component is the site of three states representing the one-level crossing
- The second component is the site of four states representing the two-level crossing

Nagatani (1993) showed that the dynamical jamming transition does not occur when the fraction c of the two-level crossings becomes larger than the percolation threshold, which gives rise to the critical behaviour However, the dynamical jamming transition occurs at higher density of cars with increasing fraction c of the two-level crossing below the percolation threshold

Torok and Kertesz (1996) have studied the sequential update version of the BML model called the Green Wave Model (GWM)

The main difference between the two models is that in the BML model single cars move while in the Green Wave Model, whole convoys (line of same type of cars with no empty space between them) travel together

In the BML model, two cars cannot move together because if they become neighbours the second car is not able to move until the first is moved away In the GWM the two neighbouring cars always stay together if the first moves the second will move in the same time step and there is no effect that could separate them The GWM shows two types of transition the free flow-jam transition and a structural transition in the jammed region

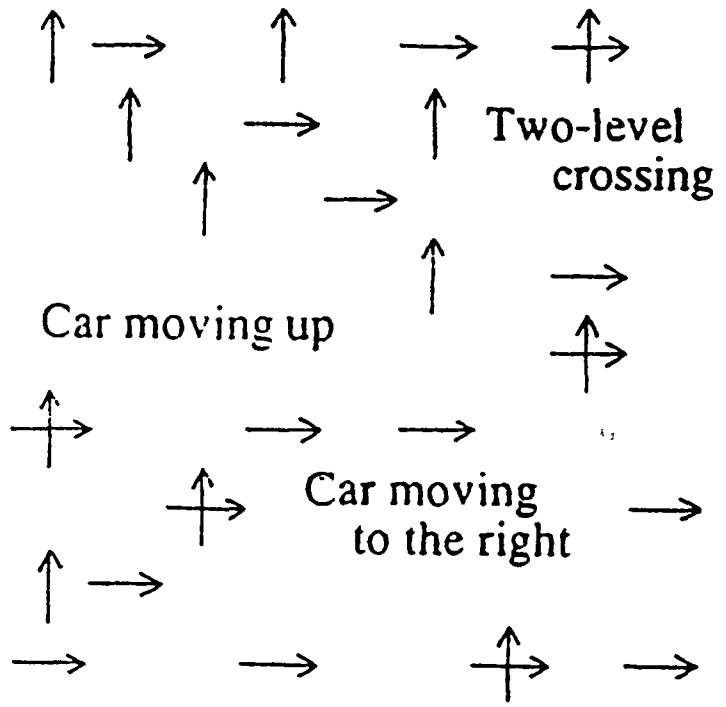

Fig (1 5) Schematic illustration of the cellular automata model of traffic flow with two-level crossings, source T Nagatani (1993)

1.1.4 Thesis Outline

The remaining chapters of this thesis are organized as follows In Chapter 2 we present a three state deterministic cellular automata model for urban traffic, then the model is adapted to simulate road traffic In Chapter 3 we move towards network traffic flow and we investigate using the simple model, developed in Sec (2 1), the network performance under different parameters that govern the traffic flow, whereas in Chapter 4 we investigate the traffic behaviour along the network with loss to flow and under short and long-term traffic events

In Chapter 5 a set of lane-changing rules for cellular automata is presented and a stochastic cellular automata model for traffic flow in inter-urban areas is presented in Chapter 6 Finally, Chapter 7 concludes this thesis by highlighting the main contributions and discussing directions for future research

Chapter 2

"Simple Cellular Automata Model for Urban Traffic Flow"

2.0 Introduction

Numerical simulations, hydrodynamic models, and queuing theory are a few of the basic theoretical tools, used to describe traffic flow on freeway networks (Leutzbach, 1988, Kuhne, 1984) Traffic control has been intensively studied also from the point of view of Operations Research (Improta, 1987) As one might expect, the theory of traffic flow is related to telecommunication and computer network theory Equally, many basic concepts in traffic flow theory have their origins in physics, (Lighthill and Whitham, 1955, Herrmann *et al*, 1959)

Cellular automata, which were developed to model simple mathematical systems, are increasingly used in the simulation of complex physical systems (Wolfram, 1986), and have helped demonstrate phenomena which are of practical interest

Congestion is a simple phenomenon cars can not move without sufficient space between them (Nagatani, 1993a,b, 1994a,b , Nagel and Herrmann, 1993) In order to simulate freeway traffic flow, Nagel and Schreckenberg (1992) extended the 1D asymmetric simple exclusion model by taking into account car velocity,(Sec(1 1 3 1)) They showed that a transition from laminar traffic flow to start-stop waves occurs with increasing car density, as observed in real freeway traffic

Control of traffic flow in cities is a more complex endeavour as it involves many degrees of freedom such as local densities and speeds Cremer and Ludwig (1986) have developed a fast simulation model for modelling traffic

flow through urban networks They simulate the progression of cars along a street using bit manipulation computer programs When compared with standard microscopic models, the computational time needed is less by a ratio of 1 / 150 The models simulate, accurately, macroscopic phenomena of traffic flow, while at the same time reproducing the main mechanisms of microscopic models

In this chapter we present a Cellular Automaton (CA) to simulate traffic flow in urban networks, which extends this approach

2.1 The Cellular Automata Model

Our model is a 3-state cellular automaton defined on a one-dimensional lattice L , of k identical sites with at most one particle per site, where each site can take one of the states 0, 1 and 2 State 0 is the empty site, state 1 represents a site occupied by a stopped car and state 2 corresponds to a site with a moving car The CA evolves in discrete time steps The state of each site at the next time step is determined from the state of the site itself and those of its two nearest neighbour sites, at the current time Applying a parallel update rule for all sites in the model, the transition rules may be described as follows

If a site is

1- Occupied by a moving car and the neighbouring site in the direction of movement is empty, then the car is advanced one site (Rule 1)

2- Occupied by a moving car and the next site in front is occupied by a stopped or moving car, the car can not advance (Rule 2)

3- Occupied by a stopped car and the nearest site in front is empty , then it will advance by one site (Rule 3)

4- Empty, and a car wishes to enter it from an adjacent cell, then the current site is occupied by a moving car if the next site ahead is either empty or occupied by a moving car, and by a stopped car otherwise (Rule 4)

2.1.1 Model parameters

The fundamental diagrams in traffic flow models are (i) flow vs density and (ii) average velocity vs density The following parameters play a central role in this analysis

The mean velocity of cars in a unit time interval τ is defined to be the number of moving cars divided by the total numbers of cars

$$v_\tau = \frac{n_\rightarrow}{n}, \qquad (2\ 1)$$

where $n_\rightarrow$ = number of moving cars in τ

and n = total number of cars

The average mean velocity over an interval of time T is

$$\langle v \rangle = \frac{1}{T}\sum_t v_t \qquad (2\ 2)$$

where v_t = system velocity at t time step

T = Length of the time interval

The density of cars in the system, ρ, and the flow, q, are defined by

$$\rho = n / k \qquad (2.3)$$

$$q = \langle v \rangle \rho \qquad (2.4)$$

where n = number of cars

and k = number of sites in the model

2.1.2 Model Dynamics

The time-evolution of the automaton follows the simple rules given earlier for applying periodic boundary conditions, (as illustrated on the space-time diagram, Fig (2.1))

When a *periodic boundary condition* is imposed on the model, cars that exit the system (on the right hand side) are fed back into the system on the left-hand side, as our traffic moves from left to right

Each site on the lattice can take one of the states 0 (empty), 1 (stopped car) or 2 (moving car) If one follows the movements of individual cars in the space-time diagram Figs (2.1 a and b), cars moving freely are characterised by diagonal lines with the symbol 2, while stationary cars are characterised by vertical lines with the symbol 1

Lines are configurations at consecutive time steps At low density, these lines show laminar traffic, with the system moving with maximum velocity subject to one gap ahead indicating *"free phase"* traffic

In contrast, at high density, we find congestion clusters, each congestion represent a traffic jam, indicating a *"jammed phase"* traffic

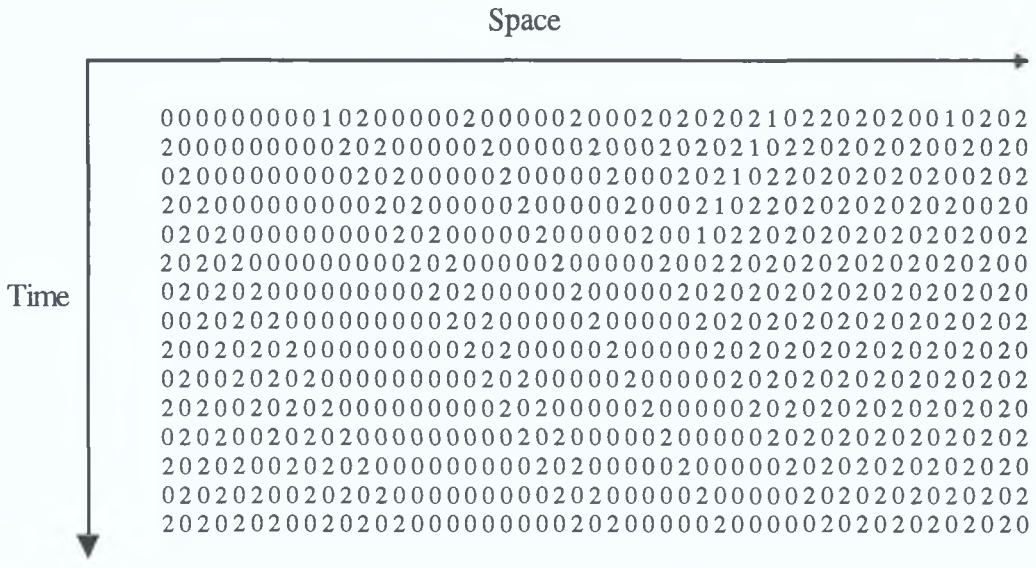

(a)

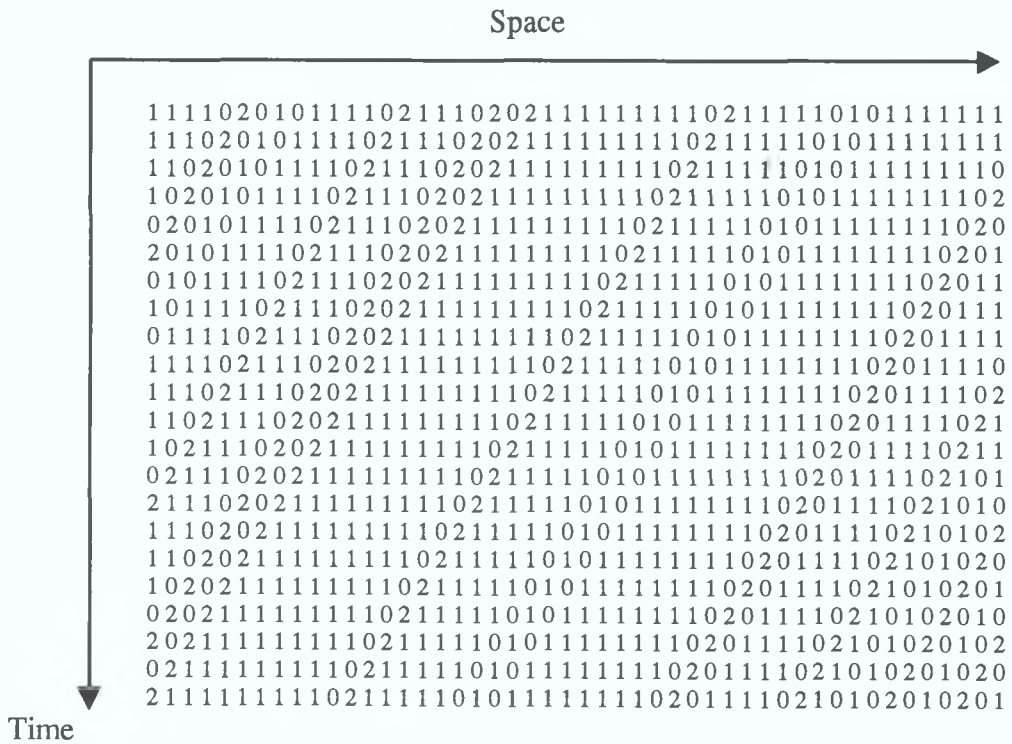

(b)

Fig.(2.1): Space-time diagrams of the Simple CA Model defined on a 100 site Lattice with closed boundary conditions, where in (a) $\rho = 0.3$ and in (b) $\rho = 0.8$

Note that when traffic is stopped, the traffic jam wave moves backwards relative to the traffic flow

2.2 Simulation and Results.

2.2.1 The model with periodic boundary conditions

We have implemented computer simulations in Borland C++ for a deterministic CA model, starting with random initial configuration of cars with density ρ and velocity = 0 Different lattice sizes (k = 60, 80, 100, 120, 140) were used In each case, the CA model ran for 1000 time steps and this process was repeated 300 times to generate the average case statistics

Most road-traffic observers have concentrated on measuring flow, q, and average velocity, v, as being the quantities of greatest practical interest The density ρ can be obtained from these measurements

The relation between the three macroscopic variables, flow, average velocity, and density, is widely known as the *fundamental diagram* In Sec (1 1 2 1 1), we have studied in detail the flow-density relation, which represents the first component of the fundamental diagram Another important relation is the velocity-density relation This is regarded as the second component of the fundamental diagram, which shows how the system density affects mean speed at different levels of concentrations The fundamental diagrams are also known as " *Empirical relations*"

Using the fundamental diagrams, our simulation results reveal that the system reached its critical state when the density $\rho_c = 0.5$

The maximum flow recorded was q = 0 5, after a transient period $t_o = \frac{k}{2}$, which does not depend on the system size.

Fig (2 2 a) shows the fundamental diagram (flow vs density) which is symmetrical about the critical density $\rho_c = 0.5$, which marks the boundary between free flowing and congested traffic

In Fig (2 2 b) we plot the average velocity against density, which indicates that the system moves with a constant average velocity <v> = 1 until ρ= 0 5 and then decreases as we increase the density

The space-time diagrams in Figs (2 3 a) and (2 3 b) are very useful in visualizing traffic and traffic jams In these figures,(2 3 a, b), each black pixel represents a car Space direction is horizontal, time is pointing downwards, cars are moving from left to right and from top to bottom.

In free flowing traffic, Fig (2 3 a), the system reaches a steady state characterised by each car advancing one site to the right at each time step In contrast, in congested traffic, Fig (2 3 b), the traffic jam moves one site to the left at each time step

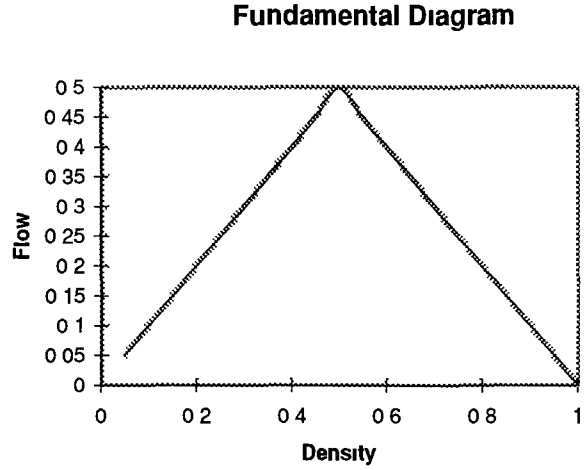

Fig (2 2 a) flow-density relation for a system of size 80 Data are averaged over long time periods (1000 time steps) using closed boundary conditions It is easy to see that the phase transition between the two regimes occurs at the critical density 0 5

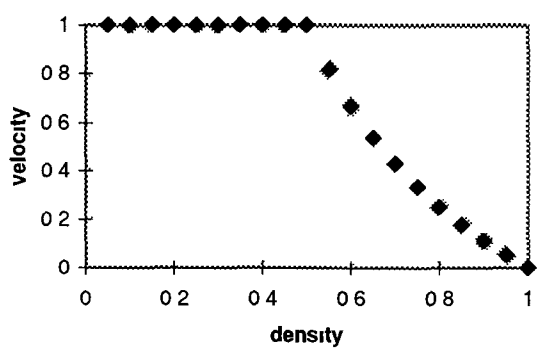

Fig (2 2 b) velocity-density relation, using closed boundary conditions, again the System moves with constant velocity until the density of 0 5, then the transition between the two phases take place

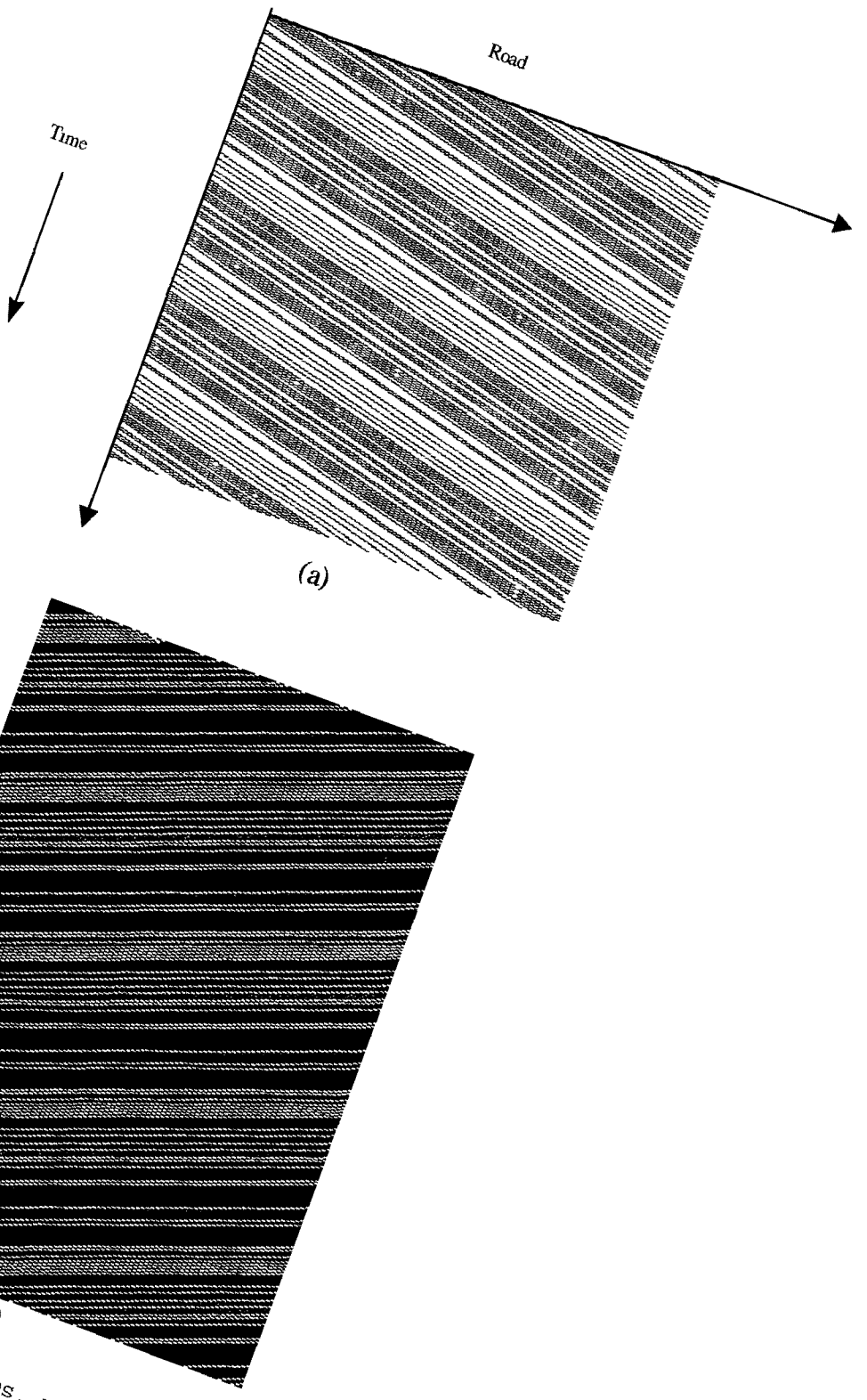

Fig(2 3) Space-time diagrams, where in (a) $\rho = 0\ 3$ and (b) $\rho = 0\ 8$

2.2.2 The Model with Open Boundary Conditions

The rules of the Simple Model with open boundary conditions are identical to the periodic case except that we work with average densities and need to consider the input to the system as well as the duration of each simulation run Different rates of injecting cars into the system were investigated These correspond to peak-time rates, such as those that occur at, say, 8 00 hrs or 17 00 hrs and off-peak time, corresponding to 11 00 hrs or 20 00hrs

In our model, exit from the road (system) is controlled by a traffic light, operating under a green and red light regime Cars can leave the system only during the green light phase, by deleting the last site of the road, and form a queue during a red light phase In this model the user fixes the duration of the green and red phases

Differing lattice sizes (60, 80) were selected, data was collected after transience k / 2, and averaged over 200 simulation runs Each simulation run consisted of 600 time steps using various regimes for the green and red phases The fundamental diagrams for the two different array sizes, k =60, 80, are presented in Figs (2 4) and (2 5) Comparing these diagrams with those obtained for closed system (closed boundary conditions), we make the following observations

1 Imposing open boundary conditions has led to lower values for the maximum flow and its density, $q_{\max}$ has decreased from 0 5 (at ρ_c = 0 5) to 0 3525 (at $\rho_c = 0\ 424$)

ii. The simulation reveals that the maximum flow and its density depend on the system size. Using a system of size 60 sites has led to a maximum flow of $q_{\max} \sim 0.36$ at density $\rho_{q\max} \sim 0.48$, whereas a lower value for $q_{\max} = 0.3525$ was obtained at lower density of 0.42 in the case of larger size network(k=80).

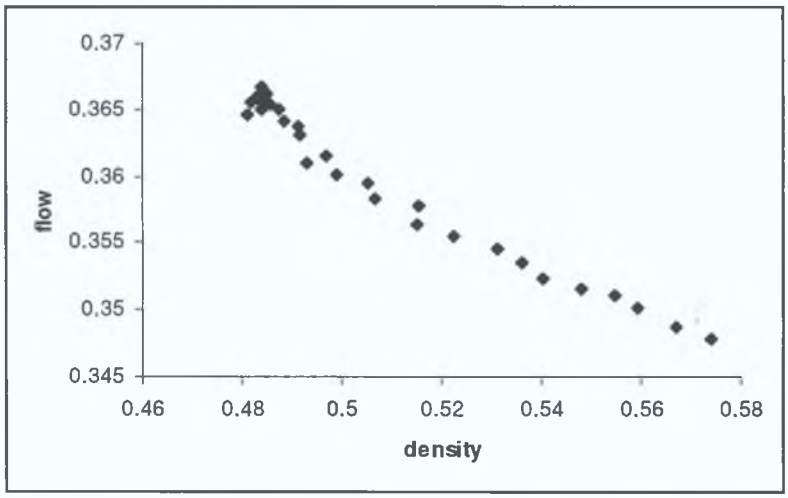

(a)

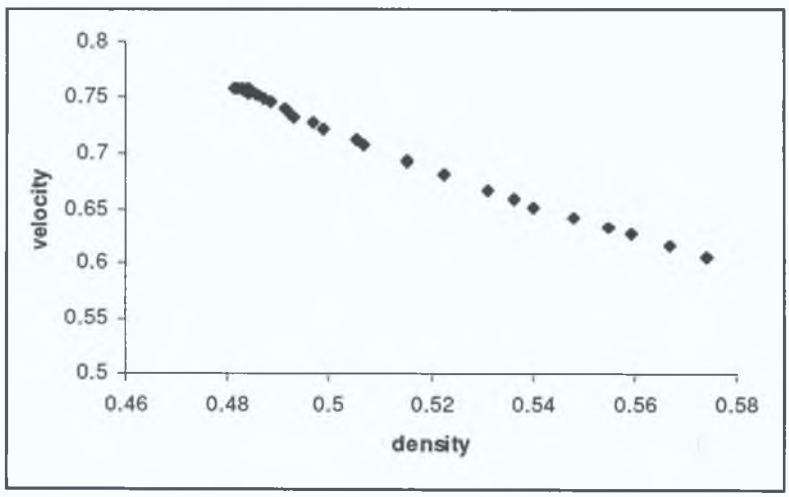

(b)

Fig.(2.4):Fundamental diagrams for the Simple Model with open boundary conditions; flow-density relation, velocity-density relation, for array size 60 cells. Data were averaged over 200 runs, where each run is 600 time steps

iii Applying open boundary conditions was also able to give, roughly, the characteristic shapes of the fundamental diagrams, flow-density relation and velocity density-relation

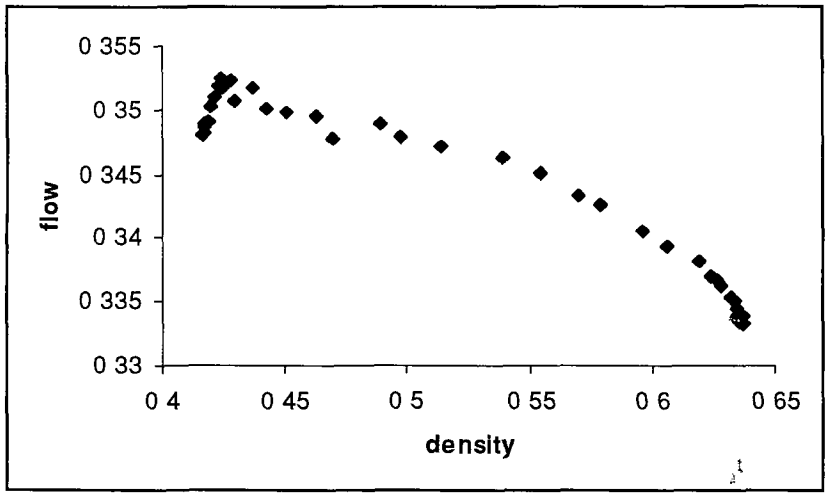

(a)

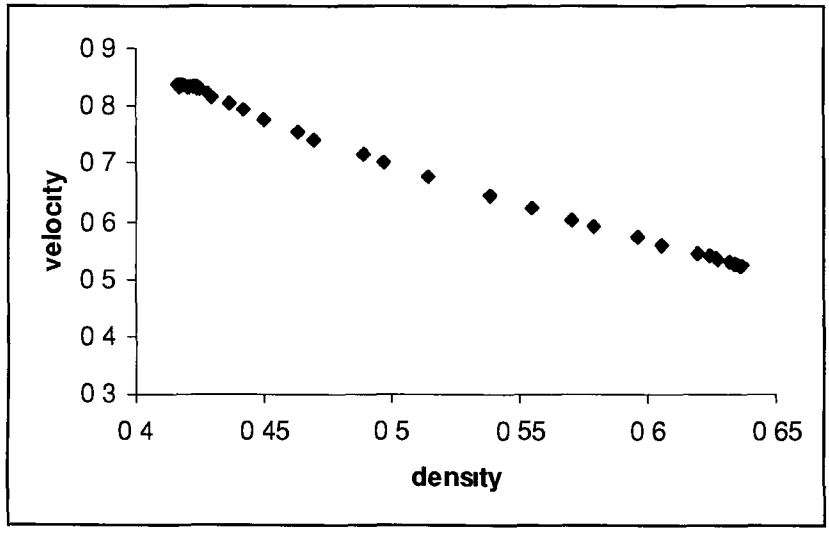

(b)

Fig (2 5) Fundamental diagrams for the Simple Model with open boundary conditions, flow-density relation, velocity-density relation, for array size 80 cells Data were averaged over 200 runs, where each run is 600 time steps

2.3 Road Traffic Simulation

We now extend our simulation to include road traffic flow, where each "road" is formed by linking more than one segment, where a segment is a one-dimensional array of k sites.

In this section we introduce a new parameter *jammed time* t_j, which represents the waiting time period cars require to leave the road. In real traffic, this parameter depends on the number of traffic lights, which are installed between the road segments, and the duration of both light cycles, red and green, as well as the traffic density. The aim of this section is to study and analyse the effect of the number of road segments and the light cycle duration on the jammed time parameter.

2.3.1 Road Description

The model looks at traffic flow for a seven-day period on two designs: a road consisting of 77 cells and three segments and another consisting of 144 cells and five segments. The choice is made in order to avoid complex situations with large number of intersections.

The simulation runs allowed for:

1- Road input and output

Cars were generated at random and input into the system according to two different injection rates: peak-time and off-peak time rates. Cars were allowed to leave the road only during the green cycle and the first site outside the road was assumed to be free throughout the simulation run.

2- Specified duration of the light cycle

The simulation was performed using different periods for both the red and green cycles

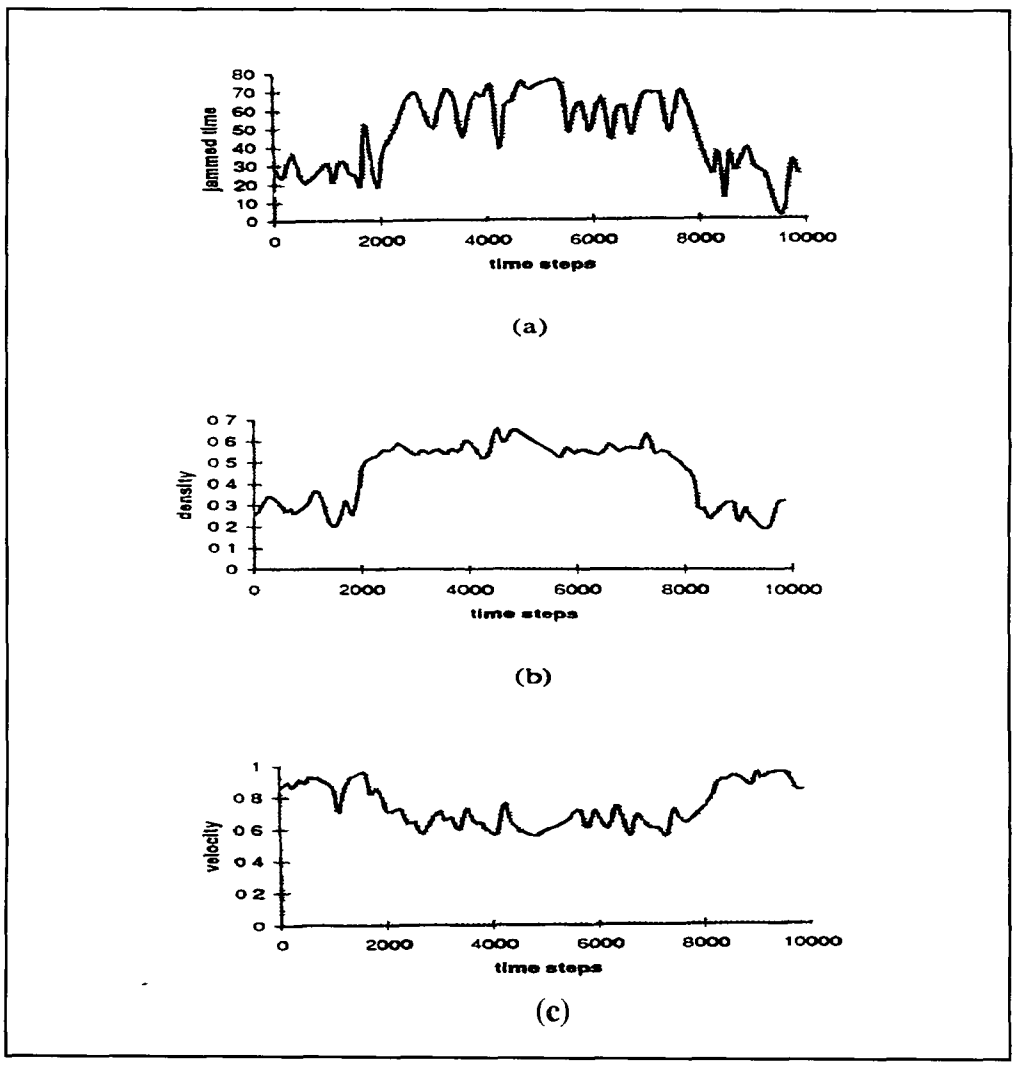

Fig (2 6) Day-one of our simulation using road of size 77 cells, with green cycle = 20 time steps, red cycle = 15 time steps and Where (a), (b), and (c) represents the relations of the time-steps against jammed time, density, and velocity

2.3.2 Simulation and results

Each simulation run is calculated using up to 10,000 time steps, where the peak-time period is considered to be inside the interval 2000-8000 time steps Fig (2 6) describes the traffic behaviour throughout day-one traffic simulation, where the roads size = 77 cells and the green time cycle is greater than the red time cycle by a factor of 4/3 The jammed time vs time steps relation, presented in Fig (2 6 a), shows the sharp transition in the jammed time parameter t_j at two points, (2000 & 8000 time steps respectively), which separates the two traffic regimes, i e free and dense traffic It also demonstrates how t_j rapidly increases over the dense traffic period and the way in which it oscillates during the two regimes These oscillations, which may occur due to the density fluctuations and the duration of the traffic light cycle, have considerable impact on the traffic velocity This is demonstrated in Fig (2 6 c) To observe the effect of the light cycle duration on the t_j parameter, we have increased the red cycle period to be the same as the green cycle, see Fig (2 7) This change in turn decreased the outflow By comparing Figs (2 6 a and 2 7 a), we find that increasing the red cycle period has result in no significant changes in the jammed-time parameter over the dense traffic period, which my be noticed by very small oscillations in the t_j parameter as it can be seen from Fig (2 7 a) This, also, was the case when the green cycle was decreased to be the same as the red cycle period

Now we investigate the effect of the number of traffic lights on the jammed-time parameter t_j by increasing the road segments to five segments

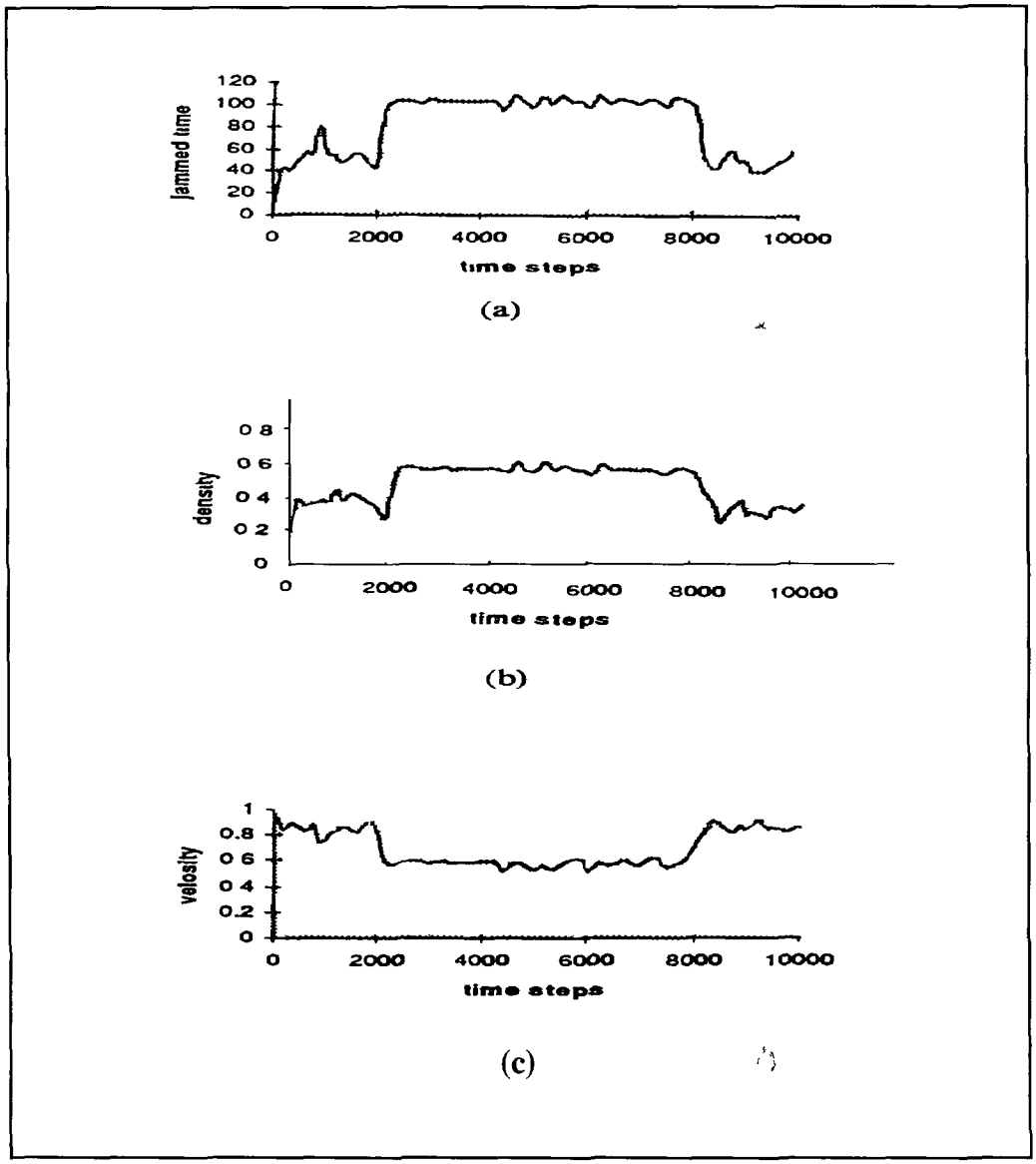

Fig (2 7) Day-two of our simulation using road of size 77 cells, with the green cycle and the red cycle the same and Where (a), (b), and (c) represents the relations of fundamental measures vs time steps

Fig (2 8) illustrates the traffic flow behaviour throughout a one-day traffic simulation, which was performed to investigate jammed-time behaviour after the number of road segments was increased to five and with green time cycle = 20 time steps and red time cycle = 15 time steps

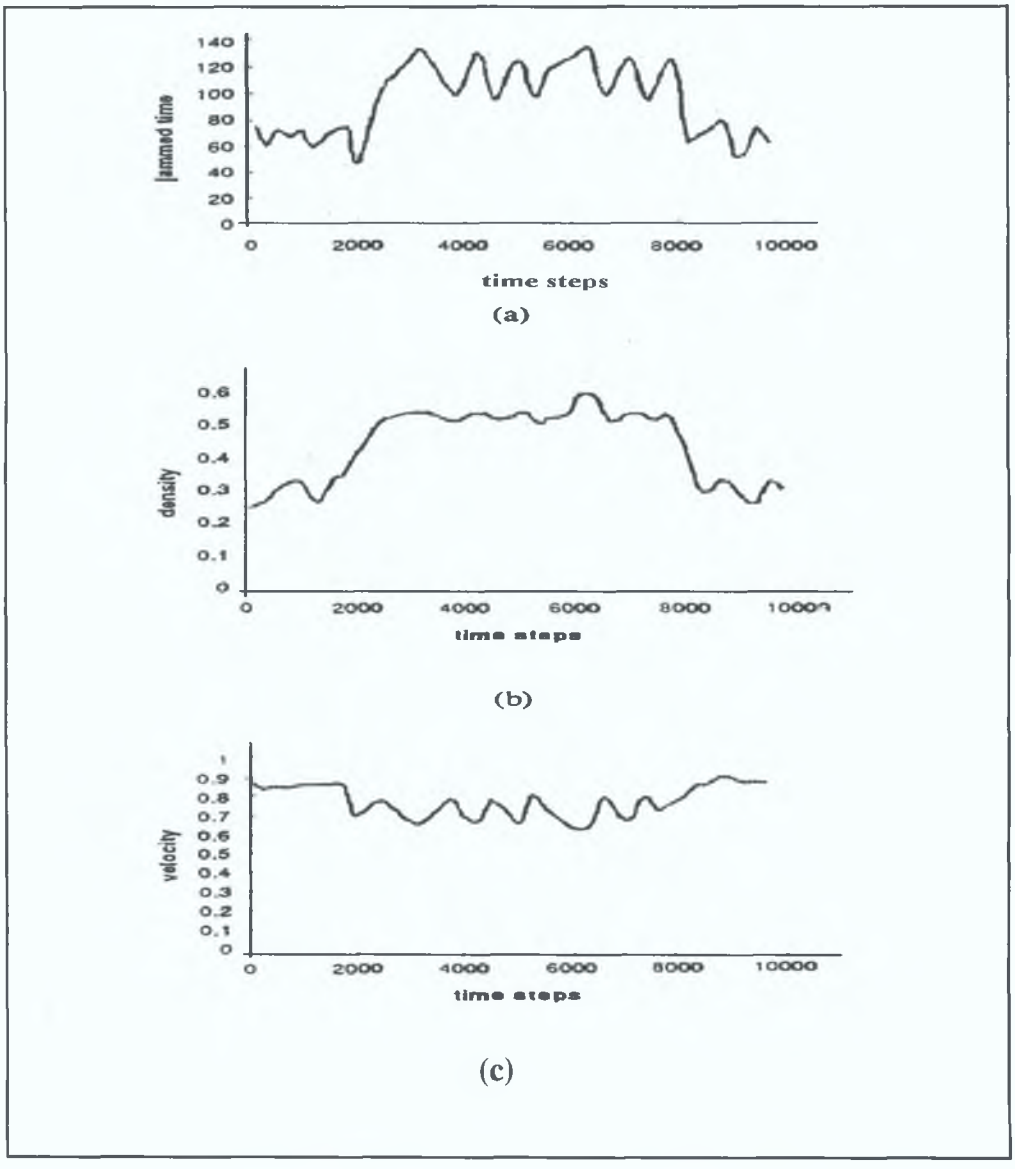

Fig(2.8): Day-three of our simulation using road of size 144 cells, and the green cycle = 20 time steps, red cycle = 15 time steps and Where (a), (b), and (c) represents the relations of the time-steps against jammed time, density, and velocity.

Comparing the results obtained in Figs (2.6 and 2.8), we may observe the following:

Increasing the number of road segments has generated the same traffic features as for the three segment road, and has also increased the jammed time as expected, see Table (2.1).

Road Size	Green Cycle =20 & Red Cycle = 15	Red cycle increased to Green cycle	Green Cycle reduced to red Cycle
77 cells	5-80	15-120	40-100
144 cells	35-135	50-140	55-140

Table (2 1) The jammed-time range, in time steps, for different road size and light cycles

Table (2 1) shows that the jammed-time range, for both roads, is affected by the changes in the light cycle duration for both red and green times For both roads, the t_j parameter attains its minimum value when the green cycle is greater than the red cycle, whereas the maximum value of t_j is obtained at higher value for the red cycle

This can be seen also from the space-time diagrams in Fig (9 (a) and (b)) From these, it is easy to visualise the traffic behaviour for a certain number of time steps

In Fig (2 9), where Borland C++ is used to plot our space-time diagrams, cars are moving to the right from top left to bottom right Straight lines indicate that cars are moving freely, while vertical lines means that cars are blocked (stopped)

Traffic jams at the traffic lights are represented by the vertical trajectories, which are moving backwards against the traffic.

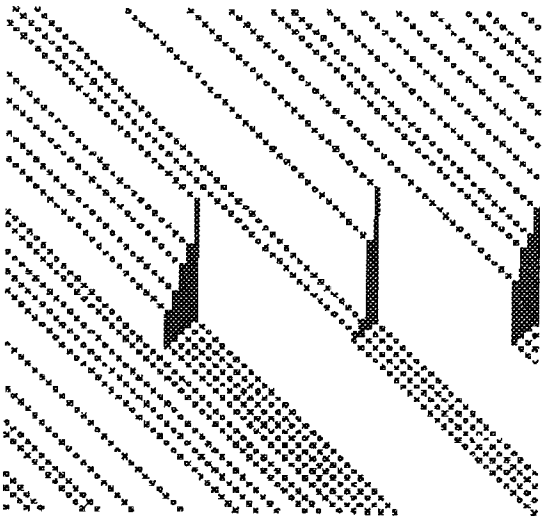

Fig.(2.9.a):Space-time diagram at off-peak time, where the road size is 77 cells

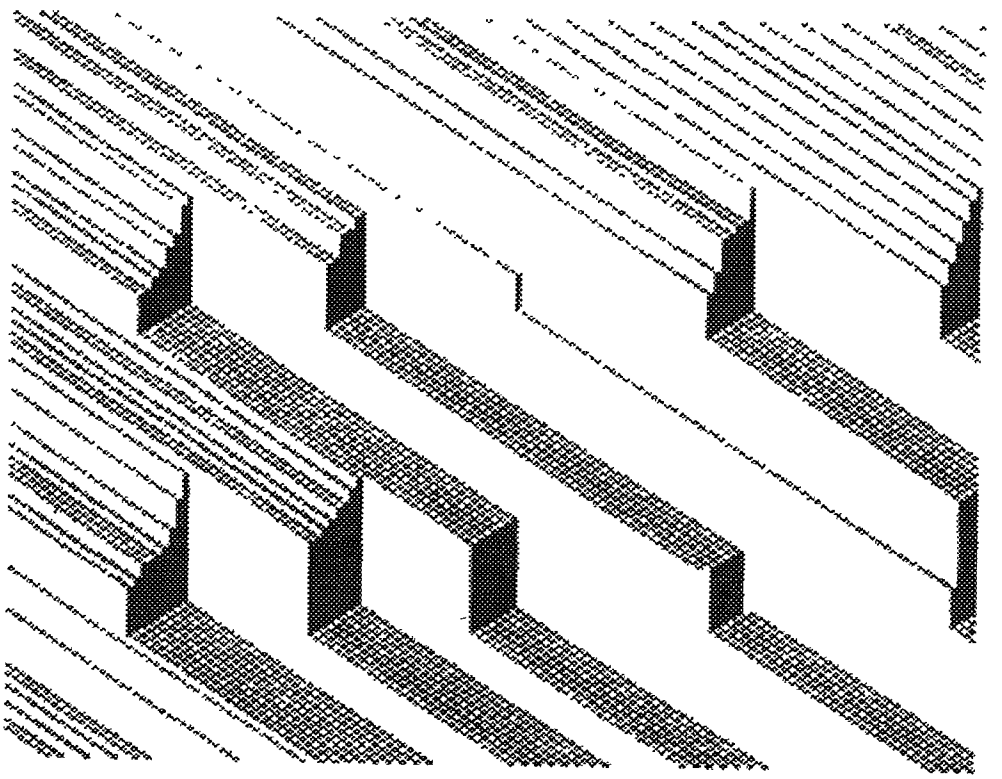

Fig.(2.9.b): Space-time diagram at off-peak time, where the road size is 144 cells

In the Figures, these jams are more noticeable, and also last for longer periods as we increase the number of the traffic lights from 3 to 5, hence the observed increase similarly in jammed time

Similar phenomena were apparent when different light cycle periods were applied, as in the three-segment road case From the above results, we conclude that the jammed-time parameter for the simulation depends on the number of traffic lights and the duration of each light cycle, red and green, and as well as the traffic density, as found for real traffic

The choice of the different cases for the light cycle's duration was destined to create three different traffic patterns as follows

- By increasing the green light cycle over the red cycle, we consider our simulated traffic to be more important than the traffic which passes the same traffic lights on the other roads,
- This situation is no longer dominant when the traffic on the other roads becomes heavier in this case we increase the red cycle for our simulated traffic, i e more green light for the other roads
- In the third choice all roads are of the same importance, but the traffic ahead is more congested In this case decreasing the green cycle will take some pressure at the front junctions

2.4 Summary and Concluding Comments

i A three state deterministic Cellular Automata Simulation Model for the dynamic process of traffic flow in urban Networks is presented in this chapter, with space and time discrete

The time–evolution of the automaton follows simple rules, the state of each site at the next time step is determined from the state of site itself and those of the nearest neighbour sites,

ii We have performed our simulation, applying a parallel update strategy, on small size lattices with open and closed boundary conditions

iii Simulations have been extended to include roads, where each road is formed by linking a finite number of segments separated by traffic lights

iv Results for the jammed time parameter t_j showed that this parameter depends on the number of traffic lights and the duration of each light cycle

v Since the update rules treat segments of the road networks, rather than individual vehicles, computational time does not depend on the number of the vehicles within the segments, but only on the segment size

Chapter 3

"Traffic System and Transient Movement Simulation"

3.0 Introduction

The development of the network level traffic approach was based on the two-fluid theory of town traffic (Herman and Prigogine, 1979, Herman and Ardekani, 1984), which relates the average speed of moving cars to the fraction of running cars in a street network Further extensive studies have been carried out on the basis of this theory (Mahamassani *et al*, 1990, Williams *et al*, 1987), which has many advantages but also involves some effort in model specification and high computational requirements However, the behaviour of the various network variables at high concentration levels of cars remains to be understood Other relevant work in the same area has involved development of a fast simulation model for progression of cars along a street through bit manipulation programs (Cremer and Ludwig, 1986) In this chapter we move from a single-lane traffic modelling to modelling networks using the Simple Cellular Automata Model described in Sec (2 1)

3.1 Network description

Road networks are represented by nodes, segments (lanes), and links This structure allows the traffic simulation in integrated networks of urban two-lane carriageways The network objects may be described by components as follows

3.1.1 Nodes

Each node can be viewed as an intersection or a T-junction. Nodes are points in the network where traffic enters or leaves the simulated network, or traffic

from one link is distributed among other links in the network The entry links of the network are located at all the peripheral nodes with the exception of the T junction nodes Each node object, Fig (3 1), has the following data items

1-*Node number*

Each node has a unique identification number

2-*Node offset*

For each node the offset is defined as the number of time steps at which the node will change its default start, (red time traffic), to green time traffic for the duration of the green cycle

The offset refers to the time relationship between the adjacent signals at network nodes The pattern of offsets in a series of signal aims to minimize the stops and delay associated with travel through network of signals

The *node offset* is calculated as follows

i the offset is set to zero for nodes, which are considered as the offset-start nodes

ii for all other nodes, the offset is considered to be the shortest path from the nearest entry and exit node up to the given node

3-*Node type*

The node type specify whether the node is an intersection, a T junction, or entry and exit node

4-*Node green cycle*

The green cycle is the number of time steps, which allows the traffic to flow from a specific direction at a specified node

Node Object

Node number:	: 15
Node offset	: 20
Node type	: I (intersection)
Node red cycle	: 15 (time steps)
Node green cycle	: 20 (time steps)
Node signal	: 0 (red)
Node entries	: 12, 34, 45, 20, 44, 21

Fig(3 1)

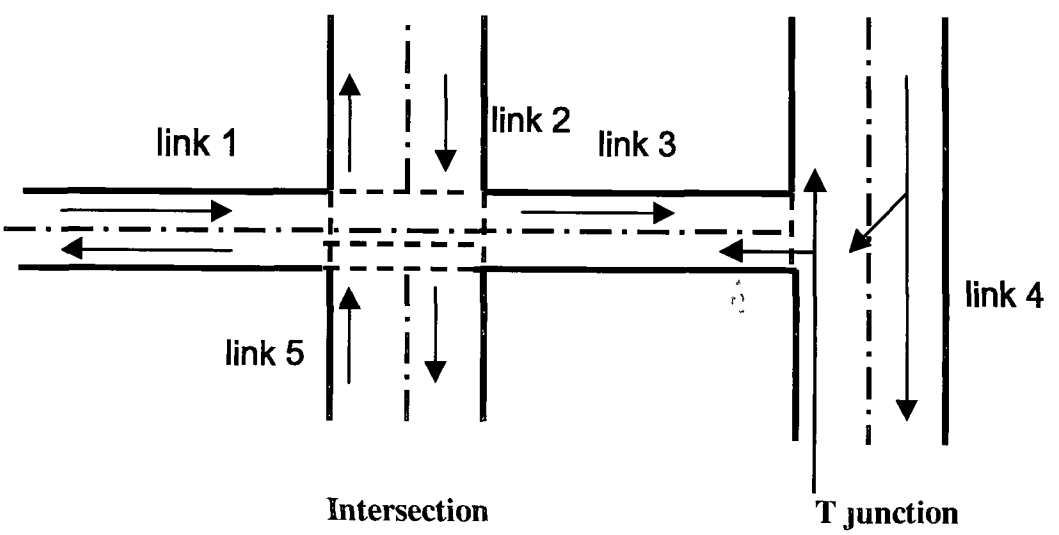

Fig(3 2)

5-*Node red cycle*

Is the duration of the opposite traffic flow at a specified node

6-*Node signal*

Two signals only are introduced in our network traffic simulation, red (0) and green (1), assuming that the default setting for each node signal is 0 (red)

7-*Node entries*

These are the segments, which link the give node to other network nodes

3.1.2 Links

A link is a set of two adjacent lanes, each of which has a different direction, which may connect any two nodes, see Fig (3 2)

Network roads are connected using links, all links in the simulated network consist of 2-lanes, with all feasible movements allowed at all intersections

3.1.3 Segments

Segments are road sections, which connect nodes Each segment object, demonstrated in Fig (3 2), has the following characteristics

1- *length*

This is the number of cells in each segment, where each cell is 7 5 m and represents the car length plus distance between cars in dense traffic

2- *configuration*

This indicates the initial state for the segment, i e the way in which the vehicles are initially placed at random

3- *transient period*

This specifies the number of time steps, which we discard before starting the

collection of our data and is based on the segment size It represents the time needed for relaxation to equilibrium

4- *starting and ending nodes*

The *starting and ending nodes* of any segment tell us the position of the segment inside the simulated network

3.1.4 Network geometry

The *geometry* of the network was chosen to be a circular grid with radius r, which indicates the number of nodes from the centre node of the simulated network to the surface node Applying this geometry, each segment object of the network can be either a straight line or a true arc, which is characterised by the co-ordinates of the start and end points (nodes) Increasing the radius of the grid would also increase the number of segments by a fixed number, which allows different size networks to be simulated Fig (3 3) shows how the proposed geometry is used to represent real networks

3.1.5 Traffic control and traffic conditions at junctions

All nodes were controlled, (signalised), in our simulated network Our signal operating condition was assumed to be a pre-timed signal, (fixed time control) By fixed time control, both the green time cycle and the red time cycle are fixed without any consideration to the vehicle arrivals and departures at junctions

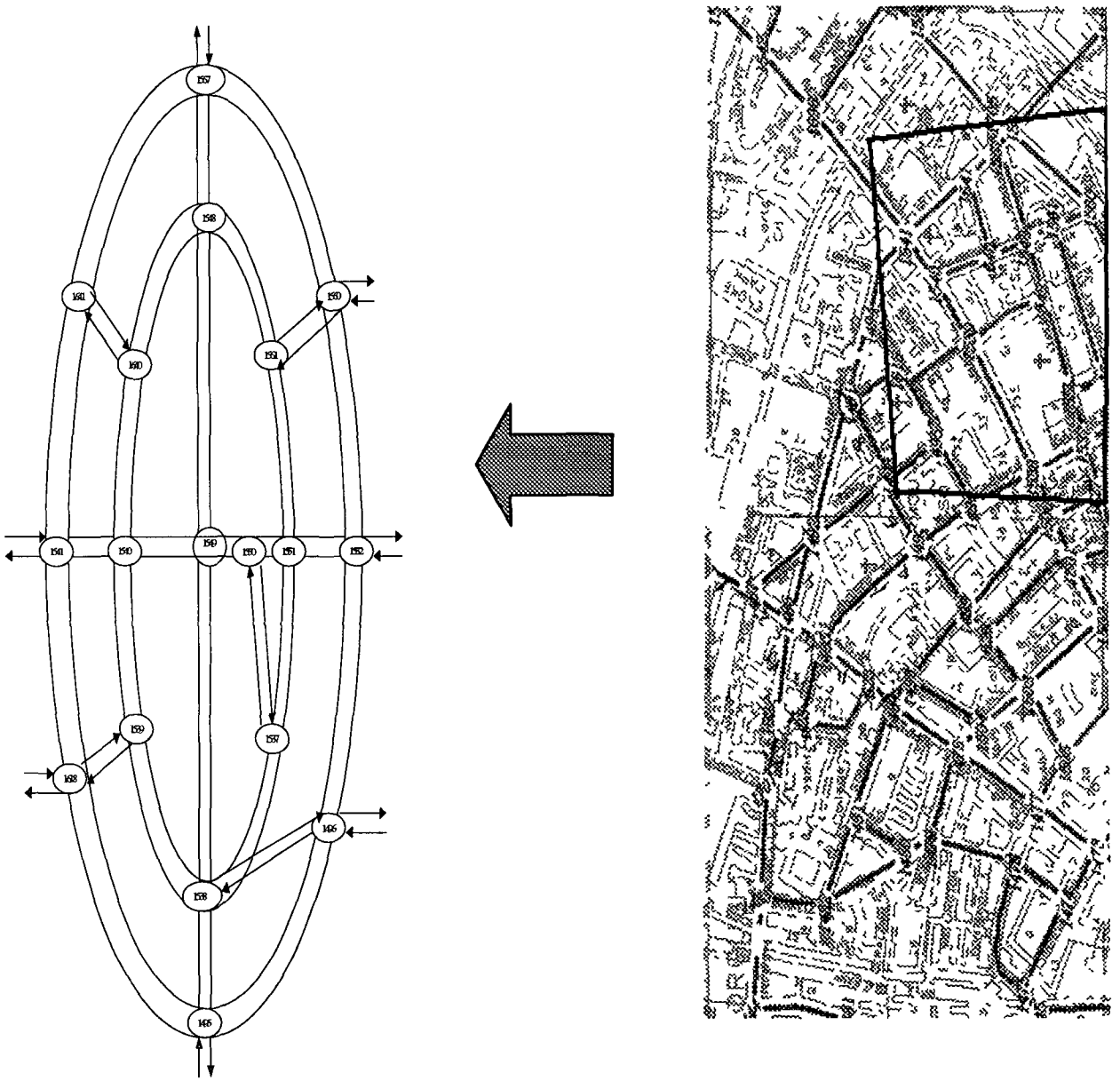

Fig (3 3) representation of a section of a real road network in Dublin by the proposed network geometry

Three deterministic traffic conditions were employed in our simulation of the number of cars passing an intersection or junction, (i) 25% turn left, 50% go straight, 25% turn right and (ii) 20% turn left, 60% go straight, 20% turn right, and (iii)12% turn left, 76% go straight, 12% turn right These conditions apply at all intersections where all three movements are allowed, and reduce to 50%-50% at junctions with two movements only

3.1.6 Traffic parameters

In this chapter we also extend the definition for the traffic parameters, density, flow, and velocity, to the network level

Network velocity is obtained at every time step as the ratio of the total number of moving vehicles, inside the network, to the total number of vehicles *Network density* is also calculated at every time step as the ratio of the total number of vehicles, inside the network, to the total number of sites

The corresponding *network flow*, at every time step, is calculated using the relation *Network flow = Network velocity * network density*

Since the density varies dramatically with time in dynamic traffic networks, the simulation time is split into intervals, which corresponds to observation periods The user can set the interval length and different values have been applied in our simulations This is because the interval length, as we will see later, has a significant effect on the traffic parameters The choice of the interval length turned out to be influenced by the dominant traffic regime, free or dense The time dependent density, velocity and flow are examined by taking averages every 30-150 time step throughout the simulation run

3.2 Description of Simulation Experiments

It is the aim of this chapter to investigate and study the behaviour of urban traffic networks and to characterise their performance using the proposed simple Cellular Automaton model

In this section, our purpose is to study the physical and operational features of the simulated network through the analysis of the fundamental diagrams, for relations such as density vs flow and density vs velocity

In general the following factors may influence the network performance

i *car arrivals to the network (at fixed or stochastic rate)*

ii *the number of the entry/ exit nodes*

iii *traffic conditions at intersections*

iv *network geometry*

v *external parameters such as weather conditions, different road conditions, different motivations for the drivers*

Vehicles were randomly distributed along the network, then thy generated at random and input into the network through all nodes of entry In our simulated traffic, vehicles did not have " Knowledge" about their complete path along the network, but only about their next time step movement Network nodes can be classified as entry/exit nodes, T-junction nodes and intersection nodes

In the following simulations four different networks were considered, whose radii varied from r=3,(8 Km length for a network of 17 nodes and 28 links), to r=6,(24 Km length for a network of 41 nodes and up to 76links) Each link is a two-lane carriageway

A stochastic feeding mechanism, see Appendix (C), in which car arrivals follow a Poisson Process, was implemented, (using different rates of arrivals), throughout the simulation experiments It is also assumed that the network neighbourhood can take any number of vehicles that might leave the network Traffic conditions may also affect the network performance For example if we increase the probabilities for turning left or right, then network density will increase, since the number of vehicles circulating inside the network will increases relative to those leaving it

In this chapter we do not consider varied network geometry, but assume a simple geometry for our simulated network throughout, keeping the number of the entry/exits are constant

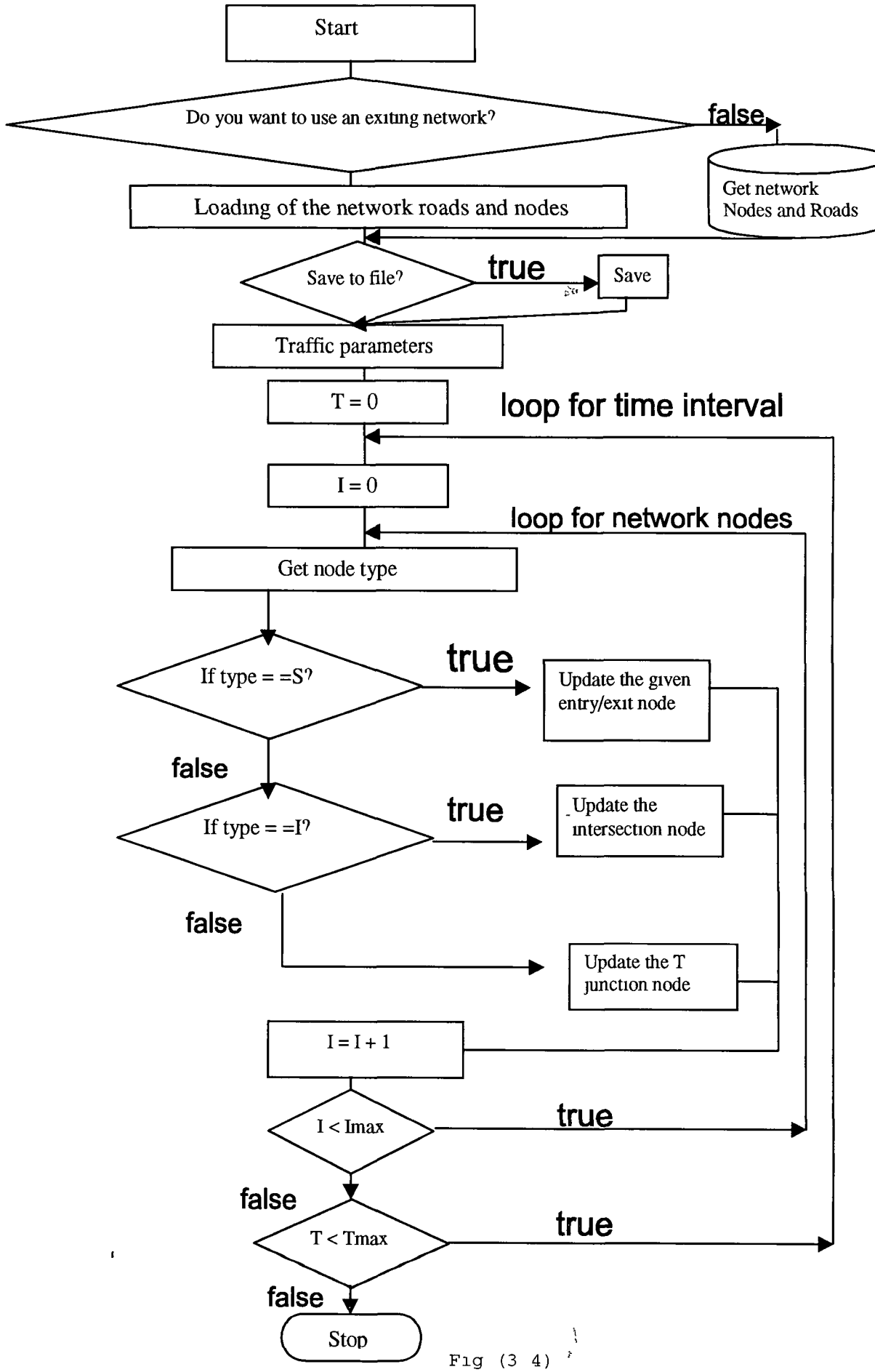
Start
Do you want to use an exiting network?
false
Get network Nodes and Roads
Loading of the network roads and nodes
Save to file?
true
Save
Traffic parameters
T = 0
loop for time interval
I = 0
loop for network nodes
Get node type
If type = =S?
true
Update the given entry/exit node
false
If type = =I?
true
Update the intersection node
false
Update the T junction node
I = I + 1
I < Imax
true
false
T < Tmax
true
false
Stop

Fig (3 4)

3.3 Simulation and Results

Using a stochastic feeding mechanism, the main factors in the following experiments are

i *arrival rate* ii *traffic conditions*

iii *interval length* iv *transient period*

In this Chapter, we consider only the transient movement of the cars along the network, whereas, in Chapter 4 we allow cars to park inside the network, so that they are temporarily lost to the flow

In the following simulation each run consists of 5000 iterations *Network parameters* are calculated every 30- 150 time steps after a discard period of 200-500 time steps with traffic conditions applied as in section (3 1 5) and using different arrival rates A summary of the simulation outputs can be found in Appendix B, Tables (B 1-B 4) We start by looking at the effect of the arrival rate, μ, on the traffic behaviour along the network

3.3.1 The effect of the arrival rate on the network parameters

3.3.1.1 The existence of jamming threshold

Fig (3 5) shows the number of cars passing through the network for a 17-node network, together with the number of cars waiting outside Arrival rate (μ) varies between 0 1 and 0 6 It is easy to observe the "*jamming threshold*" *for μ greater than the critical value μ ≅ 0 25 the network is not able to cope with the traffic, which has results in long queues outside*

The simulation also reveals that the critical arrival rate μ is independent of the network size (Fig (3 6)), where the network size has extended from 17 nodes up to 25 nodes, 33 nodes and 41 nodes, and also the traffic conditions, Fig (3 7)

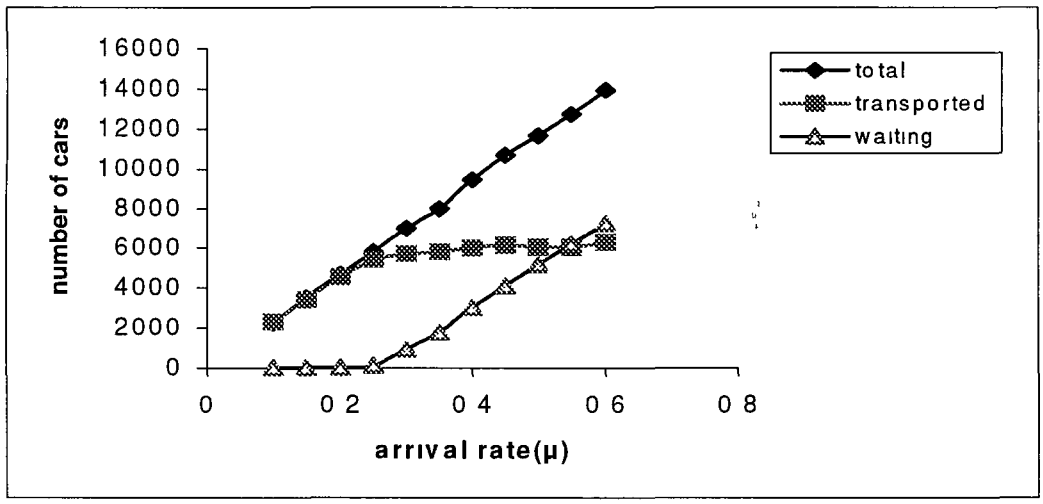

Fig (3 5) Number of cars vs arrival rate relation for a 17 node network and turning percentages 20% left, 60% through, and 20% right

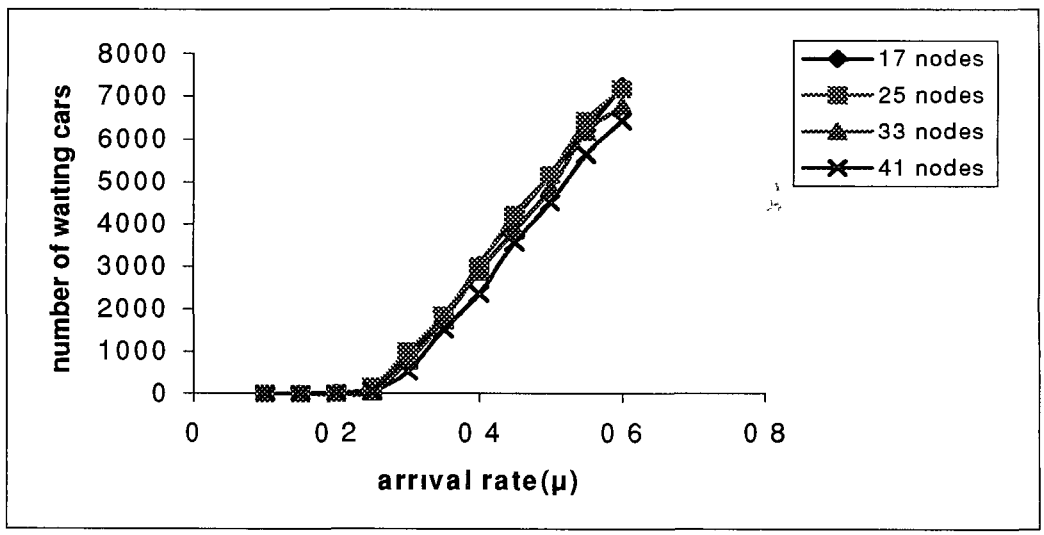

Fig (3 6) Waiting cars vs arrival rate for four different networks, and turning percentages 20% left, 60% through, and 20% right

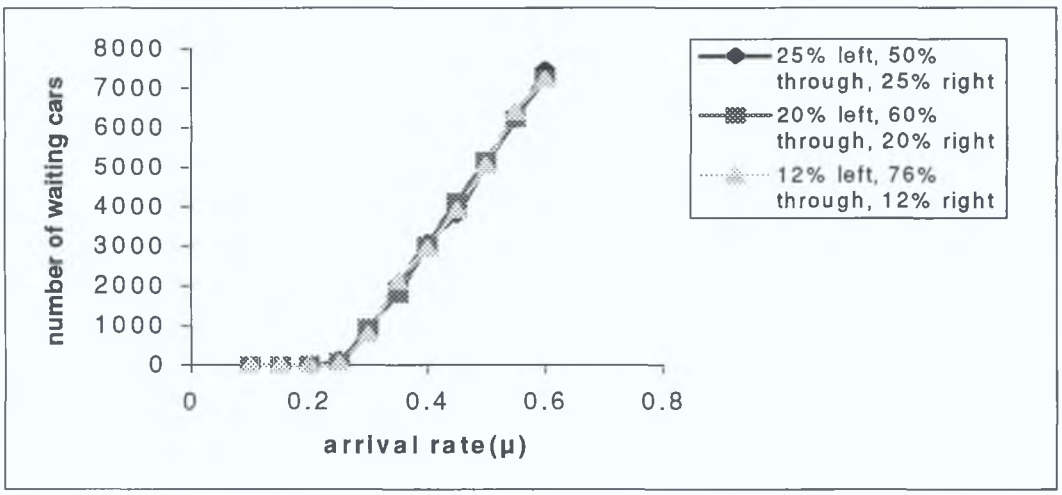

Fig.(3.7): Waiting cars vs arrival rate for various traffic conditions

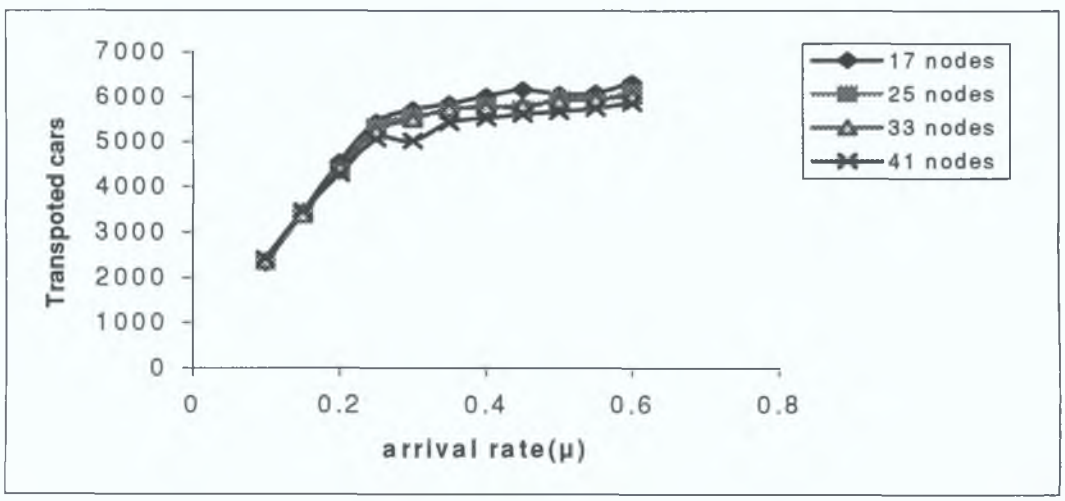

Fig.(3.8): Transported cars vs arrival rate for different size networks and turning percentages are:25% left, 50% through, and 25% right

It is however, worth noting that the number of cars transported through the network is affected by the network size, especially for μ greater than the critical value $\mu \equiv 0.25$, Fig (3.8), this is obtained for different network sizes;17, 25, 33, and 41 nodes.

This graph also suggests that the number of cars transported via small size networks is greater than those transported via larger size networks This is due to the increment of the traffic lights number, i e more delay at intersections, and also car path through the network becomes longer

3.3.1.2 Arrival rate vs Network size

In the next simulation runs we start by changing the arrival rate and keeping other factors the same, where different network sizes were used The output parameters, flow, density, and velocity, are averaged every 30-time steps after a discard period of 200-time steps to let transience die out

Performance Measure	Arrival rate	17 nodes	41 nodes
Max Flow	μ = 0.1	0.14892	0 123815
	μ = 0.3	0.247978	0.236816
	μ = 0.55	0.250189	0.236763
Density of Max Flow	μ = 0 1	0 180459	0 143406
	μ = 0 3	0 482386	0 430268
	μ = 0 55	0 414131	0 494114
Transported cars	μ = 0 1	2748	2430
	μ = 0.3	5917	5371
	μ = 0 55	6215	5810
Queue Length	μ = 0 1	3	3
	μ = 0 3	808	552
	μ = 0 55	6063	5769

Table (3 1) The influence of varying the parameter μ on the maximum flow and its density, cars transported via the network and the queue length outside it for different size networks

At all intersections the traffic conditions, as in Sec (3 1 5) case (ii), were applied The fundamental diagrams, presented in Figs (3 9) describe the flow behaviour for two different network sizes, 17 nodes and 41 nodes

The effect of changing the arrival rate (μ) can be summarised as follows

i A higher flow was obtained in the case of smaller size network and this was obtained for different values of μ, see Table (3 1) The table also shows that increasing the arrival rate from $\mu = 0\ 1$ to $\mu = 0\ 3$ has significantly increased the maximum flow (an increment of 66% was observed for the smaller network and 91% for the larger network) However, when μ was greater than the *"jamming threshold"* the flow behaviour was very similar, irrespective of the network size Statistical analysis, presented in Appendix A (Table (A 2)), reveals that the arrival rate strongly influences the flow, with a significant interaction with the network size at $\alpha = 0\ 01$ level of significance

ii Also Table(3 1) shows that the maximum flow occurred at much higher density when a high rate of arrival was used to inject the network with cars

iii Cars transported through the simulated network are influenced by both network size and arrival rate The number of the transported cars increases significantly when μ increases from 0 1 to 0 3 and this increment becomes less significant at high rate of arrivals ($\mu = 0\ 55$)

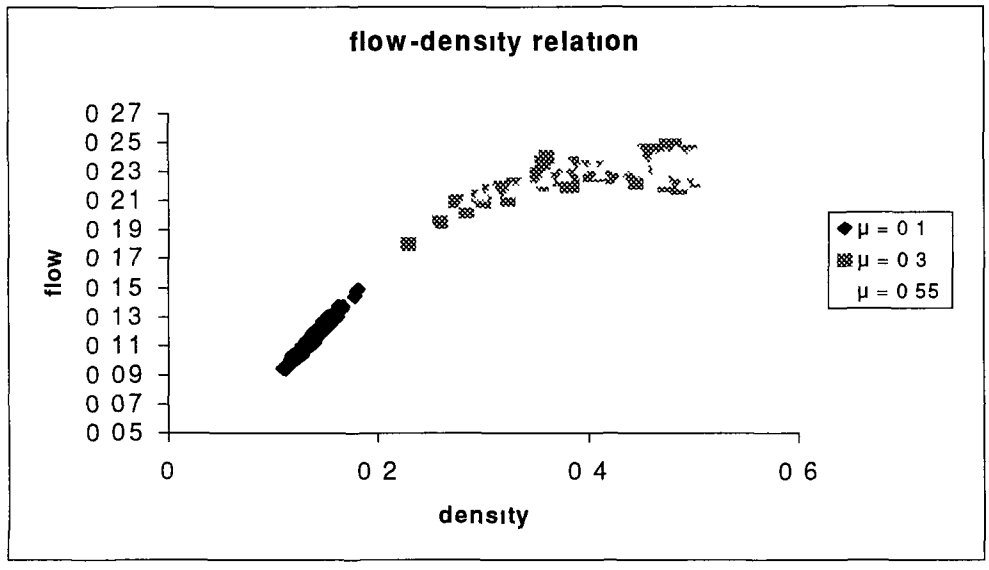

(a) Flow-density relation for a 17 nodes network using various arrival rates and the turning percentages 25% left, 50% through, and 25% right

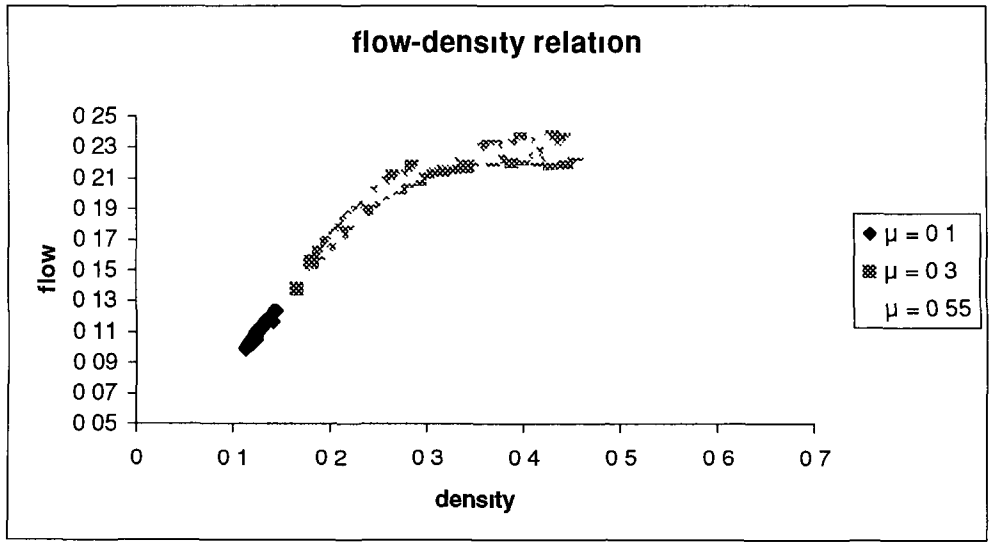

(b) Flow-density relation for a 41-node network using various arrivals rates with turning percentages are 25% left, 50% through, and 25% right

Fig (3 9)

It can be seen from Table (3 1) that cars transported via the network was much higher in the case of smaller networks irrespective of the values of μ as seen in Fig (3 8)

iv As the value of μ increases the "*jamming threshold*", a well known Macroscopic phenomena "Queues outside the networks" will occur Our simulation reveals that the queue length increased significantly as the arrival rate increased from μ = 0 3 to μ = 0 55 with the queue length longer in the case of smaller networks

The effect of varying the network size can also be seen from Fig (3 10), which shows the velocity-density relation for two different networks using a stochastic feeding mechanism, (in which car arrivals follow a Poisson process with μ = 0 55) Also, Fig (3 10) shows that the maximum velocity obtained in the case of larger size network is greater than the maximum velocity obtained for the smaller size network

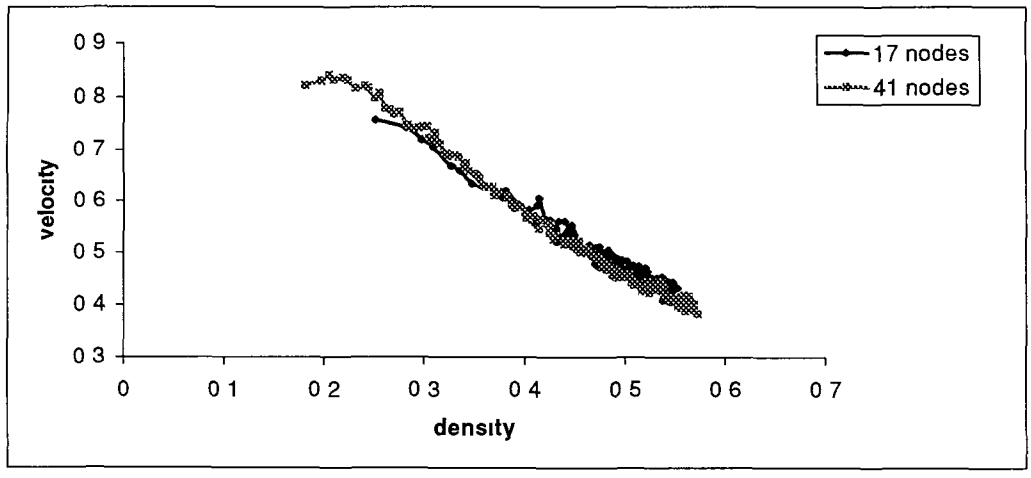

Fig (3 10): Velocity-density relation for two different networks using arrival rate of 0 55 and same traffic conditions in Fig(3 9)

3.3.2 Varying of Traffic Conditions

Two different sets of traffic conditions were applied, (i) 25% turn left, 50% go straight, 25% turn right and (ii) 12% turn left, 76% go straight, 12% turn right The influence of changing the traffic conditions on some of the network performance measures are presented in Tables (3 2) and (3 3) Also, in Fig (3 11), we present the fundamental diagrams for four different networks, applying two different traffic conditions using a moderate arrival rate $\mu = 0\ 3$ By comparing Tables (3 2) and (3 3) and studying the flow-density relations in fig (3 11), we make the following observations

i The network maximum flow was increased by increasing the headway traffic percentages from 0 50% to 0 76% and this increment was obtained for arrival rates ($\mu = 0\ 3, 0\ 55$) Also, Fig (3.11) shows that the effect of increasing the headway traffic percentages was more noticeable in the case of smaller size networks Statistical analysis, presented in Appendix A (Table (A 1)), shows a significant effect of the traffic conditions on the flow at low and high arrival rates at $\alpha =$ 0 01 level of significance Also, the analysis reveals a significant interaction between the network size and traffic conditions, using low μ, at the same level of significance

ii The change in the traffic conditions also affected the number of cars transported through the networks Tables (3 2) and (3.3) shows that for higher arrival rates, $\mu = 0\ 3, 0\ 55$.

Increasing the headway traffic percentages has decreased the cars transported through the network and this could be seen clearly in the case of smaller sized networks This is because the probability for a car to use the main roads rather than the sub-roads increases by increasing the headway traffic, which, in turn, affect the number of cars entering the network

iii The simulations also reveal an important role for traffic conditions on the queue length outside the simulated networks For smaller size networks, increasing the headway traffic percentages increased the queue length and this increment became more noticeable at higher arrival rates This is because the system density changes rapidly, increasing with every increment of μ

As the network becomes more congested, the turning percentages play an important role at the entry and exit nodes So, by increasing the headway traffic, cars tended to queue longer rather than go straight through In contrast, by increasing the network size, the network was able to cope with the incoming traffic until much latter in the simulation Hence the turning percentages were more effective for a longer period and the queue length decreased as we increased the headway traffic percentages

Performance Measure	Traffic Conditions	17 Nodes	33 Nodes	41 Nodes
Max Flow	25%, 50%, 25%	0 247978	0.2334	0.236816
	12%, 76%, 12%	0.260762	0.241085	0.245792
Density of Maxim Flow	25%, 50%, 25%	0.482386	0.419332	0.430268
	12%, 76%, 12%	0.455271	0.439291	0.459454
Transported Cars	25%, 50%, 25%	5917	5740	5351
	12%, 76%, 12%	5781	5467	5314
Queue Length	25%, 50%, 25%	808	739	552
	12%, 76%, 12%	847	672	400

Table (3 2) The Table shows the network parameters, maximum flow and its density, cars transported via the network and the queue length outside it, obtained using different traffic conditions and μ=0 3

Performance Measure	Traffic Conditions	17 Nodes	33 Nodes	41 Nodes
Max Flow	25%, 50%, 25%	0.250189	0.236959	0.236763
	12%, 76%, 12%	0.261315	0.242875	0.250523
Density of Maxim Flow	25%, 50%, 25%	0.414131	0.433432	0.494114
	12%, 76%, 12%	0.453458	0.458928	0.426943
Transported Cars	25%, 50%, 25%	6355	5989	5810
	12%, 76%, 12%	6215	5796	5740
Queue Length	25%, 50%, 25%	6063	5854	5769
	12%, 76%, 12%	6292	5744	5700

Table (3 3) The table contents are the same as in Table (2), but using higher arrival rate (μ=0 55)

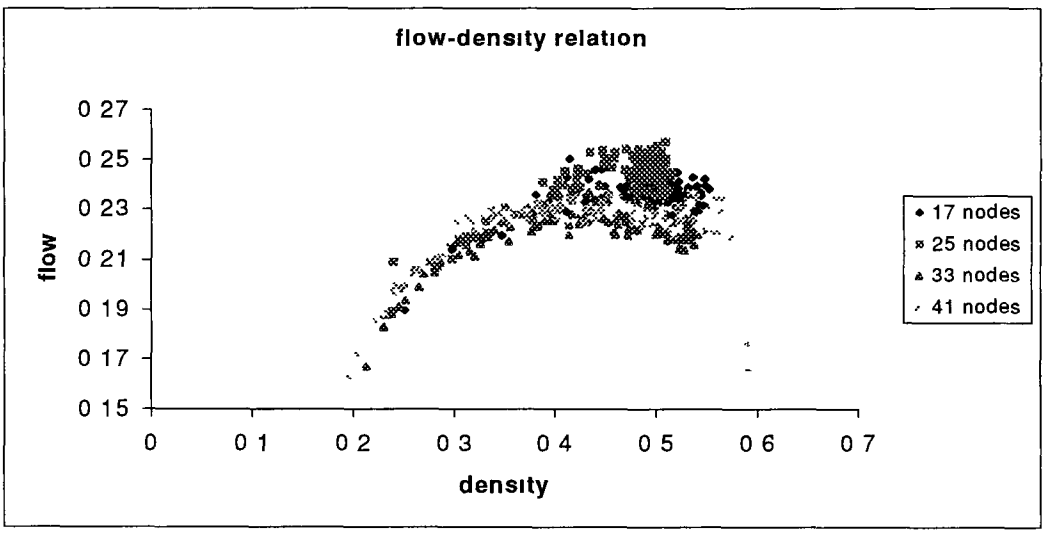

(a)

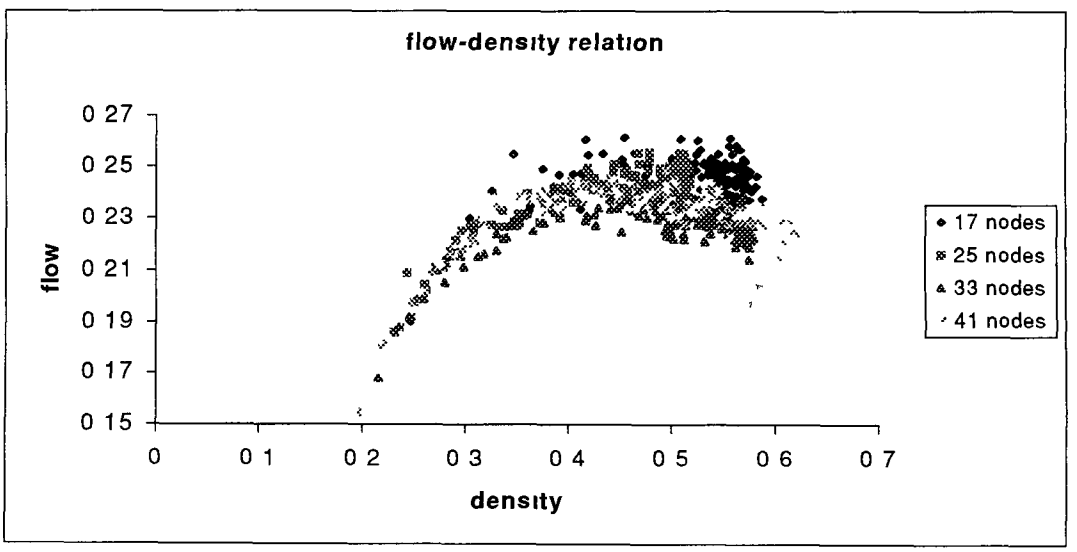

(b)

Fig (3.11). Flow-density relation using two different traffic conditions

(a) 25% left, 50% through, and 25% right and

(b) 12% left, 76% through, and 12% right

3.3.3 Time-interval Based Network Simulation

In order to observe the changes in the traffic behaviour throughout the simulation run, our simulation results were averaged over two different time-intervals

To quantify the effect of the time-interval, (interval length), on these averages, simulations were carried out using two lengths, 30 and 150 time steps (short-term and long-term averages respectively)

The output values of the traffic parameters for duration period of 600 time steps, after a discard period of 200 time steps, applying a low arrival rate for two different networks are presented in Tables (3 4) and (3 5)

Tables (3 6) and (3 7), on the other hand, present similar outputs, but with a higher arrival rate (μ=0 3) From studying these output averaged values, we make the following comments

1 Tables (3 4) and (3 5), which compare traffic parameters that gathered using both short-term and long-term averages at low μ, demonstrate the following

As long as the free traffic was dominant there were no significant changes in the *network density* and consequently, in the *network flow*

This can be seen from Table (3 4), where the changes in the *network density* did not exceed 0 0148 during the short-term averages and 0 013 over the long-term averages

As a consequence of this traffic pattern, increasing the number of data points or averaged values will not give a better idea of the fundamental diagrams,(flow-density relation here).

Short-term averages			Long-term averages		
velocity	density	flow	velocity	density	flow
0 863204	0 148	0 1278			
0 855269	0.1419	0 1214			
0 879504	0.1465	0 1288			
0 868557	0.1405	0 1220			
0 869728	0.1457	0.1267	0 888803	0.1306	0.116
0 870116	0.1464	0 1274			
0 86928	0.1476	0 1283			
0 861815	0.1424	0 1227			
0 853949	0.1392	0 1188			
0 867702	0.1378	0.1195	0 88667	0 1383	0.1226
0 862757	0.1427	0 1231			
0 872121	0.1471	0 1283			
0 862006	0 144	0 1241			
0 855352	0.1463	0 1252			
0 870685	0 1459	0.127	0 883948	0.1436	0.1269
0 876735	0.1423	0 1248			
0 850307	0.1393	0 1185			
0 868917	0.1401	0 1217			
0 863169	0.1399	0 1207			
0 871927	0.1332	0.1162	0 894586	0 1383	0.1238

Table (3 4): Sample of the simulation outputs for 600 time steps for a network of size 25 nodes at low arrival rate μ = 0 1

Short-term averages			Long-term averages		
velocity	density	Flow	velocity	density	flow
0 862791	0.1390	0 1199			
0 870016	0.1384	0 1205			
0 867203	0.1393	0.1208			
0 879202	0.134	0 1178			
0 873163	0.1364	0.1191	0 893192	0.1415	0 1264
0 875453	0.1331	0 1165			
0 866876	0.1356	0 1175			
0 860863	0.1354	0.1166			
0 863462	0.1356	0.1171			
0 866894	0.1345	0.1166	0 893607	0.1393	0 1245
0 857361	0.1315	0 1128			
0 877931	0.1334	0 1172			
0 878355	0 1315	0.1155			
0 866478	0 1318	0.1142			
0 872744	0.1315	0 1147	0 888003	0.1384	0 1229
0 880963	0.1301	0 1146			
0 876164	0.1272	0 1115			
0 871459	0.1266	0.1103			
0 871158	0.1272	0.1108			
0 8788	0.1293	0 1136	0 902559	0 1391	0 1256

Table (3 5) Same as Table (3 4), but for a larger network (41 nodes)

This was more noticeable in the case of large sized (Table (3.5)) networks, with smaller changes in the *network density*, (0.0127, 0.0035), during short-term averages and long-term averages respectively. This result in very small changes in the *network flow*, (0.0105, 0.0035), over short-term and long-term averages respectively

The statistical analysis in Appendix A (Table (A.1)) supports our findings and reveals that the interval length does not have a significant effect, at $\alpha = 0.01$ level of significance, on the network flow at low arrival rate. However, a significant interaction between the network size and the interval length at the same level of significance was obtained.

ii. When a higher arrival rate was used to feed the simulated networks, the network density increased rapidly especially in the case of smaller size networks. Everyday observations confirm that as long as the dense traffic is dominant, only small changes (increment or decrement) in the network density and in turn its flow can be obtained.

The simulation results presented in Tables (3.6) and (3.7) shows that small changes in flow behaviour, (i.e. flow-density relation), can be observed when short-term averages were used to describe the traffic behaviour, because this will generate more data points throughout the simulation run. In contrast using long-term averages has minimized the number of the data points, which describe the flow behaviour, and in turn small changes in the flow behaviour can not be observed. This can be seen also in Fig (3.12). The statistical analysis, presented in Appendix A (Table (A.1)), also reveals a significant role for the

interval length at higher rate of arrivals at $\alpha = 0.01$ level of significance

The simulations suggest that, for congested traffic, the smaller the interval length the better in order to observe small changes in the traffic behaviour through the network

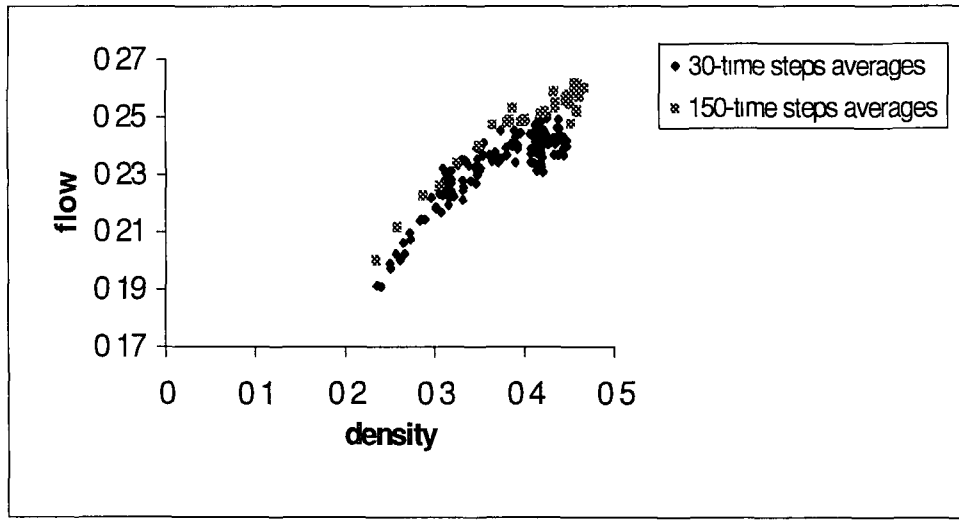

Fig (3.12) Flow-density relation for a network of size 25 nodes using $\mu = 0.3$ and the turning percentages 25%, 50%, 25%

Short-term averages			Long-term averages		
velocity	density	flow	velocity	density	flow
0.810784	0.2358	0.1912			
0.797033	0.2395	0.1909			
0.798958	0.249	0.1989			
0.799456	0.249	0.1991			
0.787616	0.2506	0.1974	0.81997	0.2579	0.2115
0.789998	0.2562	0.2024			
0.768539	0.2607	0.2004			
0.760912	0.2661	0.2025			
0.780104	0.2646	0.2064			
0.771537	0.2714	0.2094	0.775212	0.2873	0.2227
0.759717	0.2732	0.2075			
0.753567	0.2835	0.2137			
0.754227	0.284	0.2142			
0.740113	0.2896	0.2144			
0.747635	0.2966	0.2217	0.742689	0.3047	0.2263
0.726546	0.3005	0.2183			
0.724729	0.3007	0.2179			
0.729201	0.3059	0.223			
0.751688	0.3089	0.2322			
0.732638	0.3072	0.2251	0.722203	0.3242	0.2341

Table (3.6): Sample of the simulation outputs for 600 time steps for a network of size 25 nodes, $0.\mu = 0.3$

Short-term averages			Long-term averages		
velocity	density	Flow	velocity	density	flow
0.847112	0.1984	0.1681			
0.83655	0.2057	0.1721			
0.833052	0.2086	0.1738			
0.829258	0.2122	0.176			
0.832169	0.2173	0.1809	0.852978	0.2178	0.1858
0.832335	0.2199	0.183			
0.826608	0.2232	0.1845			
0.821905	0.2286	0.1879			
0.8083	0.2354	0.1903			
0.803471	0.2374	0.1908	0.833971	0.241	0.201
0.805983	0.2422	0.1952			
0.802133	0.2445	0.1961			
0.799815	0.245	0.196			
0.804715	0.249	0.2004			
0.788325	0.2549	0.201	0.809594	0.2606	0.211
0.780426	0.2588	0.202			
0.787022	0.2582	0.2032			
0.791823	0.2616	0.2072			
0.794961	0.2652	0.2108			
0.773795	0.2651	0.2052	0.794252	0.2768	0.2198

Table (3.7): Same as Table (3.6), but for a network of size 41 nodes

3.3.4 The influence of Changing the Transient Period on Network Performance

Next we look at the effect of the transient period on the simulation output by using two different transient periods, 200 and 500 time steps In the following experiments, the traffic parameters were averaged every 30-time steps by applying the following traffic conditions as in case (i), Sec (3 1 5) for a duration of 5000 time steps using two different arrival rates (μ = 0 1 & μ = 0 55) This was carried out for two different network sizes, with radii r = 3,(17 node) & r = 6,(41 node)

The results of the above simulations were as follows

At first glance, Table (3 8) reveals that the effect of increasing the transient period from 200 to 500 time steps has no significant influence on the maximum flow obtained at both rates of arrivals, no matter what network size is used in the simulation This is because no significance changes in the maximum flow occurred, for either network, or for either μ

Performance Measure	Network size	μ = 0 1		μ = 0 55	
		Trans Pd = 200	Trans Pd = 500	Trans Pd = 200	Trans Pd = 500
Maximum Flow	17 nodes	0.14892	0.141146	0.250189	0.247644
	41 nodes	0 123815	0 11531	0 236763	0 238576
Density of Max Flow	17 nodes	0.180459	0.168032	0.414131	0 528179
	41 nodes	0 143406	0 131372	0 494114	0 490861

Table (3 8) The influence of changing the transient period on the maximum flow and its density, using different values for μ and traffic conditions 25% left, 50% through, 25% right

On the other hand, statistical analysis presented in Appendix A (Table(A 1)) shows the significant influence of the transient period on the network flow at both rates of arrivals

A closer look at Table (3 8) shows the influence of transient period on the maximum flow as the statistical analysis confirms

This can be demonstrated as follows

Since no significance changes were observed in the maximum flow for either length of transient period, the increment of the transient period has not correctly reproduced the density of maximum flow This is more noticeable in the case of smaller size network at higher μ

Fig (3 13) shows how the fundamental diagrams are affected by the length of transient period, especially for smaller networks The effect of changing the transient period for different traffic conditions was also noted (Table (3 9))

Performance Measure	Network size	μ = 0 1		μ = 0 55	
		Trans Pd = 200	Trans Pd = 500	Trans Pd = 200	Trans Pd = 500
Maximum Flow	17 nodes	0.132537	0.133296	0.261315	0.264442
	41 nodes	0 137141	0 122812	0 250523	0 250281
Density of Max Flow	17 nodes	0.15784	0 154583	0 453458	0 504902
	41 nodes	0 157631	0 139498	0 426943	0 415698

Table (3 9): The influence of changing the transient period on the maximum flow and its density, using different values for μ and traffic conditions 12% left, 76% through, 12% right

The simulation reveals that using 200-time steps as a discard period is good enough to let the transience die out, where the largest road segment in our simulated networks did not exceed 60 sites, Fig (3 13)

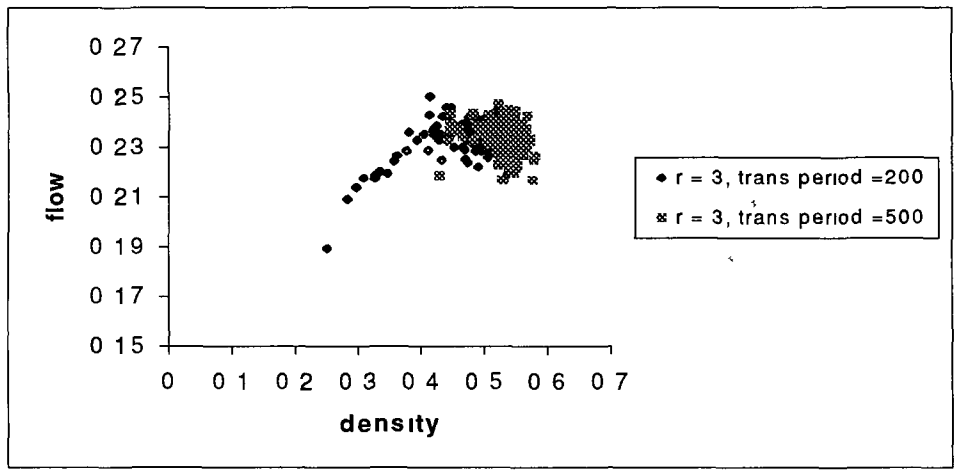

(a)

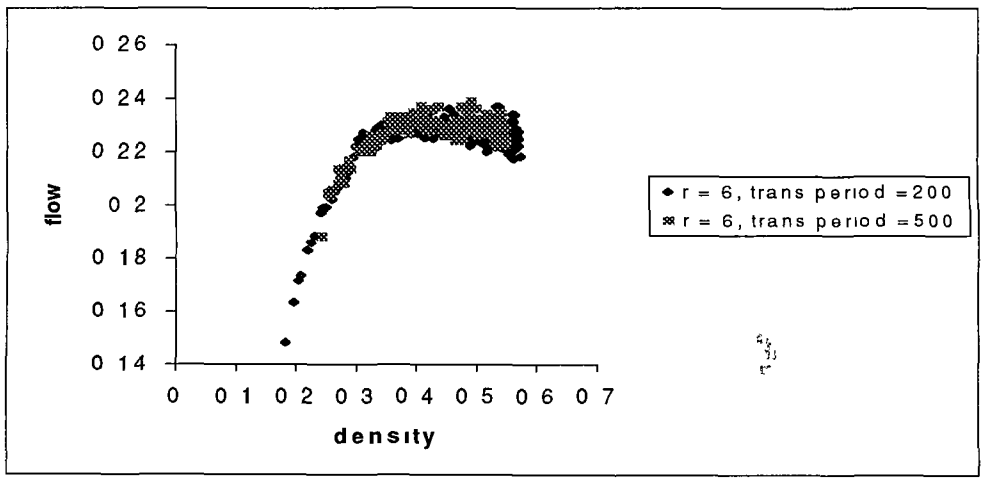

(b)

Fig (3 13) Flow-density relation using the traffic conditions of 25% left, 50% through, and 25% right and arrival rate of 0 55

(a) for a 17 node network

(b) for a 41 node network

3.4. Summary and Concluding Comments

In this chapter we moved from single lane traffic flow towards road networks Different network sizes have been tested, where all nodes were controlled by traffic lights and the signal operating conditions were assumed to be pre-timed signal Various traffic conditions were considered at the network junctions A stochastic feeding mechanism, in which car arrivals follow a Poisson process with parameter μ, has been implemented throughout the simulations using different values for the parameter μ

The work presented in this chapter suggests that parameters governing performance of urban networks may be investigated in some detail using the simple cellular automata Models

The results obtained in this chapter indicate the following

- It appears that there is a critical arrival rate *"jamming threshold"* above which the transportation through the network is not efficient any more and this rate is independent of the network size
- In a free traffic regime, the traffic conditions, defined in Sec(3 1 5), seem to involve significant interaction with network size,(α = 0 01), but for dense traffic this interaction was not significant
- The arrival rate is the principal factor of importance for larger networks A significant interaction,(α = 0 01), also exists between the arrival rate and the network size

- The simulation also reveals that the interval length used to gather the traffic parameters, average velocity, density, and flow, has a significant role,(α = 0 01), on the flow rate at higher arrival rate A significant interaction between the network size and the interval length was obtained at α = 0 01 level of significance The simulation reveals that the smaller the interval length the better, in order to calculate the traffic parameters
- The length of the transient period, warm up period, also has influenced the traffic parameters at both, low and high, arrival rate, where using 200-time steps as a transient period was good enough to let the transience die out A significant interaction (α = 0 01) between the transient period and the network size obtained at low arrival rate

Chapter 4

"Network Performance under Various Traffic Events"

4.0 Introduction

In Chapter 3, we were concerned "only" with the transient features of vehicle movements in simulating passage through the network under sustained flow

In this chapter, we investigate the traffic behaviour along the network with loss to flow Four underground parks, each of capacity up to 300 cars, were introduced in order to examine the effect on the transient behaviour of the system In the following experiments, each simulation run consists of 5000 time steps After a discard period of 200-time steps, short-term averages were used to gather the output parameters, flow, density, velocity, input of cars to the network, output of cars of the network, and the queue length outside each entry/exit node The turning percentages were 25% left, 50% through, 25% right These simulations were performed for two networks of different sizes, 17 and 41 nodes Each simulation run was divided into two stages In the first stage (1000-3000 time steps) vehicles may enter the underground parks at fixed or stochastic rate, while in the second stage (3000-5000 time steps) they leave the underground parks, also by the same manner, and hence pass through the network

4.1 Loss to Flow Simulations

4.1.1 Simulation with Loss to Flow at Fixed Rate

In the following simulation a car may enter or leave the underground park with fixed probability (p = 0 5)

The most remarkable aspect of introducing these parks is a different "*jamming threshold*" for different network sizes, as can be seen from Fig (4 1)

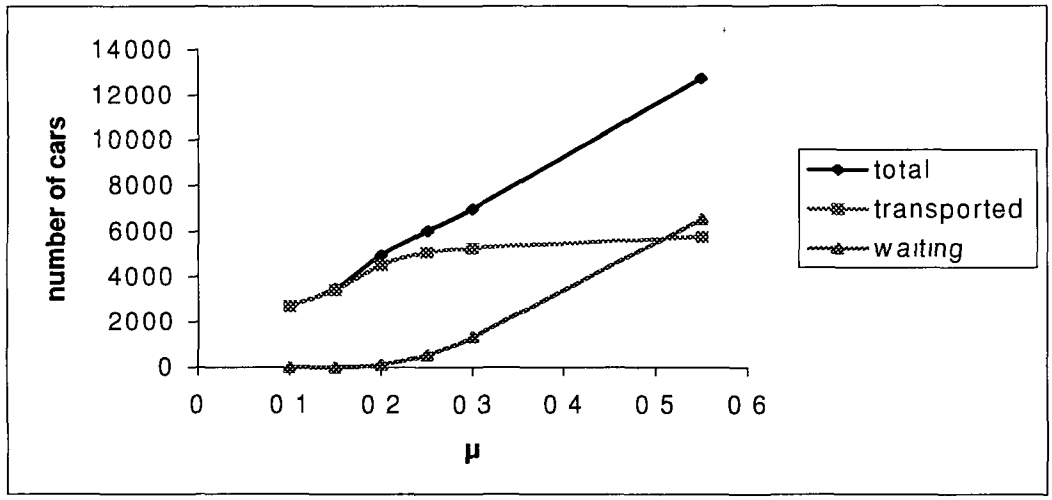

(a)

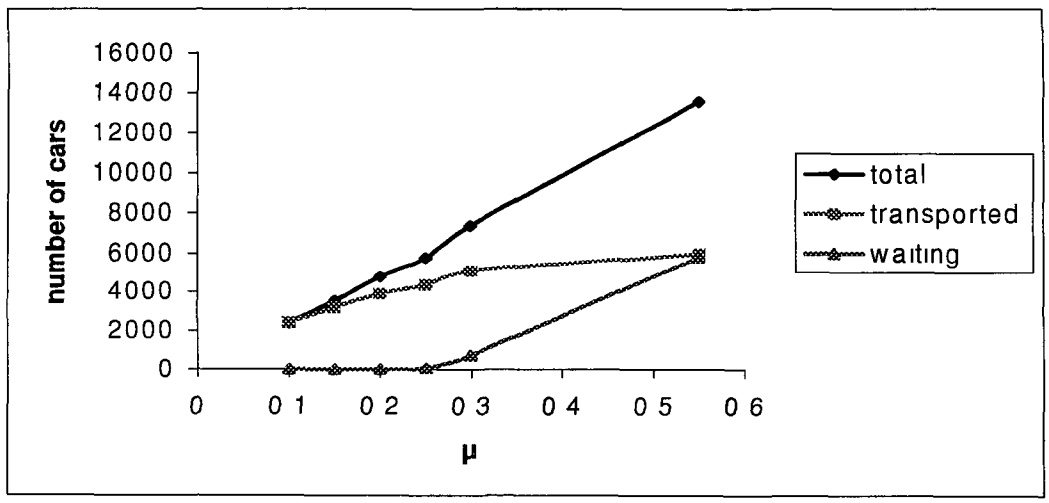

(b)

Fig(4.1) Number of cars vs arrival rate for

(a) 17 node network (b) 41 node network

By increasing the network size its ability to cope with the traffic improves, see (Fig (4 2)) This can also can be illustrated by studying the fundamental diagrams (Fig (4 3)) of one of the simulation runs, where $\mu = 0\ 3$ and the data were averaged every 30-time step after a discard period of 200 time steps

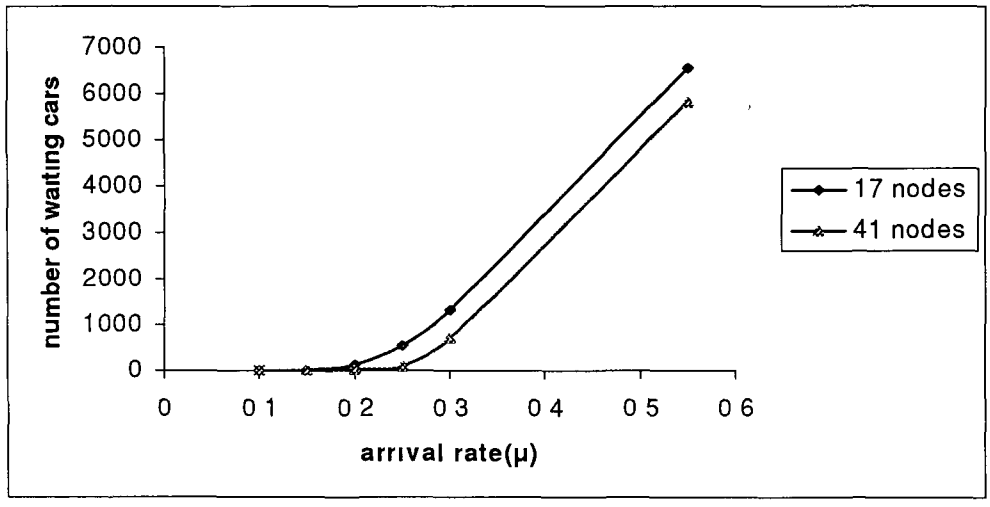

Fig (4 2) Number of waiting cars vs arrival rate for two different size networks

The first part of the flow-density relation, Fig(4 3 (a)), represents the free phase traffic, which is characterised by high velocities, see Fig(4 3 (b)), and low densities

By contrast the second part represents the jammed phase traffic, which lasts for a longer period in the case of small size network

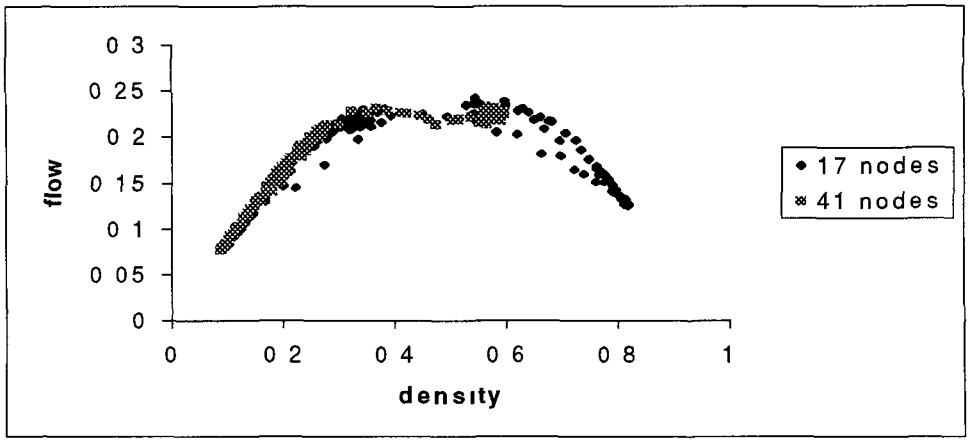
0 3
0 25
0 2
0 15
0 1
0 05
0
flow
0
0 2
0 4
0 6
0 8
1
density
17 nodes
41 nodes

(a)

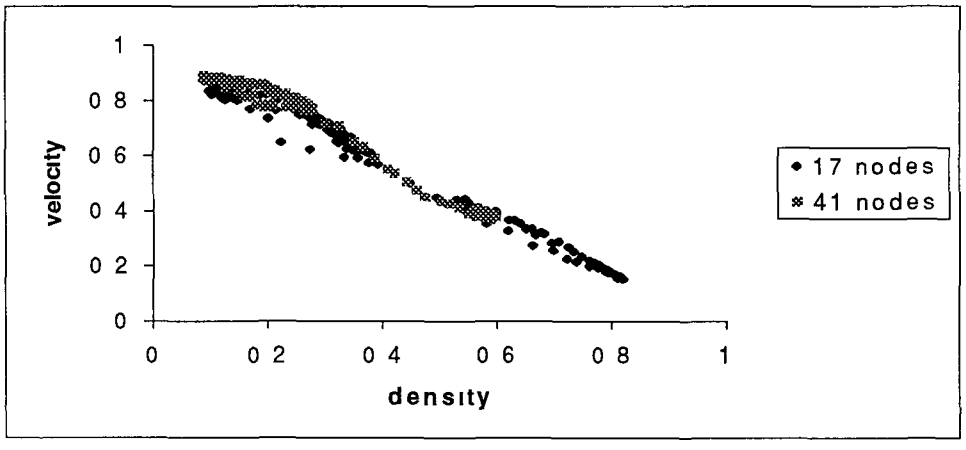
1
0 8
0 6
0 4
0 2
0
velocity
0
0 2
0 4
0 6
0 8
1
density
17 nodes
41 nodes

(b)

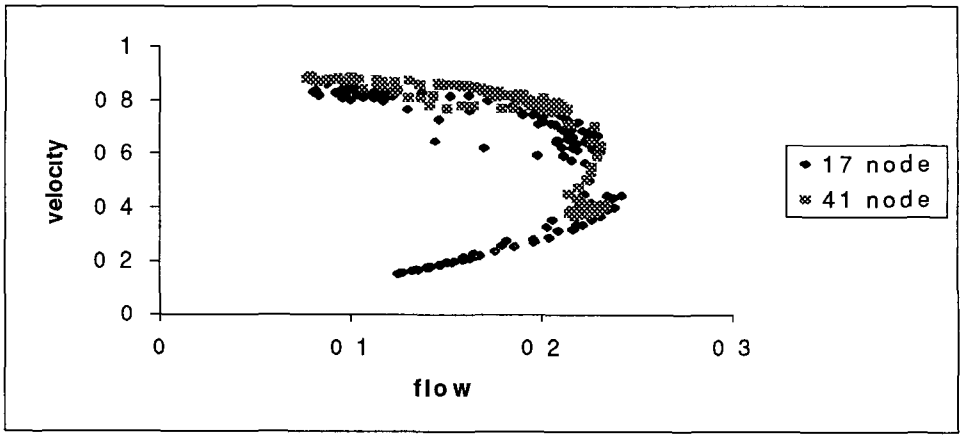
1
0 8
0 6
0 4
0 2
0
velocity
0
0 1
0 2
0 3
flow
17 node
41 node

(c)

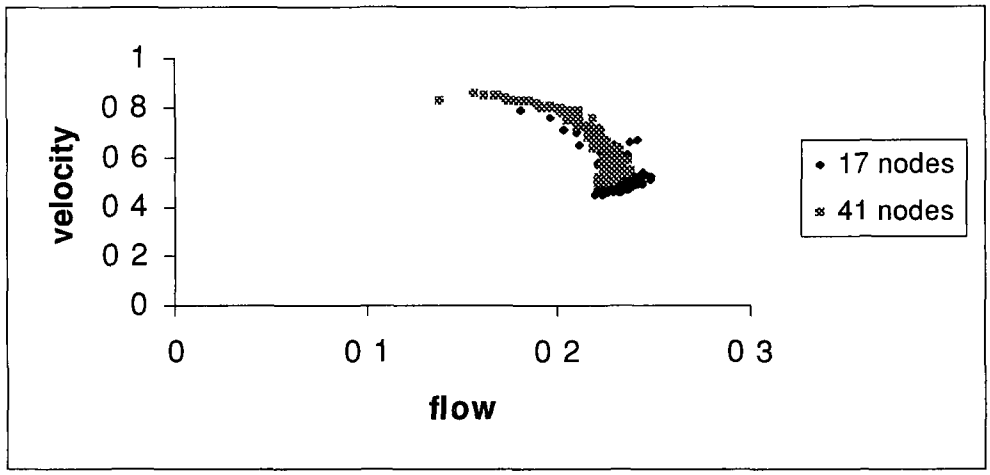

(d)

Fig (4.3) : The fundamental diagrams for simulation described above, where in

(a) flow-density relation, (b) velocity-density relation

(c) velocity-flow relation, (d)velocity-flow relation for the transient movement simulation, see Chapter 3

The above scenario can be explained as follows

Initial conditions of low density of cars and the application of arrival rate (μ = 0 3) did not much influence the network density, as long as vehicles may leave the network through the different exits and may also disappear into one of the underground parks This situation was dominant until the second stage of traffic movement when vehicles started to leave the underground parks, causing traffic jams to spread everywhere along the network due to the high density and low flow, characterised by decrease in network velocity, see Fig (4 3 (b)) This was more noticeable in the case of the smaller network, where the network density increases significantly from $\rho \sim$ 0 1, during the first stage, to $\rho \sim$ 0 81, within the second stage

In contrast the maximum network density obtained in the second stage for the larger network was ~ 0 6

These Figs (4 3 (a)) and (4 3 (b)) indicate strong similarities of the fundamental diagrams to those obtained for individual road sections when compared to those obtained in transient movement simulations (sec 2 3 1 1)

The flow vs velocity relations presented in Figs (4 3 (c)) and (4 3 (d)) show the variation of velocity with flow for the two types of simulation, simulation with loss to flow and transient movement simulation These figures may be compared and explained as follows

The upper parts of the fundamental diagrams represent the freely flowing traffic, where each car travels at the desired speed, which lasts for a longer period in the case of loss to flow systems

As the traffic becomes heavier the decrease in the average velocity begins slowly Then the continuous increase in the system density will lead to a continuous decrease in the average speed and, in turn, the average flow, which is more noticeable in the case of smaller network Also, this was more noticeable in the case of loss to flow systems as the density increases considerably due to the existence of the underground parks

4.2.1 Simulation with Loss to Flow at Stochastic Rate

In the next experiments, at every time step, within the specified periods for entering and leaving the underground parks, we assume that a car may enter or leave any of these parks according to a Poisson distribution with parameter μ1

Fig (4 4) shows that increasing the parameter μ1 from 0 1 to 0 3 has led to a lower values for the jamming threshold, which depends on the network size In the case of the smaller size network, the jamming threshold has decreased from 0 2 to ~ 0 18 and also the number waiting cars has increased

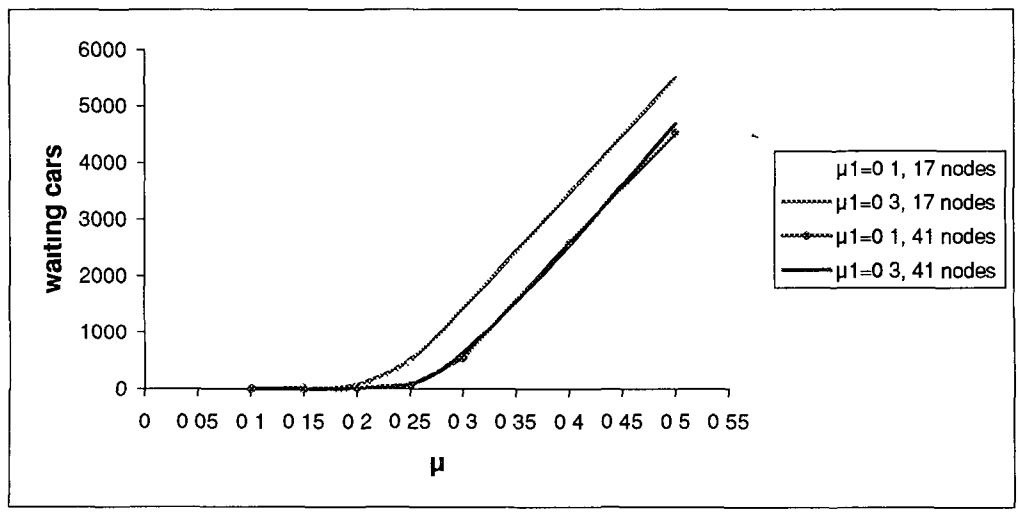

Fig.(4.4) : Number of waiting cars vs arrival rate for two different networks using different values for the parameter μ1

In contrast, using a larger size network has increased the *jamming threshold* up to 0 25 and also above the *jamming threshold* the number of waiting cars has decreased considerably compared to the smaller size network

In order to study the effect of varying the parameter $\mu 1$ on the network performance, in the following simulation we restrict ourselves to studying the behaviour of the system density over the simulation run As usual, in the next simulations each run was conducted up to 5000 time steps, then data were gathered every 30 time steps after a relaxation period of 200 time steps The turning percentages were 25% left, 50% go through, 25% right, this was performed for two different networks, 17 and 41 nodes, and using two arrival rates, $\mu = 0\ 15$ and $\mu = 0\ 5$

At low arrival rate ($\mu = 0\ 15$), Fig (4 5) demonstrates the influence of the parameter $\mu 1$ on the system density, both in (a) the system of size 17 nodes and in (b) the system of size 41 nodes

The simulation results can be summarised as follows

- Within the parking permitted period, (i e in the first stage of the simulation), increasing the parameter $\mu 1$ from 0 1 to 0 3 has increased the probability for a car to disappear into one of the parks This, in turn, has decreased the system density within this period and this was observed for both networks
- In contrast, the influence of increasing the parameter $\mu 1$ on the system density was more noticeable during the off-parking period (i e the second stage traffic) This increment has increased the probability for a car to leave the park, which, in turn, increased the outgoing traffic from the parks within a small time-interval As a consequence of this dynamic, the system density responds rapidly, i e is considerably increased

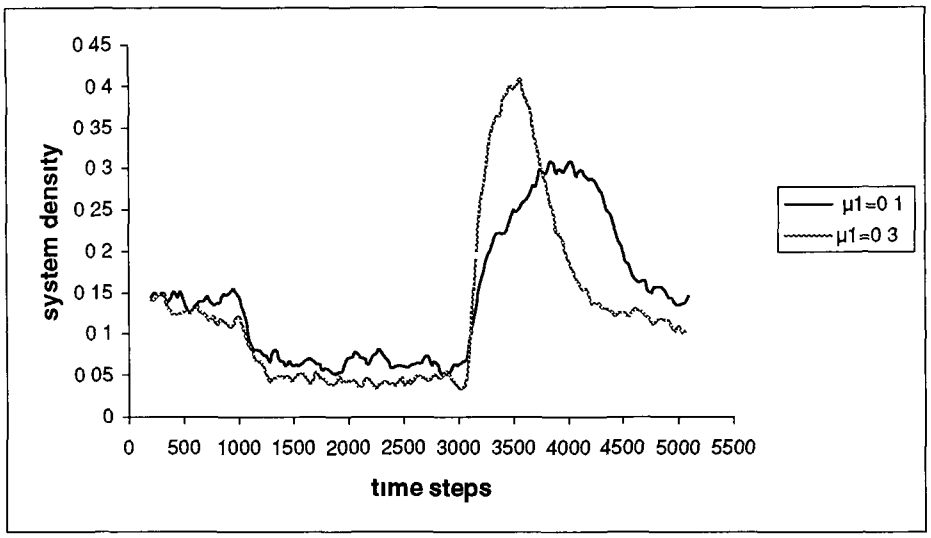

(a)

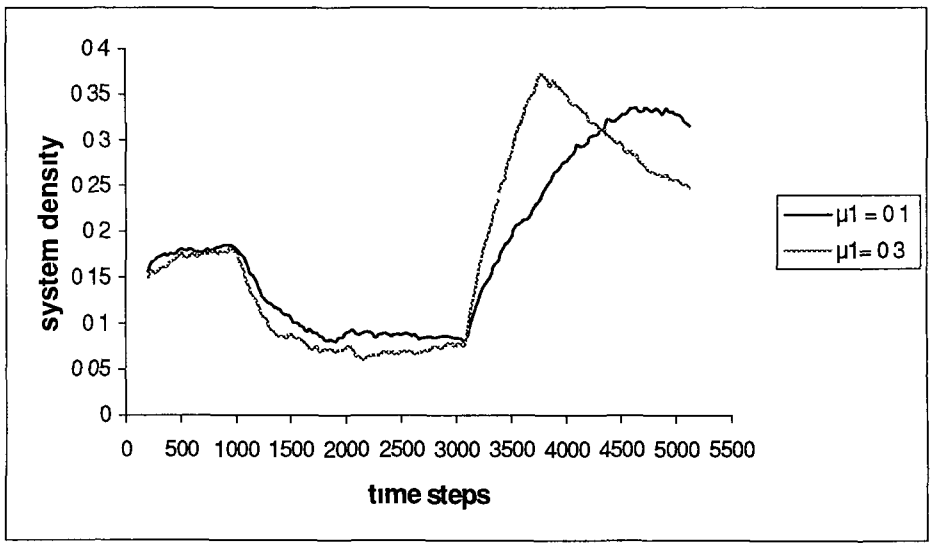

(b)

Fig (4.5) The influence of introducing underground parks on the system density over the simulation run at low arrival rate(μ = 0 15) using different values for the parameter μ1, where in

(a) The network of size 17 nodes

(b) The network of size 41 nodes

This was more noticeable in the case of the smaller size network, where the maximum density obtained was ~ 0 41 compared to ~0 36 obtained in the case of the larger network, see Fig (4 5)

This situation was dominant until all cars left the parks, which last for a longer period when $\mu 1 = 0\ 1$

At high arrival rate (μ=0 5), the influence of increasing the Poisson parameter $\mu 1$ on the system density was observable only when the underground parks were able to cope with the incoming traffic This is because the probability for a car to disappear into one of the parks has increased, which, in turn, will lead to congestion inside these parks at early stage

However, this period did not last for long and the system density increased rapidly, irrespective of the value of $\mu 1$ until the off-parking period started At this stage the parameter $\mu 1$, again, retains its influence on the system density and the outgoing traffic from the underground parks increases by the increment of $\mu 1$, see Fig (4 6)

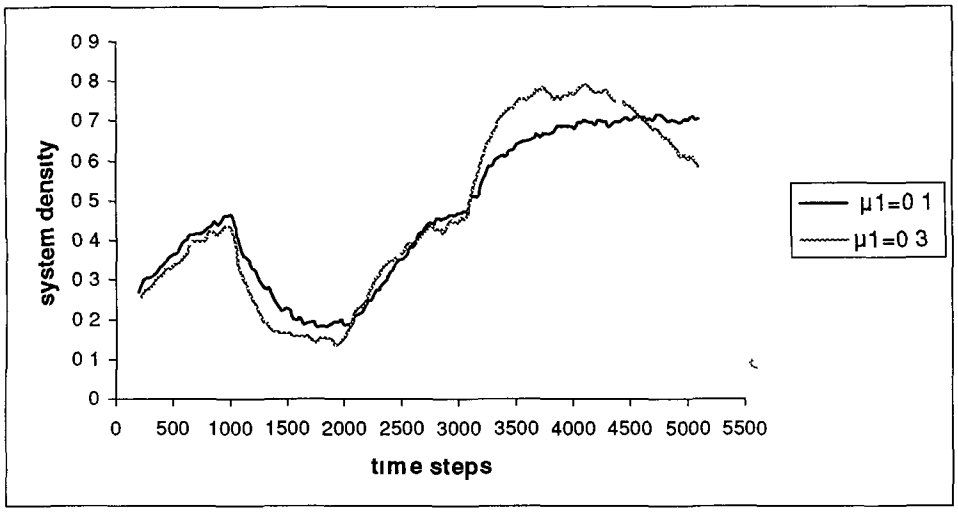

(a)

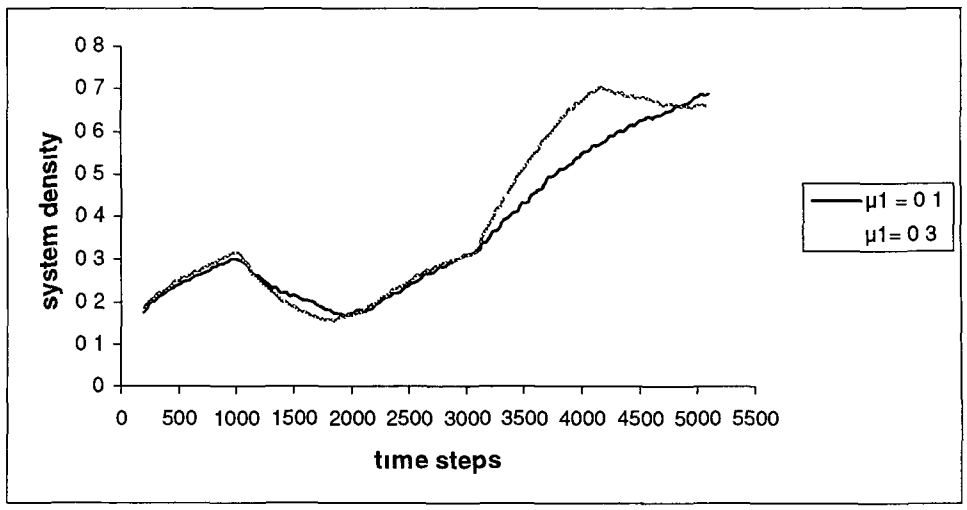

(b)

Fig (4 6) The influence of introducing underground parks on the system density over the simulation run at high arrival rate(μ = 0 5) using different values for the parameter μ1, where in

(a) The network of size 17 nodes

(b) The network of size 41 nodes

4.2 Traffic System under Short and Long-term events

In Chapter 3, we assumed that the network neighbourhood was able to cope with any number of cars that might leave the simulated network This means that the first site outside any of the network exits was always free

In real traffic, this is not always true It sometimes happens that one (or more) of the network exits is (are) closed for a short-term, due to a car accident or traffic jams, etc, or for a long-term due to road works, etc

The short-term events occur at random and last for a certain period of time, whereas the long-term events may last for days or even weeks

To approach reality these events, stated above, were modelled in our simulations In the following experiments each simulation was conducted for 6000 time steps and data were collected after a relaxation period of 200 time steps applying traffic conditions 25% turn left, 50% go straight, 25% turn right This was performed for a network of size 17 nodes by applying two arrival rates, $\mu = 0\ 15$ and $0\ 35$

4.2.1 Modelling Short-term events

The short-term events in our simulation were modelled by blocking some of the network exits at random, (i e they are exponentially distributed with parameter λ), and each event may last only for a number of time steps, which was also chosen at random, (using the function *rand()*). However, the duration of any short-term event did not exceed 50 time steps

The number of occurrences of such short-term events was fixed in our simulation and two values were used, 15 and 25

To quantify the effect of introducing such events, simulations were runs by blocking one or two of the network exits at random time steps, which were exponentially distributed with parameter $\lambda = 0\ 005$

Fig (4 7) shows the influence of introducing these events on the system density during the simulation run for a network of size 17 nodes and using a low arrival rate (μ=0 15) In (a) 15 short-term events were imposed throughout the simulation and in (b) the number of these events was increased to 25

In Fig (4 7) the changes in the system density can be interpreted as follows the way in which the system density responds to the short-term events(obstructions) depends on the following factors

i the number of occurrences of such events, how frequently they will occur?

ii and if they occur for how long?

iii the percentage of the traffic leaving the network at the time of imposing these events

iv the number of the network exits which are influenced by these events

In (i) the time-interval, which separates between any two consecutive obstruction occurrences, depends on the choice of the parameter λ The higher the values of λ the more frequent the obstructions In our simulation the value of λ was chosen to accommodate the number of the obstruction occurrences over the simulation period

Increasing the number of obstruction occurrences, provided that a longer period for the obstruction duration was randomly chosen, will increase the system density This can be noticed from Figs (4 7 (a)) and (4 7 (b)), where the number of obstruction occurrences has increased from 15 to 25 times

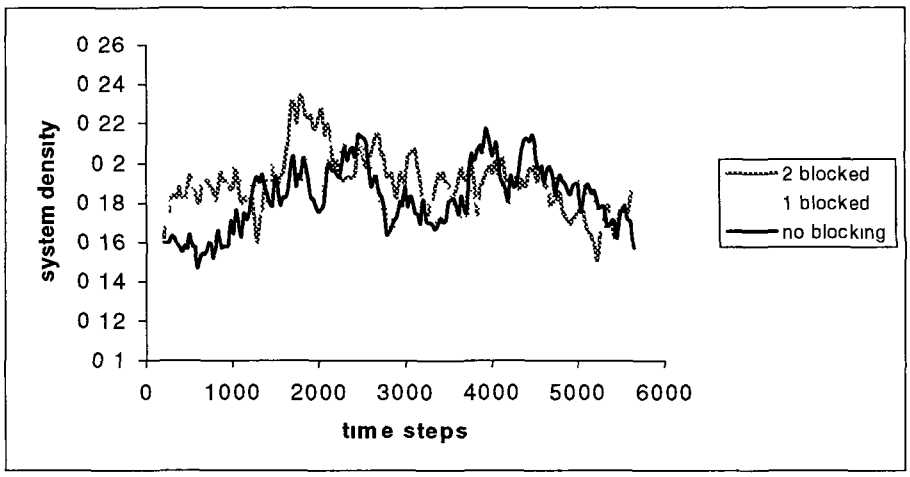

(a)

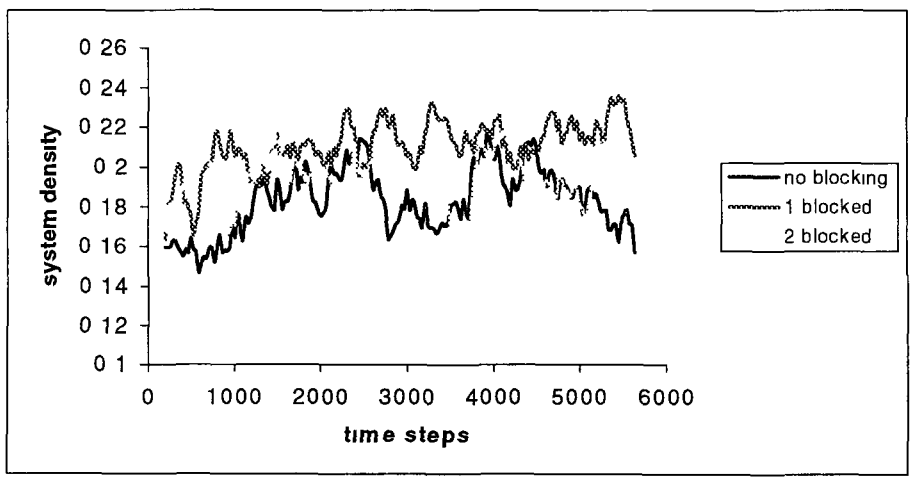

(b)

Fig (4 7) The effect of introducing short-term events on the system density, for a network of 17 nodes, over the simulation run at low arrival rate(μ = 0 15) where in
(a) The number of occurrences of these events was 15 and in
(b) the number increased to 25

To get a clear insight into the importance of (iii), let us assume that an obstruction exists outside an entry and exit node and its duration period is 20 time steps Now if 25% of the traffic is leaving the network, then there is a probability of **P** = 0 25 that car will be blocked Otherwise it will turn left (right) or go straight through

This means that the obstruction has influenced the traffic leaving the network only for 5 time steps and not 20 time steps! This explains why a higher densities were obtained in case of blocking only one exit in Fig (4 7 (b)) Further simulations, not shown here, reveal a considerable role for the traffic conditions on the system density

The influence of factor (iv) became more noticeable when the arrival rate was increased to $\mu = 0\ 35$, see Fig (4 8)

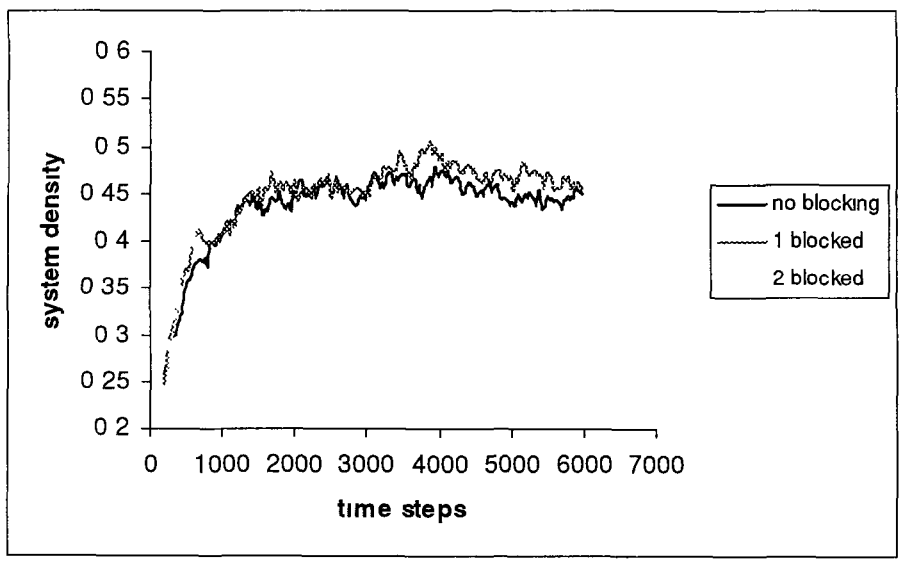

Fig (4 8) The effect of introducing short-term events on the system density, for a network of 17 nodes, over the simulation run at high arrival rate(μ = 0 35) where the number of occurrences of these events was 15

As the traffic becomes heavier, blocking more of the network exits, even for a short period of time, has significantly influenced the system density as can be seen from Fig (4 8)

4.2.2 Modelling Long-term Events

In this section, long-term events have replaced the short-term ones, (i e blocking some of the network exits over the duration of the simulation run) Also, four underground parks, each of capacity up to 300 cars, were introduced in order to simulate loss to flow (at fixed rate with P = 0 5)

The simulations were performed for two different network sizes, 17 and 41 nodes, by using different arrival rates, μ = 0 1, 0 3, and 0 55 Each simulation run was conducted for up to 5000 time steps and data were gathered every 30-150 time steps after a relaxation period 200-500 time steps The traffic conditions applied as in Chapter 3, Sec (3 1 5) cases (i) & (iii) A summary of the simulation results can be found in Appendix B (Tables (B 5) and (B 6))

In the case of the smaller size network our simulation reveals that the highest value of the maximum flow (0 2598) was obtained, when only one of the network exits was blocked and data were averaged every 150-time steps after a warm-up period of 200 time steps The turning percentages were 12% left, 76% through, 12% right and the arrival rate used was μ = 0 3 In contrast, the lowest value of the maximum flow (0 2097) was obtained when two of the network exits were blocked and using the same simulation parameters as above but at lower arrival rate (μ = 0 1)

To get a clear insight into the effect of introducing both the long-term events and the underground parks on the network performance, we therefore study the above two extreme cases (i e. q_{max} = 0.2598 and q_{max} =0.2097).

The traffic behaviour for these simulation runs compared with the case of maximum flow obtained in the transient movement simulation, Chapter 3, may be described with the help of the fundamental diagrams presented in Fig (4 9)

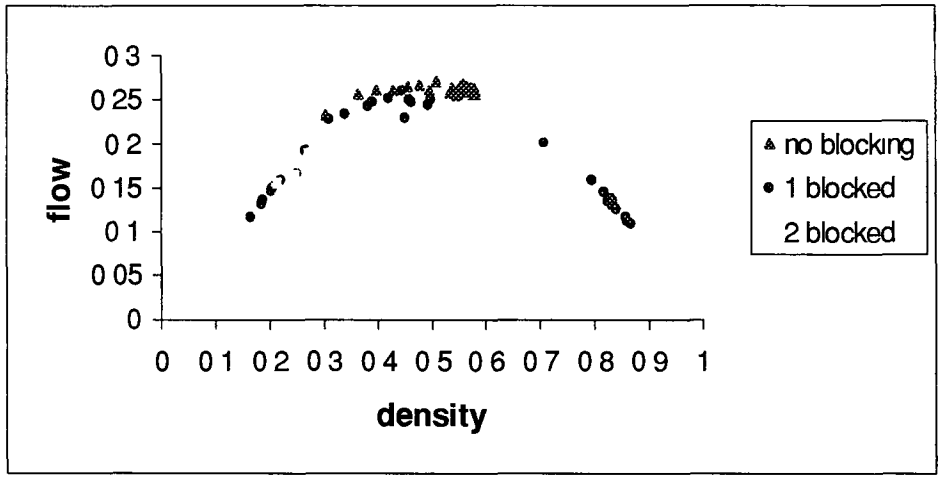

(a)

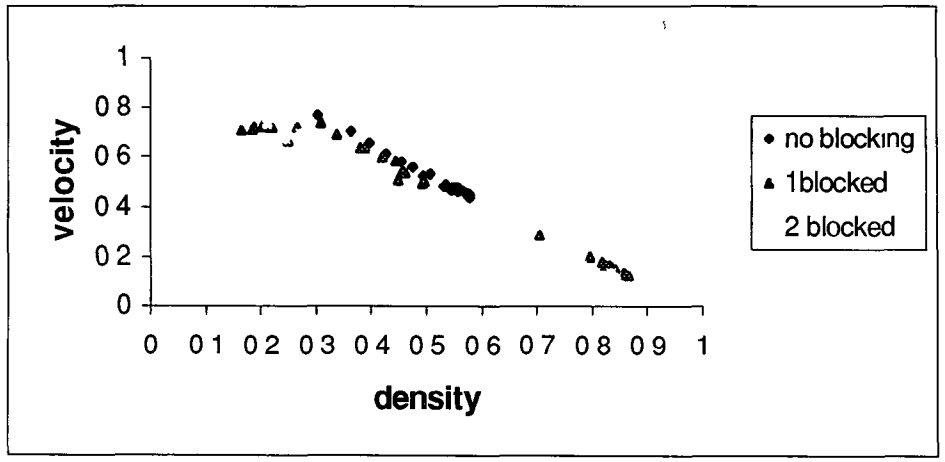

(b)

Fig (4 9) Fundamental diagrams of the above two extreme cases, where in
(a) flow-density relations (b) velocity-density relations

From Fig (4 9), we can observe the effect of blocking one or more of the network exits as follows

- The first striking feature of Fig (4 9), flow-density relation, is this gap, which isolates the dense traffic regime This occurs due to the increment of the network density from 0 330629 to 0 5969, when two exits were blocked and from 0 4963 to 0 7059, when only one exit was blocked This in turn results in dropping the network velocity from 0 63 to 0 33 and from 0 5 to 0 28 for the above cases respectively, which can be seen from Fig (4 9 (b))
- This discontinuity in the fundamental diagram has been obtained in road traffic measurements, (Edie, 1974, Hall, 1986), which lead to the assumption, that there is a point of discontinuity in the fundamental diagram around the maximum traffic flow, between the left part of the diagram, representing the free traffic, and the right part of the diagram, representing the dense traffic The fundamental diagram obtained for the case of highest value of q_{max} (Fig (4 10 a) gives a good approximation to the experimental data in Fig(4 10 b)
- Also, introducing long-term events such as underground parks and blocking some of the network exits has decreased the network maximum flow from q_{max} = 0 2702, which obtained in the case of transient movement simulation in Chapter 3, to q_{max} = 0 2097, which obtained by blocking two of the network exits at low arrival rate(μ = 0 1)

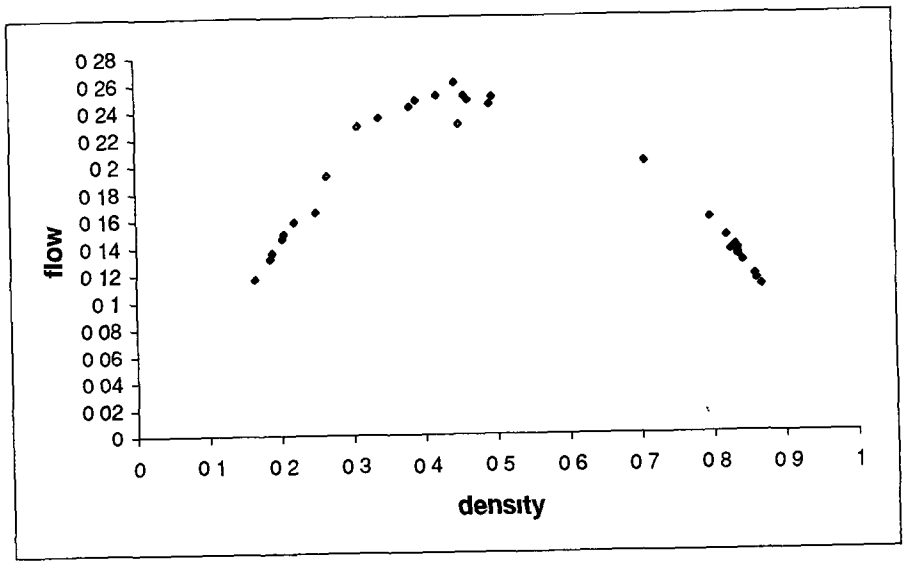

Fig(4 10 a) The fundamental diagram obtained for the case of highest value of q_{max} = 0 2598

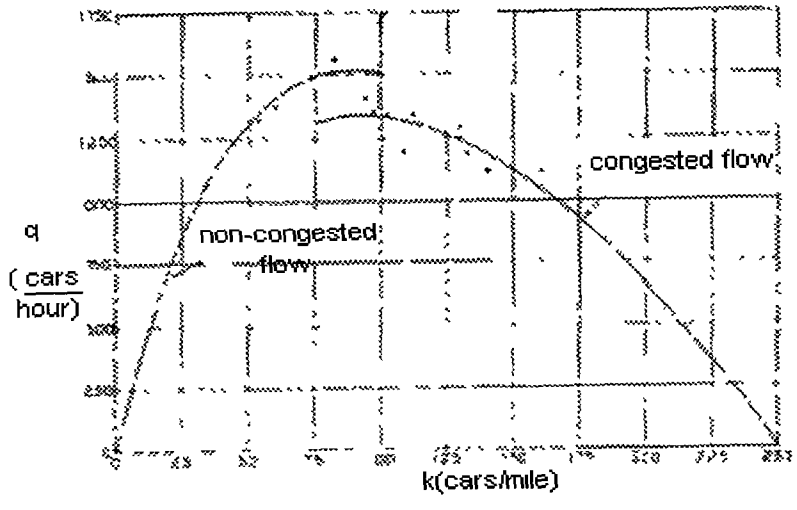

Fig(4 10 b) Fundamental diagram for road traffic flow, source· Edie (1974)

- Fig (4 9) reveals that introducing long-term events has resulted in lower densities for the maximum flow In the case of transient movement simulation, q_{max} was observed at density $\rho_{q_{max}} = 0\ 50$, whereas progressively blocking network exits has decreased the density of $\rho_{q_{max}}$ from 0 41, which was observed in case of blocking one exit, to 0 33 when two of the network exits were blocked
- Increasing the network size to 41 nodes has results in lower densities for the extreme values of q_{max} The results are summarised in Table (4 1)

  It can be seen from Table (4 1) that, in the case of larger size network, slightly lower values for the maximum flow were obtained at lower densities The statistical analysis presented in Appendix A (Table (A 1)) reveals a significant interaction between the network size and the number of the blocked exits at $\alpha = 0\ 5$ level of significance

Performance Measure	17 nodes network		41 nodes network	
	Highest	Lowest	Highest	Lowest
Maximum flow	0 2598	0 2097	0 254654	0 2054
Density of max flow	0 4439	0 3309	0 4199	0 3168

Table (4 1) Comparison between the highest values and the lowest values the maximum flow obtained for two different networks, where some of the network exits were blocked

4.3 Summary and conclusion

In first part of this chapter we have studied the non-transient movement of cars along the networks by introducing underground parks and allow cars to park inside the network, so that they are temporarily lost to flow This was performed at fixed rate (i e car may leave (enter) the park with probability P) and also at stochastic rate (i e car arrival or departure to any of the parks follow a Poisson distribution with parameter $\mu 1$)

In the second part of this chapter, we investigated, in brief, the influence of imposing short and long-term events on the network performance

Short-term events in our simulation were modelled by blocking some of the network exits at random, they were exponentially distributed with parameter λ, and this blocking lasts only for a certain number of time steps, which did not exceed 50 time steps

In contrast, blocking some of the network exits during the simulation run have simulated the long-term events Our findings can be summarised as follows

i The most remarkable aspect from introducing underground parks was a different "*jamming threshold*" for different network sizes, and simulation with loss to flow at stochastic rate shows that the *"jamming threshold"* for each network depends on the parameter $\mu 1$

ii The simulation also reveals that small size networks respond rapidly to external changes, especially for networks with loss to flow

iii The simulation reveals that the way in which the system responds to the simulated short-term events depends on their number and how frequently they will occur and the duration of each occurrence and also the arrival rate used to feed the system with cars The influence of these events was more noticeable at higher rate of arrivals More work needs to be done to investigate the influence the traffic conditions and the change in the parameter λ, which determine how frequently these events will occur, on the network performance

iv By modelling long-term events such as blocking one or more of the network exits, over the simulation run, a significant interaction between the network size and number of blocked exits was obtained, ($\alpha = 0\ 01$), at high level of concentration of cars

v Despite the complex interactions in urban networks, the characteristic shape of the fundamental diagrams was also obtained at network traffic level

Chapter 5

"Simple Lane-Changing Rules for Urban Traffic Using Cellular Automata"

5.0 Introduction

To approximate reality the simulation tool has to be efficient and represent some of the basic traffic features, which can be observed or tested Using single-lane networks, important features like lane changing and its effect on the traffic stream behaviour cannot be observed and studied

The basic idea behind the lane changing mechanism is either to maintain a regular, (desired), speed or to improve the current speed, where in both cases the driver is hindered from doing so in his current lane

This situation is not always the case inside urban traffic areas, where drivers may change their lane due to different motivations, such as performing a right turn at intersections, to avoid obstructions and so on

In the first regime, (highway traffic), one set of lane-changing rules was shown to be able to reproduce some of the macroscopic aspects of traffic flow on highways such as density inversion between the two lanes, which take place long before the density of the maximum flow (Rickert *et al*, 1996, Wagner *et al*, 1997)

Due to the complexity of the second regime (urban traffic), we may raise the following question

Can we find a perfect set, "super set", of *lane-changing* rules in order to accommodate all the different motivations for lane changing inside the urban areas?

In this chapter, we present three different sets of rules for lane changing as follows urgent *lane-changing* conditions, *minimal* and *maximal* conditions for *lane-changing* each of which is used in order to accommodate the driver need to change lane (Gipps, 1986)

5.1 Motivations for Lane Changing

Lane-changing will occur in one of the following cases

I To gain some speed advantage

If the driver on the left lane, (slow lane), evaluates the other lane traffic to be better, (i e the second lane has a lower flow and higher speed), then with probability P_chg he will change lane and with 1-P_chg he will not

II To avoid obstruction

Obstructions, such as cars making delivery, Bus stops, and cars intending to perform a left, (or right), turn, have been imposed at random with probability P_obs This obstruction is located on the left lane with probability P_lobs and with probability 1- P_lobs on the right lane Cars will move to overtake the obstruction as they enter the obstruction zone

III To turn at the next intersection

If the driver on the left lane intends to perform a right turn or the driver on the right lane intends to perform a left turn, then *lane-changing* will occur and this depends on how close the car is to the intersection zone

IV To avoid slow platoons on the fast lane

Since all cars evaluate the fast lane to be the better one, this will result in clusters of slow moving cars At this stage cars can change lane in order to pass those platoons provided that the slow lane allow this change

5.2 The two-lane Model:

The two-lane model consists of two parallel single-lane models and three sets of rules for *lane-changing* defined below, (Equations (5 1)-(5 3)

Our lane changing rules are based on the following steps

(a)- check for vehicles that are qualified for lane-changing according to the specified lane-changing rules

(b)- move the chosen vehicles for lane-changing to the neighbouring sites in the second lane

(c)- use the model rules to update each single lane independently

In step (a), normally, cars must overtake on the right lane but overtaking on the left lane is permitted-

1 When the driver intends to turn at the next intersection

2 Where the traffic is moving more slowly on the right lane than the left lane

Step (b) is needed for the simulation purpose only, as in real traffic the car will advance to the destination site directly

Let us assume that, in reference to Fig.(5.1):

dx is the headway distance to the leading car on the destination lane

dy is the backwards distance to the following car on the destination lane, where both dx and dy are measured from the empty neighbouring site on the destination lane

v is the speed of the car which intends to change lane

vb is the speed of the following car on the destination lane

dz is the headway distance to the car ahead in the current lane

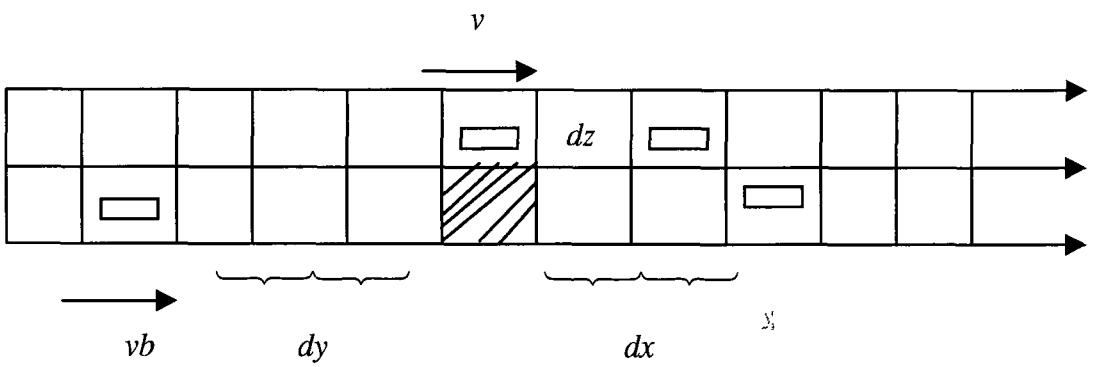

Fig (5 1)

Then, the necessary conditions for lanes-changing are

1 $dx > v + k_1$ $\qquad k_1 \in [0, v_{max}]$

and in order not to disturb the traffic on the second lane

2 $dy > vb + k_2$, $\qquad k_2 \in [0, v_{max}]$

If we set $k_1 = k_2 = 0$, then we obtain the *minimal conditions* for lane changing as follows

$$dx > v,$$

$$dy > vb \qquad (5\ 1)$$

However, as the driver gets closer and closer to the given intersection or obstruction, he is prepared to accept less headway distance on the other lane (i e $dx = v$) This will result in the *urgent conditions* for *lane-changing* as follows

$$dx \geq v,$$

$$dy > vb \qquad (5\ 2)$$

Setting $k_1 = k_2 = v_{max}$ yields the *maximal conditions* for *lane-changing* as follows

$$dx > v + v_{max},$$

$$dy > vb + v_{max} \qquad (5\ 3)$$

To apply Equation (5 3), we must have $dz < \alpha$, where α is a parameter which defines the headway distance on the left lane that satisfies the driver in order to stay in his current lane

In order to simulate the stochasticity element in the *lane-changing* mechanism, with probability P_chg the driver will accept the *maximal* or *minimal* conditions to change his lane and with probability 1- P_chg he will not

In case (I), Sec (5 1), the intention of the driver to improve his speed, by changing his lane, is dependent on whether the traffic in the present lane or the target lane is more likely to affect his speed

If the driver is hindered in his current lane, (left lane), he requires the *minimal conditions* to change lane Otherwise, the driver will move to the second lane if it is worthwhile to do so, which means that the driver is not satisfied with his current headway distance ($\alpha < dz$) and evaluates the second lane as the better lane In this case, the *maximal conditions* for *lane-changing* are required Fig (5 2) presents the flow-chart for the *lane-changing* mechanism.

In case (II), Sec(5 2), the obstruction zone is defined as being 3 sites distance from the obstruction As the driver movers nearer to the obstruction, he is ready to accept the *minimal* or *urgent condition* to change lane, in order to avoid being blocked by the obstruction

In case (III), Sec(5 1), as long as the driver is outside the turning zone, it has no influence on the *lane-changing* decision and the driver is concerned only about improving his speed, case (I)

When the driver enters the turning zone, he ignores any attempt to change lane in order to improve his speed and looks for *minimal conditions* to change lane

As the driver moves closer to the junction and enters the urgent zone for *lane-changing* he looks for the *urgent conditions* for *lane-changing* in order to be in the right lane to perform the required turn

In case (IV), Sec (5 1) to avoid slow platoons on the fast lane the driver looks for the minimum requirements to change his lane A *platoon* is defined as a block of 5 or more occupied sites, for most of which are stopped

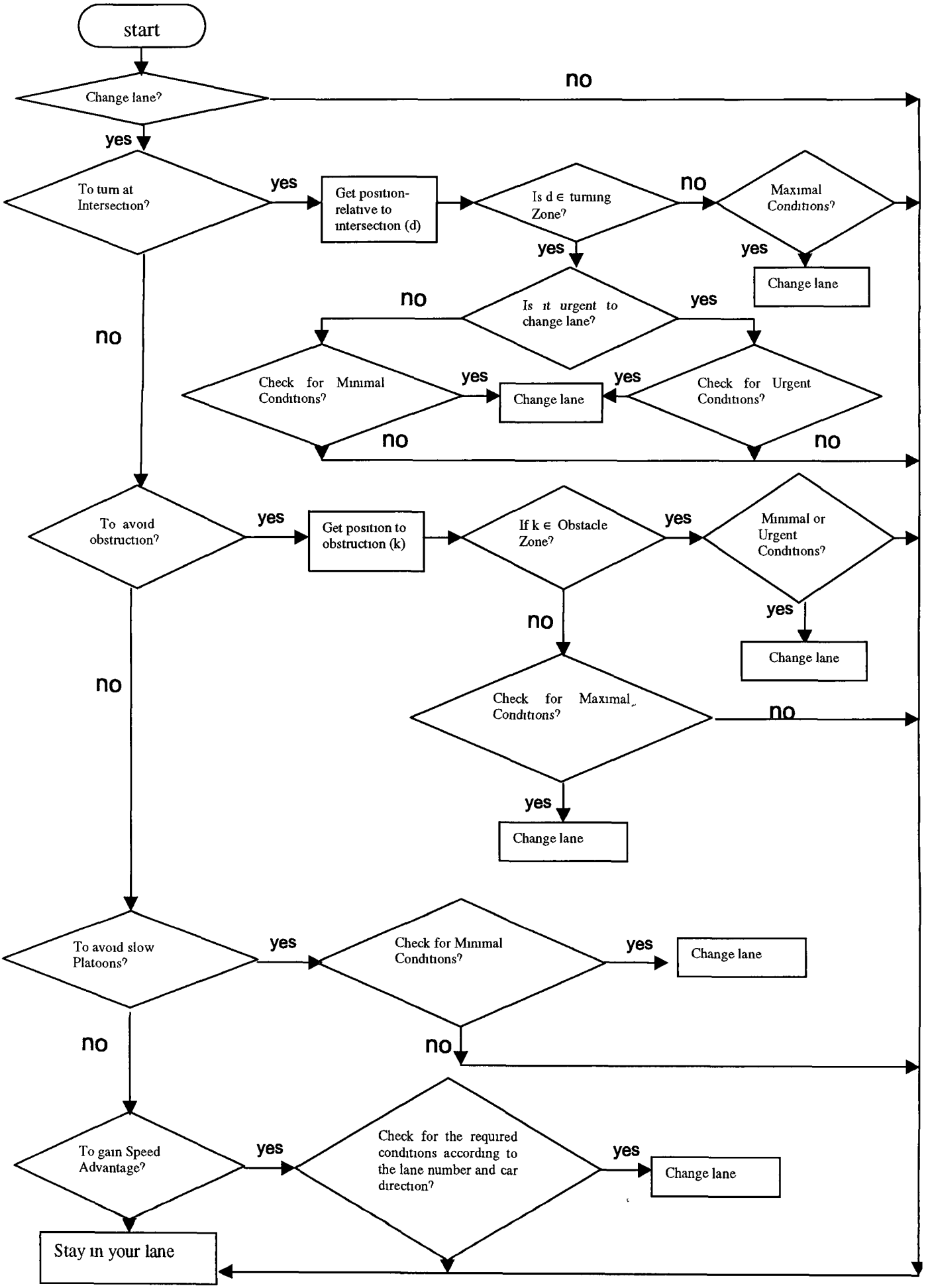
start
Change lane?
no
yes
To turn at Intersection?
yes
Get position-relative to intersection (d)
Is d ∈ turning Zone?
no
Maximal Conditions?
yes
yes
Change lane
yes
Is it urgent to change lane?
no
no
Check for Minimal Conditions?
yes
Change lane
yes
Check for Urgent Conditions?
no
no
To avoid obstruction?
yes
Get position to obstruction (k)
If k ∈ Obstacle Zone?
yes
Minimal or Urgent Conditions?
yes
Change lane
no
no
Check for Maximal Conditions?
no
yes
Change lane
To avoid slow Platoons?
yes
Check for Minimal Conditions?
yes
Change lane
no
no
To gain Speed Advantage?
yes
Check for the required conditions according to the lane number and car direction?
yes
Change lane
Stay in your lane

Fig (5 2)

5.3 Simulation and results

In the following simulation experiments, each simulation is conducted for 50 runs, where each run is calculated up to 2000 time steps to generate the average case statistics Imposing periodic boundary conditions, we simulated a system of size 2x100 sites, two-lane, which is large enough for an urban street The turning probabilities at the intersections are 0.4 left and 0 30 right The intersection zone is considered to be 10 sites (or less) under *minimal conditions* and 5 sites or less for *urgent conditions* at the same intersection. Headway parameter, α = 3 (i e *headway distance* = 22 5m), which is reasonable for urban traffic The basic *lane-changing parameters* in our simulation are

i lane-changing probability (P_chg)

ii obstruction probability (P_obs)

iii lane obstruction probability (P_Lobs)

5.3.1 Lane-usage behaviour

In order to get clear insight about the impact of the *lane-changing parameters* on the *lane-usage frequency*, we have performed two different simulations by changing the value of the above parameters as follow

Experiment I:

In the first simulation experiment, we have fixed the *lane-changing probability* at P_chg = 0 4 and modified the values of the other two parameters (P_obs = (0.3, 0.4) and P_Lobs = (0.7, 0.3), (0.6, 0.4), (0.5, 0.5)).

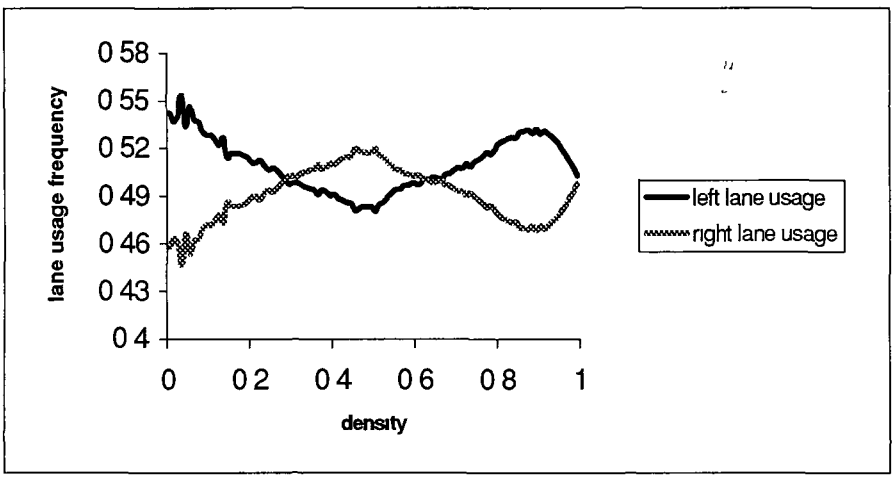

(a)

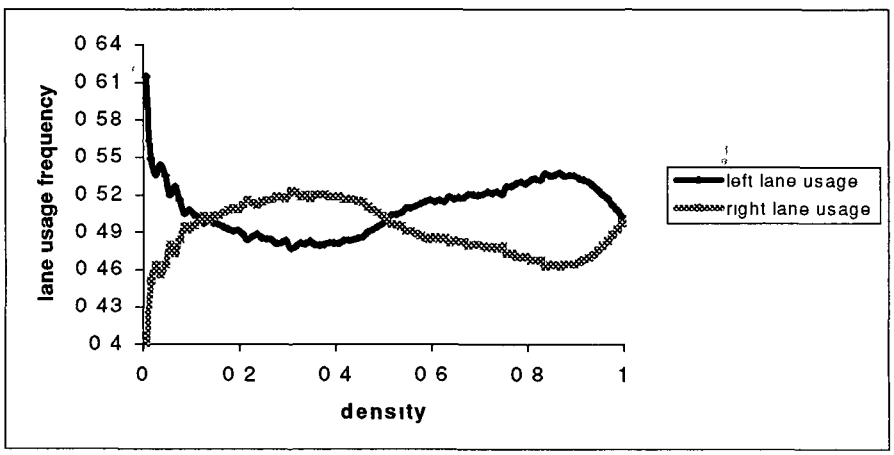

(b)

Fig (5 3) Lane usage frequency vs traffic density for two different simulation of size 2xk, k=100, where P_chg = 0 4, P_obs = 0 3 and in

(a) P_Lobs = 0 5, 0 5 for left and right lane respectively

(b) P_Lobs = 0 6, 0 4 for left and right lane respectively

Simulation	P_chg	P_obs	P_Lobs Left	P_Lobs Right	Low density Inversion point	high density Inversion point
Run1	0 4	0 3	0 7	0 3	0 075	0 475
Run2	0 4	0 3	0 6	0 4	0 115	0 505
Run3	0 4	0 3	0 5	0 5	0 295	0 625
Run4	0 4	0 4	0 7	0 3	0 065	0 485
Run5	0 4	0 4	0 6	0 4	0 105	0 515
Run6	0 4	0 4	0 5	0 5	0 275	0 715

Table (5 1) Simulation Experiment I each "run" refers to an average of 50 Experiments over 2000 time steps each to obtain average case statistics

The relationship between the *lane-usage frequency* and the simulation density using different values for P_obs and P_Lobs is presented in Table (5 1) and Fig (5 3) The observations can be summarized as follows

i It can be seen from Fig (5 3) that both lanes have the same *lane usage-frequency* at three different points The first two points are called "*density inversion*" points At these points, high traffic-density switches from one lane to the other lane

ii The first "*density inversion*" point has occurred at density $\rho = 0\ 295$ in case (a) and at $\rho = 0\ 115$ for case (b), while the second one has occurred at much higher density $\rho = 0\ 625$, $0\ 505$ for both cases (a) and (b) respectively

iii The location of these points depends on the *lane-changing parameters*, which from Table (5.1) may be summarised as follows

(a) The effect of lane obstruction probability(P_Lobs)

This parameter has considerable effect on *lane-usage frequency* For example, using P_Lobs = 0 6 for the left lane and P_Lobs = 0 4 for the right lane has influenced the *lane-usage frequency* for both lanes at an early stage, (low density) The first "*density inversion*" point has occurred at ρ_1 = 0 115, where usage of the right lane becomes higher than usage of the left lane, and again the two lanes switch traffic at ρ_2 = 0 505, where the left lane becomes more crowded than the right one In contrast, using both lanes with the same P_Lobs = 0 5 has increased the above densities (ρ_1, ρ_2) to a much higher values (ρ_1= 0 295 and ρ_2 = 0 625), see Fig (5 3)

This can be explained as follows

Increasing P_Lobs for the left lane will disturb its traffic, even at low density, due to the frequent, randomly occurring obstructions

This results in the right lane again becoming more crowded at ρ = 0 505 At this stage, a car will again switch lanes in order to avoid traffic jams However, applying the same P_Lobs to both lanes has increased the low-density inversion point from 0 115 to 0 295 This increase is to be expected as the motivation for *lane-changing* reduces Fig (5 4) shows the location of the inversion points for different values of P_Lobs

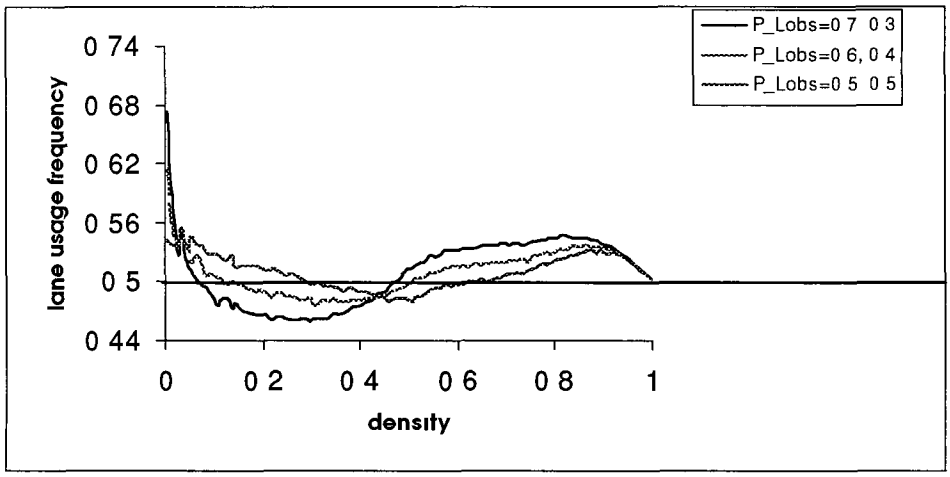

Fig (5 4) left lane usage vs traffic density for different values of P_Lobs and P_chg = 0 4, and P_obs = 0 3 Each intersection between the lane-usage curve and the horizontal line represents an inversion point

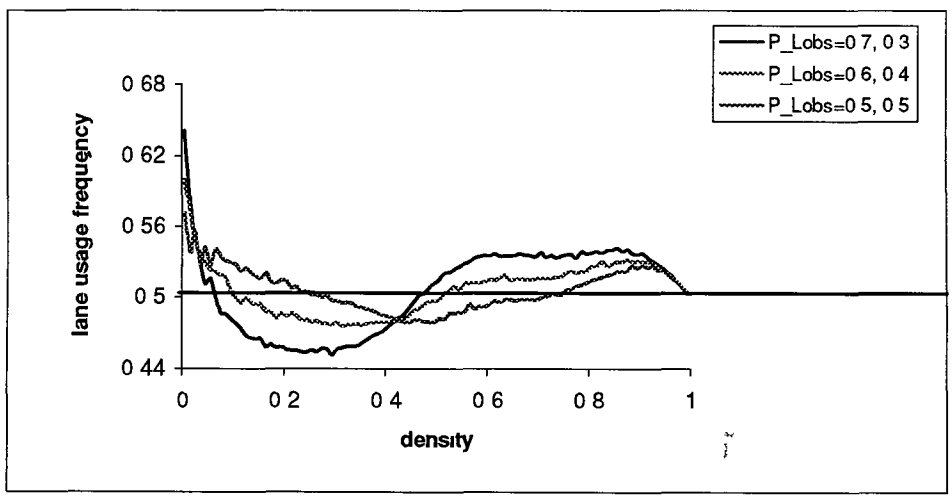

Fig (5 5) left lane usage vs traffic density for different values of P_Lobs and P_chg = 0 4, and P_obs = 0 4 Each intersection between the lane-usage curve and the horizontal line represents an inversion point

(b) The effect of obstruction probability(P_obs)

The *obstruction probability* also influences the *lane-usage frequency* for both lanes, especially when there is no considerable difference between the values of P_Lobs or when the two lanes are used with same P_Lobs, (see Run3 and Run6 in Table (5 1)) For these runs, increasing P_obs has resulted in lower value for the low density inversion point and higher value for the higher density inversion point, see Figs (5 4) and (5 5)

This can be explained as follows

Increasing the value of P_obs will result in more obstruction occurrences on both lanes, which, in turn, increases the usage of the right lane over the left lane at density (0 27) This is to be expected as the chance for a car to overtake on the right lane is greater than its chance for overtaking on the left lane This increase in the usage of the right lane, will continue, followed by decrease in the left lane usage, until $\rho \sim 0\ 5$, where the usage of the right lane attain its maximum value over the left lane At this stage traffic starts to switch gradually from the right lane to the left lane and due to the increase in obstruction probability (P_obs), the second inversion point occurs at higher density (0 71)

Experiment II

To examine the effect of the *lane-changing probability* on the lane usage behavior, in the second experiment, presented in Table (5 2), we have increased the *lane-changing probability* to P_chg = 0 5 and also used different values for the other two *lane-changing parameters* In general the same macroscopic phenomenon, "density inversion" points, was observed

Table (5 2) shows the effect on the *" density inversion" points* of increasing P_chg to 0 5 This means that the "*density inversion*" is modified by the *lane-changing parameters* and more simulations are needed in order to determine if there is a limit for such changes For example, Table (5 2) demonstrates that increasing *lane-changing probability* as well as *obstruction probability* resulted in a smaller density for the first inversion point (from ρ= 0 295 to ρ= 0 275) and higher density for the second inversion point (from ρ= 0 635 to ρ= 0 735)

Simulation	P_chg	P_obs	P_Lobs Left	P_Lobs Right	Low density Inversion point	high density Inversion point
Run7	0 5	0 3	0 7	0 3	0 085	0 465
Run8	0 5	0 3	0 6	0 4	0 135	0 505
Run9	0 5	0 3	0 5	0 5	0 295	0 635
Run10	0 5	0 4	0 7	0 3	0 065	0 475
Run11	0 5	0 4	0 6	0 4	0 115	0 519
Run12	0 5	0 4	0 5	0 5	0 275	0 735

Table (5 2) Simulation Experiment II each " run" refers to an average of 50 Experiments over 2000 time steps each to obtain average case statistics

5.3.2 Flow Behavior

i Despite adding another set of lane-changing rules, the maximum flow for the two-lane model is much higher than the maximum flow for the single-lane model This can be seen clearly from Fig (5 6) These results in Fig (5 6) are based on simulating two systems, the first of size k=100 representing a single-lane road, the second of size k = 2x100 representing a two-lane road In both cases data were averaged over 50 runs and each run is conducted up to 2000 time steps

ii The two-lane flow reaches its maximum, approximately, at $\rho \sim 0\,5$, which is the density of maximum flow for the single-lane model, (see Fig(5 6))

iii In the case of the single-lane model, there is a sharp bend in the flow-density curve, which is not found in the two-lane model This bend means that the dynamics below and above the density of maximum flow($\rho_{q\max}$) for the single-lane model are different from those of the two-lane model, i e flow breaks-down quickly in single-lane model

iv The change in the *lane obstruction probability* (P_Lobs) seems to have a great impact on the flow behavior on both lanes as follows

a) Applying P_Lobs=0 7 for the left lane and P_Lobs = 0 3 for the right lane has decreased flow on the left lane compared to the right lane Even at lower densities The flow is correspondingly increased on the right lane, see Fig (5 7 (a))

b) When P_Lobs =0 5 for both lanes, flow for both was similar at low densities but, at higher densities, (ρ > 0 5), we observed a considerable change in the traffic flow between the two lanes, see Fig (5 7 (b)) The first intersection point of the two curves obtained at low density "*inversion point*", while the last one occurred at the high density "*inversion point*" The graph also shows a third inversion point which does not appear in lane-usage vs traffic density relation presented in Fig(5 3)

For both cases (a) and (b) we obtained similar traffic patterns by using different values for P_chg,(0 4, 0 5, 0 6), but maximum flow on both lanes decreased when the value of P_obs was increased, as can be seen from Fig (5 8)

v Fig (5 9) shows that as we increased the *obstruction probability*, the maximum flow for the two-lane model decreased from q ~ 0 77 for P_obs = 0 3 to q = 0 68 for P_obs = 0 5, (i e a decreases of 11 6 %), no matter whether the obstacle was located in the left or right lane

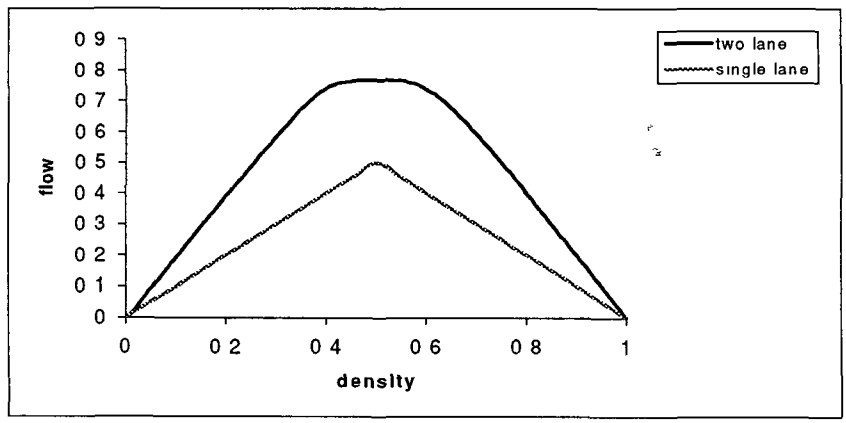

Fig (5 6) flow vs density relation for both single-lane and two-lane Models

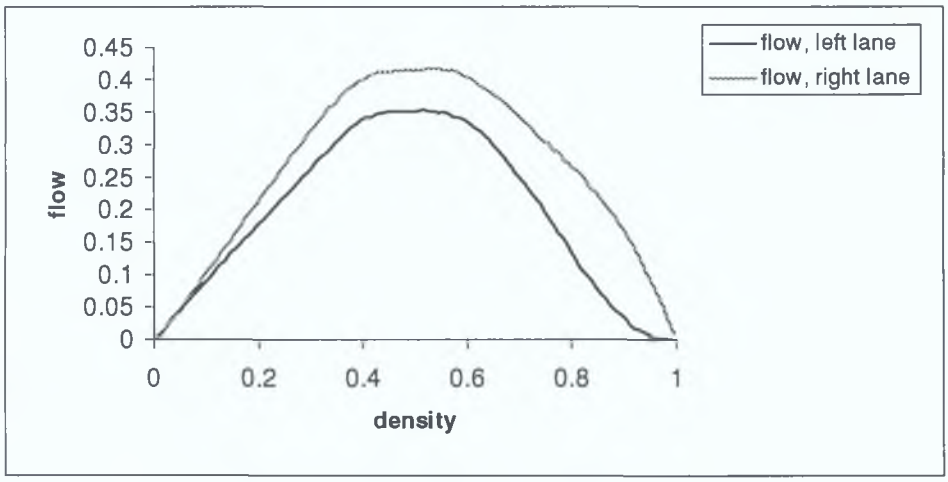

(a)

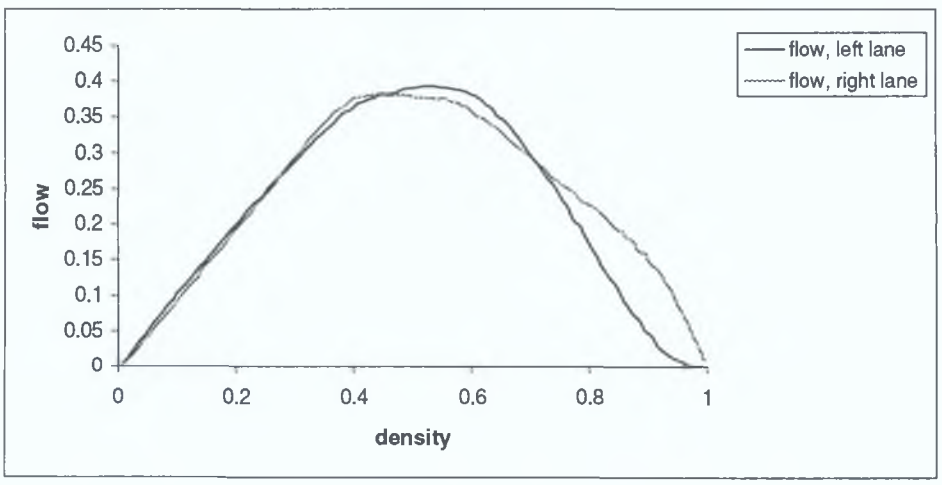

(b)

Fig.(5.7): flow-density relation for two different simulations of size k = 2x100; two lane .Data were averaged over long time periods over 50 runs using P_chg=0.4, P_obs=0.4, where in (a) P_Lobs=0.7, 0.3 and in (b) P_Lobs=0.5, 0.5 for both left and right lanes respectively.

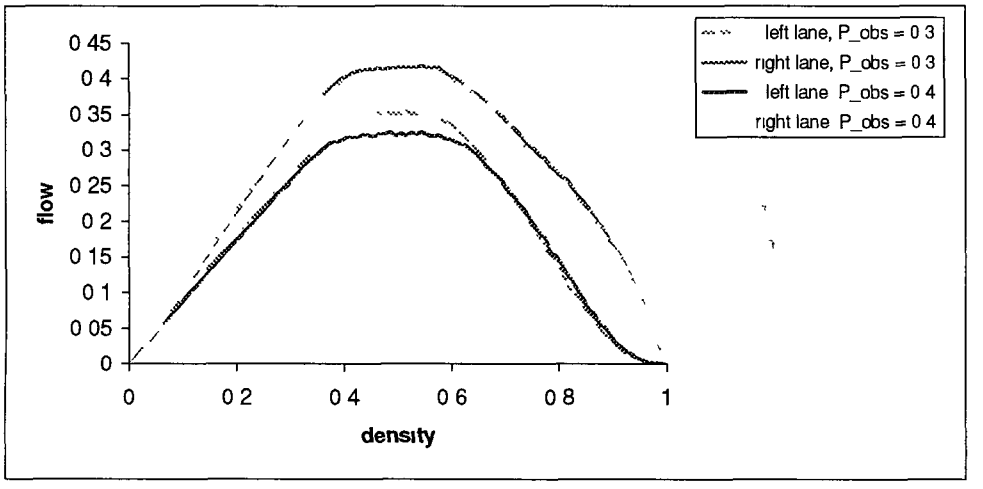

Fig (5 8) flow-density relation for different simulation of size k = 2x100, two-lane, using different values for P_obs, where P_chg = 0 4 and P_Lobs = 0 7, 0 3 for both left and right lanes respectively

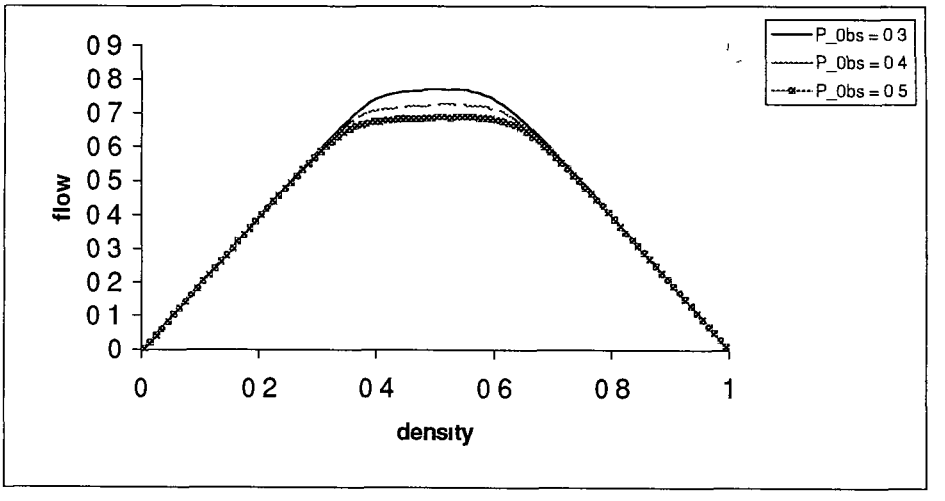

Fig (5 9) comparison of flows for different values of P_obs, where P_chg and P_Lobs are fixed as in Fig (5 8)

5.3.3 Lane-changing behavior

To understand lane-changing dynamics, we have to study the relations between *lane-changing frequency* and *lane-changing parameters* This study can be summarized as follows

i The influence of varying P_Lobs on *lane-changing frequency* is presented in Fig (5 10) The maximum value of *lane-changing frequency* (0 001706) was obtained at a traffic density of 0 295,when P_Lobs = 0 5 for both lanes However, increasing P_Lobs for the left lane decreased the frequency of lane changes to 0 001527 at the same density This dynamic is observed at different values of P_obs = 0 3, 0 4, and 0 5

ii Fig (5 10), also shows that *lane-changing frequency* increases linearly at low densities, ($\rho \leq 0\ 125$), and this is observed for all values of P_Lobs Further simulations, see below, also show that as we exceed the density $\rho = 0\ 125$, different values of the *lane-changing parameters* will influence the *lane-changing frequency* Fig (5 10) shows two significant peaks when P_Lobs =(0 5,0 5), the first at the first inversion point while the second occurs before the second inversion take place

iii The maximum number of lane changes occurred at density $\rho \sim 0\ 3 \pm 0\ 01$, which is well below the density of maximum flow for the 2x100 site system ($\rho = 0\ 5$)

iv The maximum frequency of lane-changes to the right lane (0 000889) was much higher than the maximum frequency to the left lane (0 000655) and was obtained at density ρ = 0 295 This is higher than that found for maximum frequency of changes to the left lane (ρ = 0 245) This can be seen from Fig (5 11), for different values of P_Lobs and P_obs

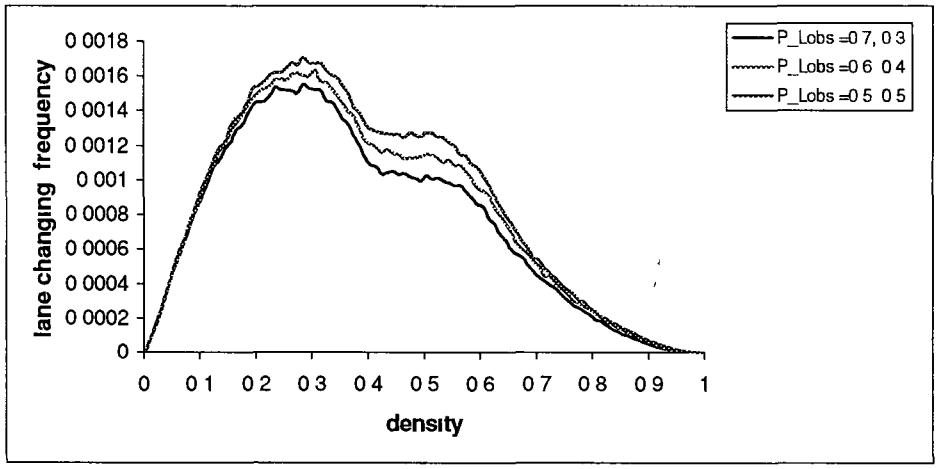

Fig(5 10) lane-changes frequency vs traffic density for different values of P_Lobs while P_chg = 0 4 and P_obs = o 4

v Increasing the value of P_obs from 0 3 to 0 5 has increased the maximum frequency of lane changes to 0 001704 (at ρ = 0 275), from 0 001486 (at ρ = 0 285) This is to be expected, because drivers have to change their lane in order to avoid being halted behind an obstruction and these lane changes increase, as the occurrence of obstructions becomes more frequent

vi The effect of *lane-changing probability* (P_chg) seems to be influenced by the values of the other two lane-changing parameters, P_obs and P_Lobs, as follows

Applying P_chg = 0 4, P_obs = 0 4 and P_Lobs = 0 5, (for each lane), the maximum lane-changing frequency obtained was 0 001706, see Fig (5 12 (a)) However, when we increased *lane-changing probability* to P_chg = 0 6 and reduced the value of P_obs to 0 3, also increasing P_Lobs for left lane to 0 7, the maximum *lane-changing frequency* dropped to 0 001447, see Fig (5 12 (b)) This example demonstrates that increasing the value of P_chg will not always yield a higher frequency of lane changes without controlling values of the other two parameters However, further simulations are required in order to quantify more the effect of changing of P_chg

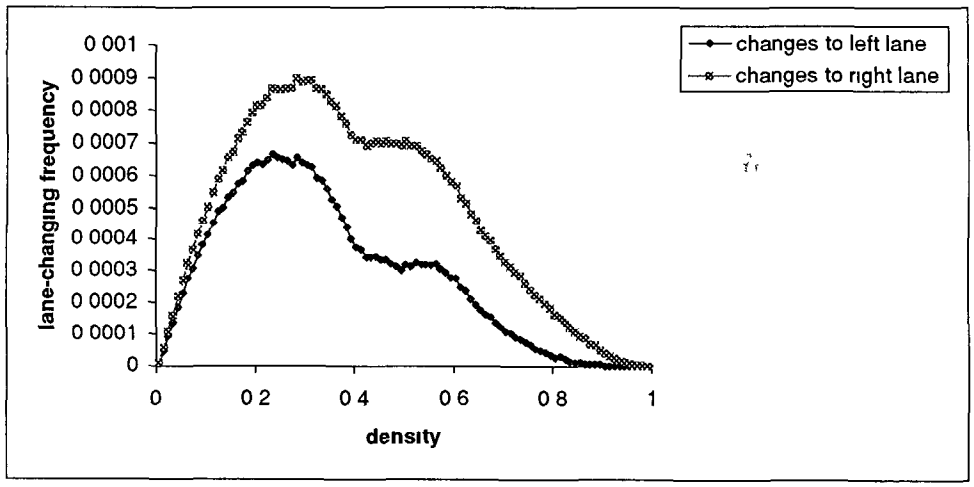

Fig (5 11) comparison between lane changing frequency to left lane and right lane When ρ > 0 125 the increase in right changes over left changes becomes more noticeable.

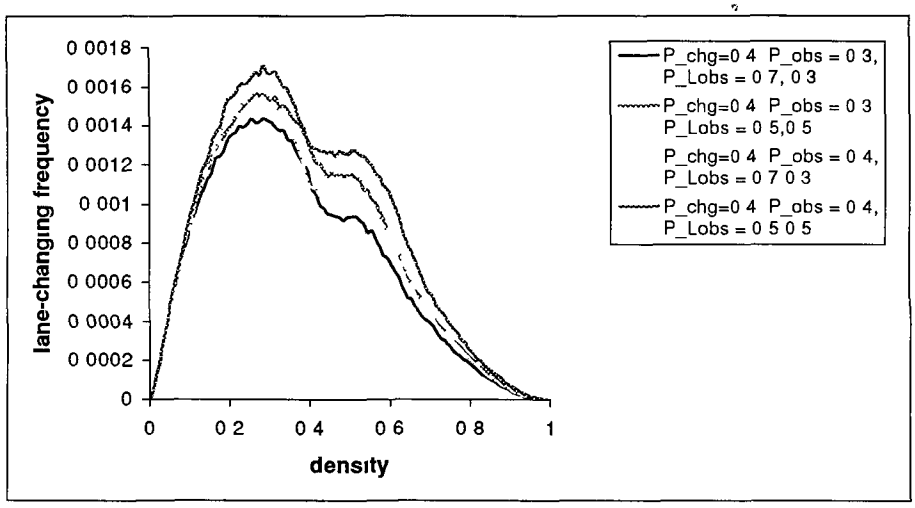

(a)

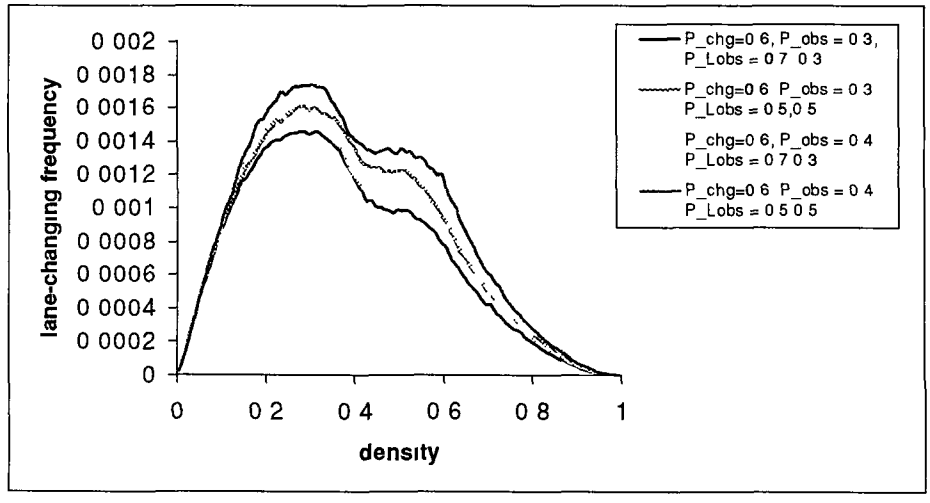

(b)

Fig (5 12) The effect of lane-changing probability on the frequency of lane changes It is easy to observe that the effect of increasing P_chg on the frequency of lane changes depends on the other parameters, P_Lobs and P_obs

5.4 Model validation

Unfortunately, there exists no source of real data, which studies lane-usage characteristics on two-lane roads in urban areas In this regard none of the available studies were devoted for urban traffic, but they were concerned only with highway traffic So, in order to calibrate our *lane-changing* rules, we have, performed a simple study on one of Dublin's two-lane streets This was attempted in May 1998, as follows A video camera was set up on a high building, overlooking the street of interest The street, which is 250m in length, is controlled by traffic lights from both sides at two intersections and has one pedestrian crossing We were interested in calculating the lane usage frequency for each lane Data were obtained for 4-hours per day for four different consecutive days One limit of this empirical study was the lack of required equipment for surveying a longer urban street with many intersections Another, clearly, was the limited period of time for which the survey could be considered and we acknowledge Dublin Corporation, Traffic Section, for facilitating us on this Unfortunately, we did not find any study of urban traffic in relation to *lane-changing* to compare our data with

On highway traffic, Sparmann (1978) has demonstrated an important macroscopic phenomenon called " *lane-usage inversion*" or " *density inversion*", which occurs long before maximum flow

The *lane-changing* rules, presented in this chapter, appear to reproduce the same phenomenon for urban traffic, within the limitations of the simulation employed, c f Figs (5 13) and (5 14)

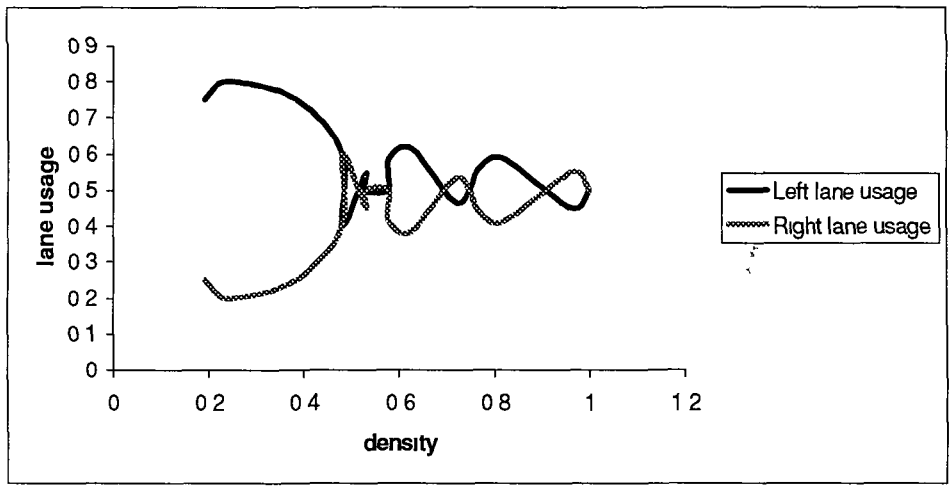

Fig (5 13) lane-usage vs traffic density for empirical data Data were averaged every 3-minutes for a small Road segment in Dublin City

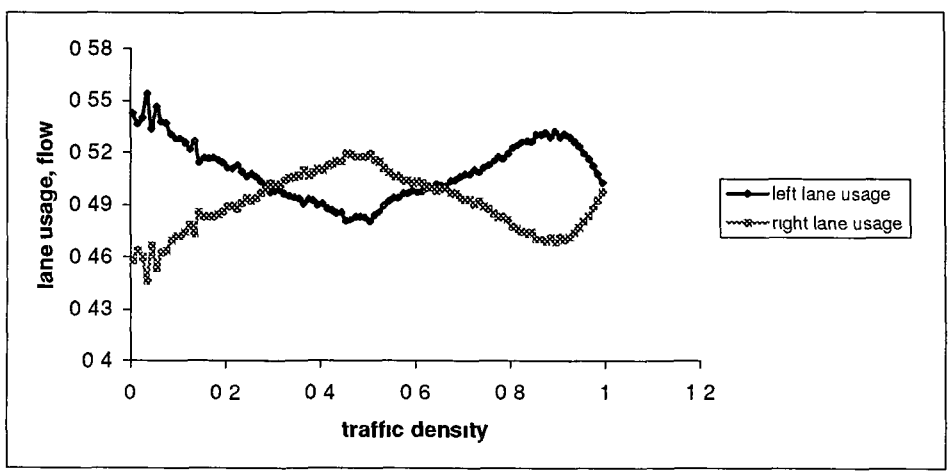

Fig (5 14) lane-usage frequency vs traffic density It can be seen that the first *"density inversion"* has occurred also long before maximum flow density

The first "*density inversion*" in our simulation has occurred long before the density of maximum flow This is in agreement with Sparmann (1978)

As has been described in Sec (5 3), the "*density inversion* " point is adjustable by the *lane-changing parameters*, P_chg, P_obs, and P_Lobs The choice P_chg = 0 4, P_obs = 0 3, P_Lobs = 0 5 for both lanes left and right, gives a reasonably good approximation to our observed data

The data, presented in Fig (5 13) indicate that the lane-usage frequency for both lanes is not correctly modelled at very large densities ($\rho > 0\ 7$) The left lane flow is higher than the right lane flow This, for example, may be due to the fact that long vehicles were not modelled in our simulations, which have a great influence on the city traffic However, the limitations of this study in regard of street and time for data collection have been noted earlier clearly, further experimental or observational studies on larger roads are needed

Chapter 6

"Stochastic Cellular Automata Model for Inter-urban Traffic"

6.0 Introduction

In this chapter, we move from one-speed deterministic cellular automaton models, where stochasticity was introduced through the random feeding mechanism and probabilistic lane-changing rules, to a completely stochastic cellular automaton model, with more than one-speed

The need for such models becomes necessary as we move from urban areas, where links between junctions do not exceed 50-500 m, to inter-urban areas with links, which may exceed 10-15 km

In the latter case, cars have a good chance to interact with each other, generating a very complex driving process or "traffic dynamics"

In this model we try to simplify the above, complicated dynamics by concentrating on the most important elements of driving, of course without losing the essentials of the start-stop waves dynamic

According to the rules of road traffic in Ireland, the following Table (6 1) demonstrates the car velocity and the safe distance needed in order to brake without colliding with the leading car (or car in front)

Table 6.1

Velocity	Safe distance in sites
v = 1	1 site
v = 2	3 sites
v = 3	5 sites

Where one velocity unit is equivalent to 13 5 mph

The following relation can give the safe distance *ds* for a car moving with velocity *v* relative to the front car

$$ds = 2(v - 1) + 1, \qquad v = 1, 2, 3 \qquad (6\ 1)$$

Car acceleration or deceleration at the next time step is then dependent on the above safe distance

6.1 The model

The model is defined on a one-dimensional lattice, which is regarded as a road segment, of k identical sites (cells) The state of every cell is either empty or occupied by a car, where each car has an integer velocity varied between 0 and maximum velocity v_{max} The number of empty sites ahead of a given car is called *gap*

6.1.1 Definition of the Model

For any given car, the number of empty sites to the front car after securing the safe distance for the current car speed is called "*free headway distance*" and denoted by "*dx*", which can be defined as follows

$$dx = gap - ds \qquad (6\ 2)$$

The model update rules depend on the relation between the car velocity and its *free headway distance* This means that starting from an arbitrary configuration of cars, the following rules are applied in order to update the cell state at time instant $t+1$, given its state at time t This is applied simultaneously for all cars

Rule 1 "**Irregularities in the driver behaviour**"

Let v be the current car speed and its target speed at the next time step

$v \pm a$*

If ds $(v \pm a) > gap(v \pm a)$, $a = 0, 1, 2, 3$

Then, with probability P_inc, the driver will replace

$gap\ (v \pm a) + b$ by $ds(v \pm a)$, $b \in Z,\ 1 \leq b < v \pm a$

Rule 2 "**acceleration**"

If v< v_{max} and $ds\ (v + 1) \leq gap\ (v + 1)$

Then, with probability P_ac, the car will accelerate to

$S = v + 1,$

Rule 3 "**deceleration**"

If $v > dx(v)$ and $ds(v\text{-}a) \leq gap(v\text{-}a)$,

Then the car will decelerate to

$S = v\text{-}a,$ $a = 1, 2, 3$

Rule 4 "**speed fluctuation**"

If the car is moving with constant velocity, then with probability P_rd the car will reduce its speed to

$S = v\text{-}r,$ $r \in Z$ and $r \in [1, 3]$

Rule 5 "**car movement**"

Every car advances d sites ahead where

d = max(v, S)

---

a = 1 in case of acceleration

6.1.2 Implementation of the Model

In what follows, we chose $v_{max} = 3$ to confirm with traffic regulations in Dublin, which allow a speed of 40 MPH (~ 3 in the model)in inter-urban areas

The use of the above probabilities, P_inc, P_rd, and P_ac, is essential in order to simulate realistic traffic flow in inter-urban areas They generate three different traffic properties, which characterise the inter-urban traffic as follows

i. Irregularities in the drivers behaviour

In inter-urban areas its is obvious that not all the drivers will comply with the rules of the road and keep the required safe distance to the car ahead

In Rule 1, our aim is to model this " irregular behaviour" of the driver using the probability P_inc, which control the irregularities in the driver behaviour This can be demonstrated as follows

Example:

Assume that we have the following configuration of cars, where each number represents the current car velocity and "dots" are empty sites

....2.....3....

Now the following car has the velocity $v = 2$, which means that the required *safe distance* for this speed from Equation (6 1) is

$$ds(v=2) = 2(2-1)+1 = 3$$

and the *free headway distance* for this car from Equation (6 2) is

$$dx(v=2) = 6 - 3 = 3$$

As $dx(v) > v$, the driver will try to accelerate to $v + 1$ and the requirement for this acceleration, according to Rule 2, is that

$$ds(v + 1) \leq gap(v + 1)$$

According to the above configuration

$$ds(v + 1) = 5 \text{ and } gap(v + 1) = 3$$

which implies that

$$ds(v + 1) > gap(v + 1)$$

Now Rule 1 applies, because $b = 2 < v+1$ Therefore, with probability P_inc the driver will replace $gap(v + 1) + 2$ by $ds(v + 1)$ and with probability 1- P_inc he will not

ii. Delay factor

Rule 2 reads as follows

With a certain probability, P_ac, only, a car will accelerate to the new speed $v + 1$ and with probability $1 - P\_ac$ it will not, even if the requirements for acceleration are completely fulfilled

The reason behind introducing the above probability is to model a very important property of realistic traffic flow in inter-urban areas, which is the delay in acceleration For example, this delay may occur in the following cases

i The car is travelling with $v < v_{max}$ and it has *enough free headway distance* to accelerate, but the car is coming to a pedestrian or traffic light

ii Other problems not related to normal road features, e g bad weather, Road works, and faulty car performance

iii. Speed fluctuations

Traffic through urban areas is controlled by many factors such as; traffic lights, pedestrians, zebra crossings.....etc.

Therefore, the *free headway distance* is not always the main cause behind the oscillation in the car movements between acceleration or deceleration.

The above factors lead to a stochastic sequence of changes in car speed and speed fluctuations, which vary, from one car to another. In our stochastic model, a fluctuation in speed occurs, with probability P_rd, provided that a car is moving with constant speed as follows: If $v = v_{max}$ or $v = dx(v)$ then, with probability P_rd, the velocity v is reduced to $v - r$, where r is an integer randomly chosen from the interval $[1, v_{max}]$.

Using the above probabilities, P_inc, P_rd, and P_ac, will generate stochastic sequences for the changes in the car speed as follows:

$$0 \rightarrow 0 \rightarrow 1 \rightarrow 1 \rightarrow 2 \rightarrow 2 \rightarrow 2 \rightarrow 0 \rightarrow 1.....$$

Where each integer number represents the current car velocity.

6.2 Simulation and Results

We have performed simulations with the Stochastic Cellular Automata Model (SCAM) with various initial conditions. The Lattice size = 200 cells and closed boundary conditions have been applied. In our simulation, car velocity ranges from $v = 0$ to $v_{max} = 3$ and different values for the model parameters, P_inc, P_rd, and P_ac, were investigated, see Sec(6.2.3).

Each run was calculated up to 3000 time steps, and the data averaged over 50 runs, after a discard period of 500 time steps Each curve contains about 100 data points

6.2.1 Model Dynamics

Model dynamics are easier to follow by visualising the time-evolution of the Automaton with the help of the space-time diagrams e g (Fig (6 1))

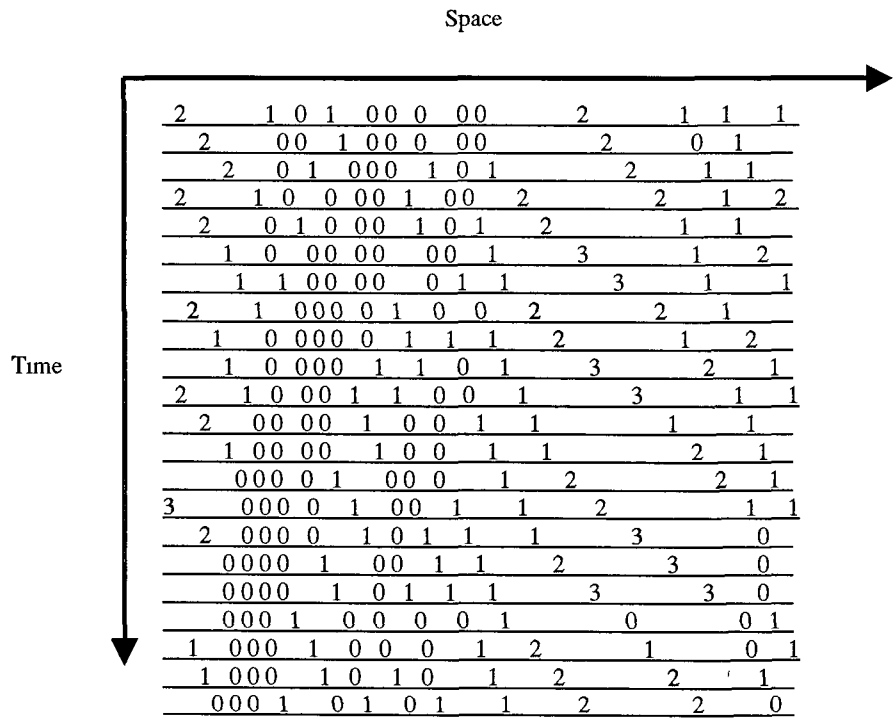

Fig (6 1) space-time diagram at density (ρ) of 0 22 for a system of size 200 cells and v_{max} = 3, P_inc= 0 5, P_rd= 0 3, P_ac =0 5 Each new row shows the traffic system after one update step and just after the car motion

Rows are configurations at consecutive time-steps Dots represent empty sites, and integer numbers indicate the car velocity located at the given site.

The most impressive way to describe the traffic flow is by a diagram, which shows the space-time curves of a set of cars over a road segment Such diagrams have been produced by Treiterer (1975) in the United States by aerial photography The typical patterns of car configuration for the car densities 0 16 and 0 22 are presented in Fig (6 2 a and b), where the first density is slightly below the density of maximum flow, see below, and the second is slightly above the density of maximum flow

In Fig (6 2) each black Pixel represents a car, with trajectory indicated by a dotted curve Cars are moving from left to right and from top to bottom, i e from top left corner to bottom right corner Vertical trajectories mean that cars are completely blocked, whereas diagonal trajectories show car movement

Traffic jams or *jam waves* are identifiable as solid areas in the space-time diagrams At low densities, slightly below the density of maximum flow, (as in Fig (6 2 a)), we find that laminar traffic is the dominant pattern, despite the appearance of small jams, which occurs randomly due to speed fluctuations

The appearance of these small jams becomes more noticeable as we exceed the density of maximum flow, see Fig (6 2 b), and their lifetime becomes relatively longer

On the other hand, the high-density regime, (Fig (6 3)), is characterised by random formation of congested clusters, due to the stochasticity elements in our model The lifetime of these traffic jams becomes continuous to increase compared to those obtained at low densities (Fig (6 2 (a) and (b))

The Figure also shows the backward movement of the traffic jams, i e against the traffic flow

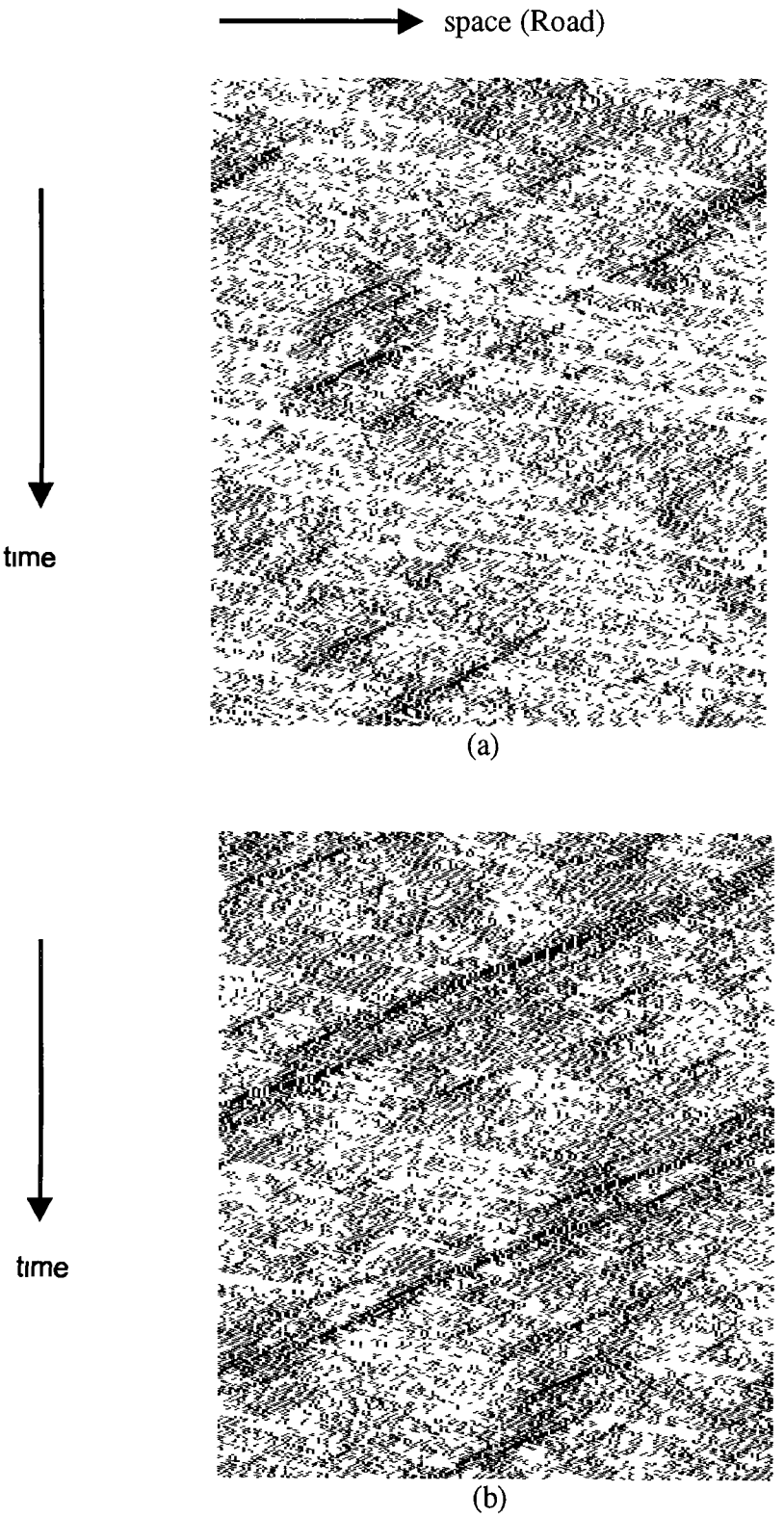

Fig (6 2) The typical patterns of car configurations up to 1500 time steps, where L =200, v_{max} = 3, P_inc= 0 5, P_rd= 0 3, P_ac =0 5
(a) the pattern for density of 0 16 (b) the pattern for density of 0 22

Fig (6 3) shows that these congested clusters represents a typical start-stop wave and, due to lack of real data in our study, may be compared to data obtained for simulated highway traffic (Nage and Schreckenberg(1992) On this basis, the model appears to produce fairly realistic results

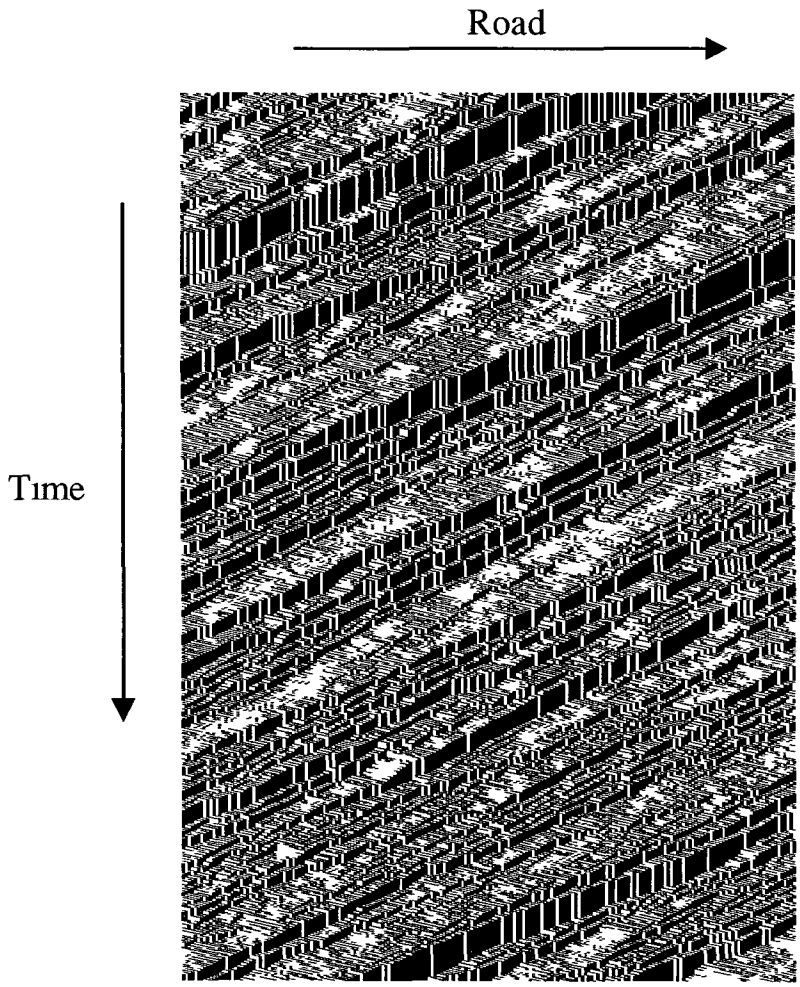

Fig (6 3) Space-time diagram for the SCAM, v_{max} = 3, P_inc= 0 5, P_rd= 0 3, P_ac =0 5, and ρ = 0 5 Black dots represent cars, consecutive horizontal lines represent configurations at consecutive time steps It can be seen that the traffic jams,(sold areas), are moving backwards

6.2.2 Fundamental diagrams

Next we study the fundamental diagrams, flow-density relation q-ρ and velocity-density relation v-ρ, of our SCAM

The definitions of the above macroscopic aggregate variables, q, ρ, and v, for which data are shown in the fundamental diagrams, have been introduced in Sec (2 1 1), using Equations (2 1)-(2 4)

The simulation reveals that the maximum flow obtained was $q_{\max} \sim 0\ 24 \pm 0\ 02$ at the density $\rho_{q\max} = 0\ 18 \pm 0\ 01$ (Fig (6 4 a)) In contrast the maximum flow obtained by Nagel and Schreckenberge (1992), in highway traffic, was $0\ 318 \pm 0\ 0005$ and obtained at lower density ($0\ 085 \pm 0\ 004$), where $v_{\max} = 5$

Further simulations, (Fig (6 4 (b)) shows that the system size does not have a significant effect on the above two extremes, $q_{\max}$, $\rho_{q\max}$, where data were long-term averaged

The flow-density relation (Fig.(6 4)) can be characterised as follows

i Low-density phase, where the drivers change their speed according to rules of the road and the traffic control system In this regime, flow increases linearly by increasing the traffic density

ii High-density phase, where the drivers change their speeds according to the needs of driving in a queue The high-density phase is characterised by periodic start-stop waves (Fig (6 3)) and the significant drop in the system flow as in Fig (6 4)

In between the above two-regimes, the traffic dynamic is hard to explain In Sec (1.1 2 1) we outlined the explanation given by Hall (1995)

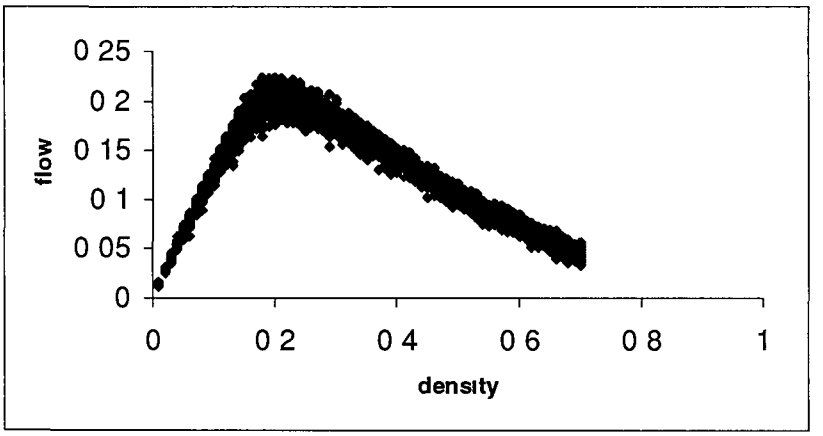

Fig (6 4 a) flow-density relation Points are averaged over short time periods (50 time steps) for a system of size = 200 after a transient period of 500 time steps, where v_{max} = 3, P_inc= 0 5, P_rd= 0 3, P_ac =0 5

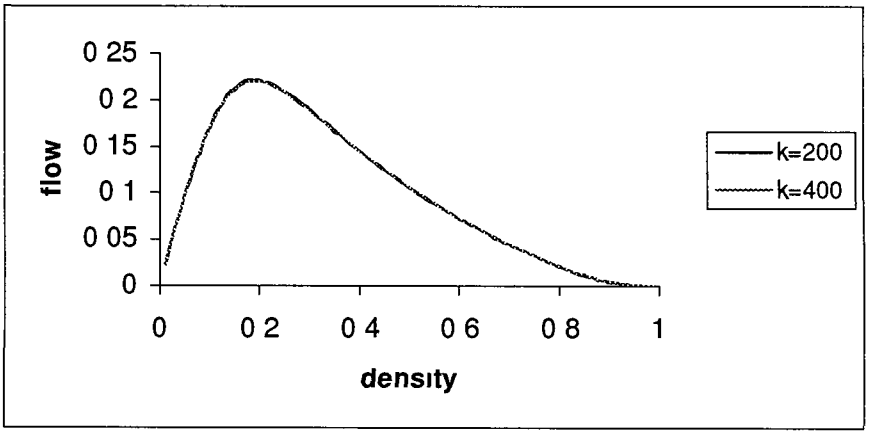

Fig (6 4 b) flow-density relation Lines are averaged over long time periods (2000 time steps) for systems of size = 200, 400 after a transient period of 500 time steps, where v_{max} = 3, P_inc= 0 5, P_rd= 0 3, P_ac =0 5

6.2.3 The Effect of Varying the Model Parameters

Firstly, we look at the influence of changing the model maximum integer velocity on the two-extremes, $q_{\max}$, $\rho_{q\max}$

Our simulations, (Fig (6 5)), show that the position and the form of the maximum flow depend strongly on the maximum integer velocity Reducing the value of $v_{\max}$ in the model has shifted the maximum flow $q_{\max}$ to higher values of density ρ while decreasing its value This is more noticeable for $v_{\max}$ = 1, where the value of $q_{\max}$ has decreased from 0 2209, in case of $v_{\max}$ =3, to 0 1286 obtained for $v_{\max}$ =1(i e a decrement of 58% approximatly) Also, the fundamental diagrams show the asymmetry seen for real data obtained for highway traffic (Hall and Gunter, 1986)

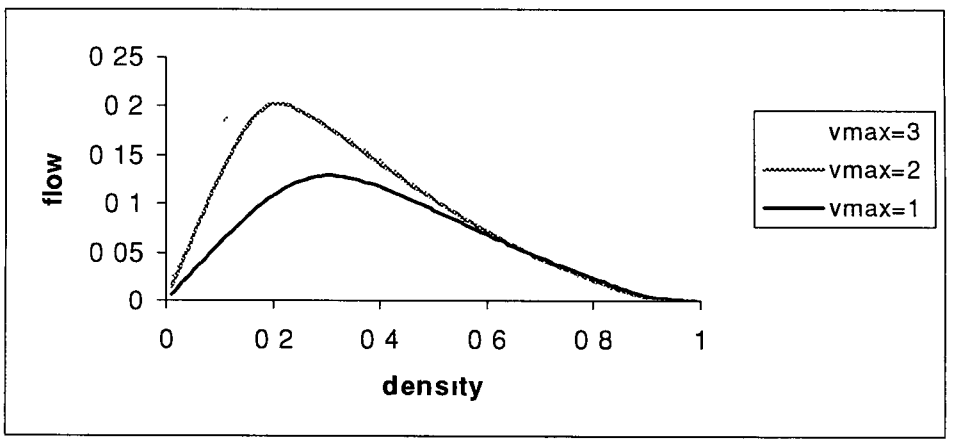

Fig(6 5) Fundamental diagrams obtained by varying the model maximum integer velocity, where P_inc = 0 5, P_rd= 0 3, P_ac = 0 5

The system velocity as a function of the traffic density for different values of v_{max} is presented in Fig (6 6)

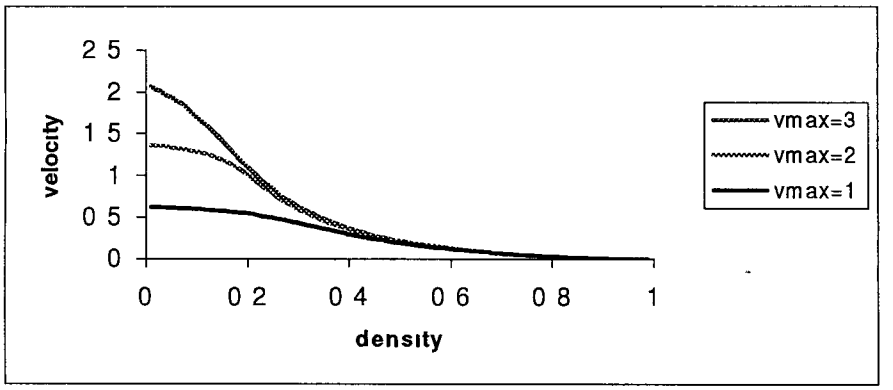

Fig (6 6) Velocity-density relations obtained by varying the model maximum velocity, where P_inc = 0 5, P_rd= 0 3, P_ac =0 5

Fig (6 7) shows that the changes in the acceleration probability (P_ac) have significantly influenced the flow behaviour and the maximum flow obtained

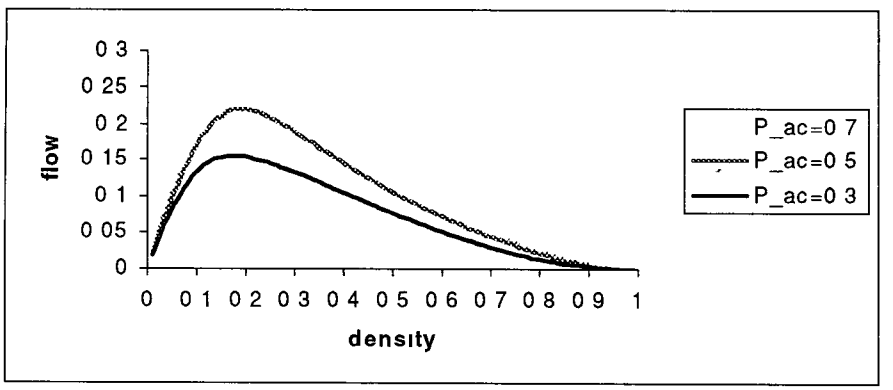

Fig (6 7) Different fundamental diagrams obtained by varying the value of P_ac, where v_{max} = 3, P_inc = 0.5, and P_rd= 0.3

Increasing the value of P_ac from 0 3 to 0 7 has increased the maximum flow from 0 1554 to 0 2557(i e an increment of 65% approximately)

In contrast using higher values for P_rd has reduced the maximum flow from q_{max} = 0 2209 to q_{max} = 0 2008, which means a decrement of 9% approximately, see Fig (6 8)

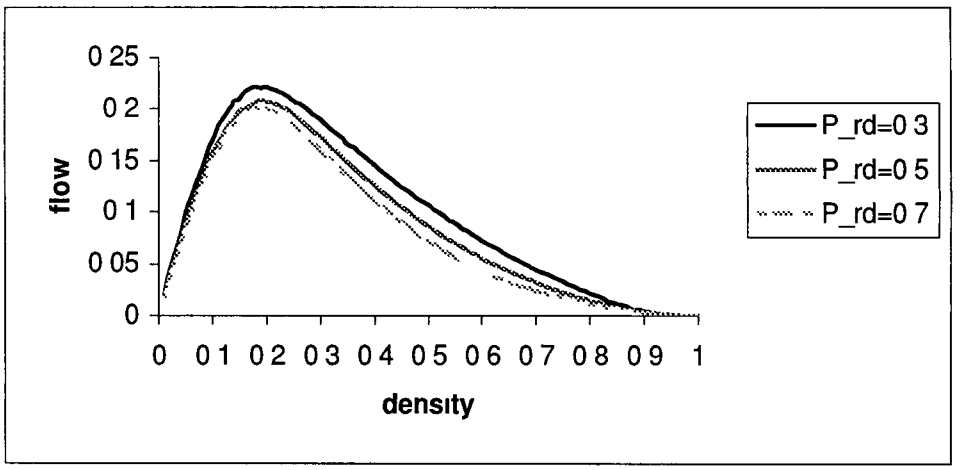

Fig (6 8) fundamental diagrams obtained by varying the value of P_rd, where v_{max} = 3, P_inc = 0 5, and P_ac= 0 5

Fig (6 9) shows that varying the value of P_inc has influenced both the position and the values of maximum flow Increasing the value of P_inc from 0 3 to 0 7 has shifted the maximum flow to higher values of ρ (0 22) and slightly decreases its value from 0 2237 to 0 2181 At this density, 0 22, the two curves crossover and the flow becomes higher as P_inc increases from 0 3 to 0 7 This situation was dominant until ρ ~ 0 55, then the flow becomes similar on both lanes All the above experiments involve changing the model parameters individually, i e varying one of the model's parameters while keeping others at the same values

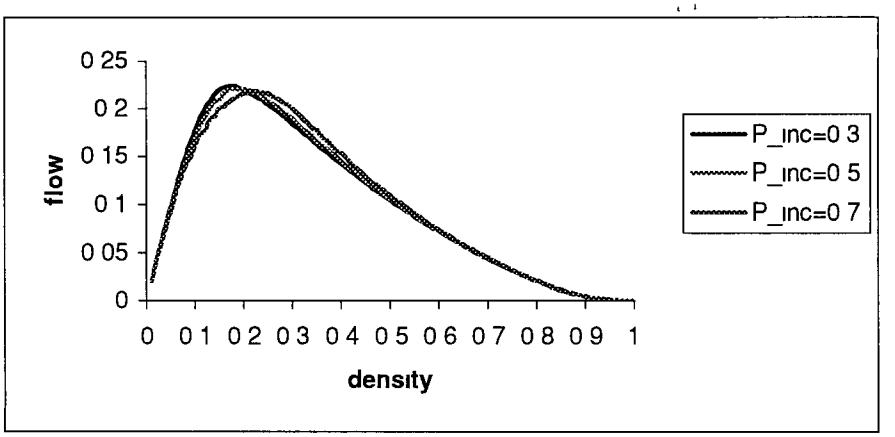

Fig (6 9) Flow-density relations obtained by varying the value of P_inc, where v_{max} = 3, P_ac = 0 5, and P_rd= 0 3

This has resulted in different traffic flow patterns, which can be interpreted as changes in the traffic behaviour, due to different circumstances, (e g speed limits, bad weather, road conditions, etc)

Secondly, by keeping v_{max} =3, we look at different combinations of the model parameters(P_inc, P_rd, P_ac) The summary of the simulation runs can be found in Table (6 2), where three values for each parameters were used(0 3, 0 5, and 0 7)

Looking at the values of q_{max} , $\rho_{q\,max}$ in Table (6 2), it is easy to see that the model can be adapted to model a wide range of traffic circumstances, as above The minimum value of q_{max} is obtained at bad driving conditions (P_rd = 0 7, P_ac = 0 3), with maximum velocity obtained 1 6447 (i e 22 2 mph)

P_ınc	P_rd	P_ac	$\rho_{q\max}$	$q_{\max}$
0 3	0 3	0 3	0 17	0 1565
0 3	0 3	0 5	0 18	0 2231
0 3	0 3	0 7	0 16	0 2521
0 3	0 5	0 3	0 17	0 1483
0 3	0 5	0 5	0 18	0 2093
0 3	0 5	0 7	0 16	0 2395
0 3	0 7	0 3	0 16	0 1427
0 3	0 7	0 5	0 17	0 2025
0 3	0 7	0 7	0 16	0 232
0 5	0 3	0 3	0 17	0 1557
0 5	0 3	0 5	0 18	0 2219
0 5	0 3	0 7	0 17	0 256
0 5	0 5	0 3	0 17	0 1464
0 5	0 5	0 5	0 19	0 2083
0 5	0 5	0 7	0 18	0 2433
0 5	0 7	0 3	0 17	0 1404
0 5	0 7	0 5	0 19	0 2005
0 5	0 7	0 7	0 19	0 2352
0 7	0 3	0 3	0 18	0 1533
0 7	0 3	0 5	0 22	0 2181
0.7	**0.3**	**0.7**	**0.18**	**0.2609**
0 7	0 5	0 3	0 18	0 1445
0 7	0 5	0 5	0 21	0 2054
0 7	0 5	0 7	0 20	0 247
0.7	**0.7**	**0.3**	**0.18**	**0.1389**
0 7	0 7	0 5	0 21	0 1981
0 7	0 7	0 7	0 20	0 2389

Table (6 2) The ınfluence of varyıng the model parameters on the two extremes

In contrast, improving the driving conditions by decreasing P_rd to a lower value (P_rd = 0 3) and increasing the value of P_ac to a higher value (P_ac=0 7) has lead to the maximum value of q_{max} (0 2609) and also increased the system velocity to a higher value (2 2044)

Further, the two extreme values of q_{max} ,(minimum and maximum values), were obtained, suprisingly, at the same traffic density ($\rho_{q\,max} = 0\ 18$)

Table (6 2) shows that most values of $\rho_{q\,max}$ are obtained at the density of 0 18 $\pm$ 0 01, with some cases where $\rho_{q\,max}$ is obtained at a lower (higher) densities than 0 18 $\pm$ 0 01 This is due to due to different combinations of the extreme values of the model parameters in order to obtain a realistic traffic patterns

6.3 Open Systems

In this section, we apply different boundary conditions and apply the same rules of the stochastic cellular automata model The system inputs and outputs are treated as follows

- At the left side of the road, a stochastic feeding mechanism, in which car arrivals follow a Poisson process, has been implemented throughout the simulations for different arrival rates
- On the other hand, cars may leave the system at the right side of the road This is achieved by ensuring that the last three sites of the road are empty

The above conditions for the system input and output will create open boundary conditions

The fundamental diagram for the stochastic model (Fig (6 10)) was obtained, starting with a random initial configuration of density 0 2 and velocity $v = 0$, by applying open boundary conditions and employing different rates of arrivals The simulations included a system of size 300 sites for duration of 10,000-time step After relaxation, 1000 time steps, the maximum flow obtained is

$$q_{\max\ open} = q_{\max,closed} + c, \qquad \text{where} \quad 0\,0 < c < 0\,03 \qquad (6\,3)$$

at density of

$$\rho_{q_{\max\ open}} = \rho_{q_{\max,\ closed}} - c_1 \qquad \text{where} \quad 0\,0 < c_1 < 0\,04 \qquad (6\,4)$$

The above results mean that a higher flow is obtained at lower density, compared to the model with closed boundary conditions

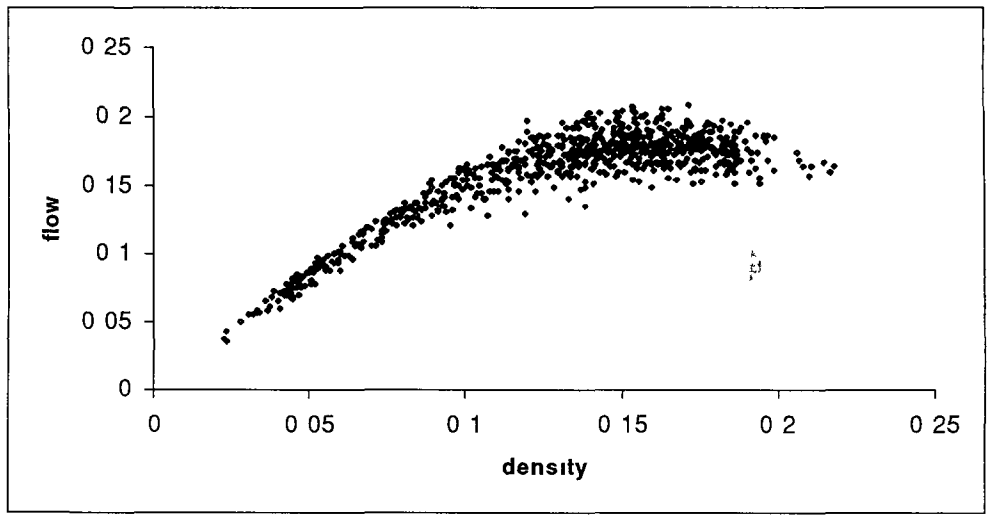

Fig (6 10) Fundamental diagram of the stochastic model using open boundary conditions Points are averaged over short-time periods (50 time steps) for a system of size = 300 after discard period of 1000 time steps Duration of system evolution = 10,000 time steps Data relate to different arrival rates, where $v_{\max}$ =3, P_inc=0 5, P_rd=0 5, P_ac = 0 4

6.3.1 Bottleneck Situations

One of the important factors in traffic science is the existence of bottlenecks, i e sections that have less capacity of accommodating traffic than do other sections of the road A very common example of a bottleneck situation is a two-lane directional road merging into one lane only

In order to obtain a bottleneck situation in the following simulation, we apply a high rate of arrivals ($p = 0\ 6$) starting from a high initial density Duration of the simulation is 10,000 time steps for a system of size 300 cells

6.3.2 Self-organization of the Maximum Throughput

For the conditions specified in the previous section, our model shows that the outflow from a jam appear to self-organize into maximum throughput This phenomenon of self-organized criticality was reported initially by Bak et al (1987) using a one-dimensional sand-pile cellular automata model as the transport process, but our model indicates a state of non-trivial critical density (i e $\rho_c \neq 0$) in agreement with Nagel (1994, 1995) This can be seen from Fig (6 11), where the system size k=300 and the initial density is 0 56 with P_inc = 0 5, P_rd = 0 5, and P_ac = 0 5 After a relaxation of 1000 iterations, we started to collect our averages every 50-time steps The maximum flow obtained is $q_{\max open} = 0\ 2185$, which is 0 0102 greater than the maximum flow obtained in closed systems, at lower density ($\rho_{q_{\max\ open}} = 0\ 15$)

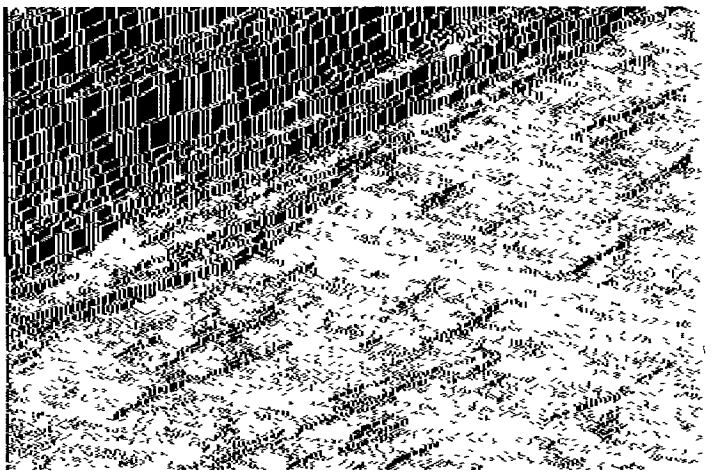

Fig(6 11) space-time plot of the outflow from a jam, where the system size = 300, starting from a dense traffic ρ = 0 56,and apply high arrival rate on the left boundary μ = 0 6,

v_{max} =3, P_inc=0 5, P_rd=0 5, P_ac = 0 5

6.4 Summary and Conclusion

A stochastic cellular automata model for the traffic in inter-urban areas is presented in this chapter The model is defined on a one-dimensional lattice of k-identical cells, where each cell is either empty or occupied by a car, where each car has an integer velocity varied between $v = 0$ and $v = v_{max}$

The model update rules depend on the relation between the car velocity and its free headway distance and take into account some of the basic features, which characterise the inter-urban traffic such as delay in acceleration, speed fluctuations, and irregularities of the driver behaviour only in term of gap acceptance

Our simulation results can be summarized as follows

- The maximum flow $q_{max} = 0\ 24 \pm 0\ 02$ was obtained at density $\rho_{max} = 0\ 18 \pm 0\ 01$, further simulation reveals that the system size does not effect these values
- At low densities, we found that laminar traffic was the dominant pattern despite the appearance of small jams, whereas the high density regime was characterized by congested clusters, which represent typical start-stop waves
- The simulation conducted in Sec(6 3 3) shows that the model can be adapted to model various traffic conditions such as bad weather, rush hours, etc, by modifing its parametrs
- When open boundary conditions were applied, a higher values for the maximum flow was obtained at lower densities
- Applying open boundary conditions with higher arrival rate, the model indicates that the outflow from a traffic jam appears to self-organise to a maximum flow

Chapter 7

"Summary and Conclusions"

7.0 Research Contribution

The main contribution in this research lies in developing three cellular automata models for traffic flow in urban and inter-urban areas, which can be summarized and discussed as follows

A simple cellular automata model for urban traffic is presented, the model is a three state deterministic cellular automaton with both space and time, discrete

The state of each site at next time step is determined from the state of the site itself and those of the nearest neighbour sites, where $v_{max} = 1$ is the maximum possible jump for each particle For an arbitrary configuration, one update of the system consists of the transition rules described in Sec (2 2), which are performed in parallel for all sites

It is hard to classify the cellular automata models in the frame of car following theory, (described in Chapter 1, Sec (1 1 1 1)) In our model the stimulus can be regarded as the gap between adjacent sites in the automata

Car movements, (described by rules, Rule 1, Rule 3, and Rule 4, defined in Sec (2 1)), can be viewed as the response, in the case of acceleration, whereas Rule 2 may be considered as the deceleration due to insufficient space ahead

Our simulation reveals that the system, (imposing periodic boundary conditions), reaches its critical state at density $\rho_c = 0\ 5$ and the maximum flow obtained was $q_{max} = 0\ 5$ after a discard period $t_o = \frac{k}{2}$, which does not depend on the system size

This was also obtained by Nagel and Schreckenberg (1992) in the deterministic limit of their stochastic model using $v_{max}=1$, but after a much higher transient period For densities less than the critical density ($\rho < \rho_c$), the kinematic waves move forward with velocity 1 In contrast, for densities higher than ρ_c, the kinematic waves move backward with velocity -1 The open boundary conditions, (described in Chapter 2, Sec (2 3 2)), have led to lower values for maximum flow and its density, compared to maximum flow obtained for closed systems, which depends on the system size

The model, then, is adapted to model road traffic, where the road is formed by linking a finite number of segments separated by traffic lights In urban traffic, our experience and every day observations says that cars have to wait for a certain period of time in order to leave a specific road

This time period depends on the number of the traffic lights installed between road segments and the duration of both light cycles, red and green, as well as the traffic density To examine the realism of our simulation model, a new parameter" jammed time t_j" is introduced, which represents the number of time steps a car has to wait in order to leave the road Our simulation results show that this parameter, as in real traffic, depends on the number of traffic lights and the duration of each light cycle

The real task for our "toy" model was its ability to simulate traffic flow at network level Four different networks, varying from 17 nodes, (8 km length), to 41 nodes, (24 km length), have been used in the simulation, the limitations of this

range is due to the effort needed to represent larger size networks However, future work has to incorporate larger size networks

Each network node corresponds to a signalized intersection, timing of signals at all nodes followed two-phase timing scheme At all nodes traffic movements followed turning percentages as described in Chapter 3, Sec (3 1 5) Cars are injected into the network according to a Poisson process with parameter μ, where different values for μ are used

Two types of simulation were executed, the first considers the transient movement of cars along the networks, whereas in the second cars were allowed to park inside the network, using underground parks, and the network behavior under short and long-term events were also investigated

The simulation results strongly suggest that traffic flow in urban street networks and the parameters governing its performance may be characterized using the Simple Cellular Automaton Models

Our findings indicate the following

- The characteristic shape of the fundamental diagrams as observed for highway traffic is, surprisingly, obtained at urban network level, despite the complex interactions in urban traffic This is in agreement with Williams (1986), and results obtained here appear to reflect realistic traffic behaviour
- The simulation reveals that there is a critical arrival rate" *jamming threshold*" above which the network is not able to handle the incoming traffic any more, which results in " *queues outside the network*" This "*jamming threshold*" is

independent of the network size in the case of transient movement simulation, whereas different "*jamming thresholds*" for different network sizes were obtained in the case of non-transient movement simulation

- At low arrival rate and also slightly above the "jamming threshold" a significant interaction,(α = 0 01), between the traffic conditions, transient period, and the interval length was obtained for smaller size network, 17 nodes This interaction became insignificant for larger size network, 41 nodes
- Modelling long-term events, such as blocking some of the network exits, has successfully reproduced the jamming effect typically seen in highly congested networks at peak-times

Using single-lane networks, important features such as *lane-changing* and its impact on the flow behavior in urban networks cannot be observed and studied Compared to highway traffic, *lane-changing* in urban areas is more complex This is because the decision to change lane in urban areas depends on a number of objectives and at times these may conflict

Despite this complexity, our aim is to find the minimal sets of lane-changing rules, which are capable of reproducing important macroscopic features such as lane-usage inversion, which is observed long before maximum flow in highway traffic and also observed in urban traffic flow in our study, but at higher density, see Sec (5 4)

In this regard a two-lane model is introduced, which consists of two parallel single-lane model and three sets of rules for lane-changing defined as follows urgent lane-changing conditions, minimal and maximal lane-changing conditions Our simulation reveals that the above lane-changing rules were able to reproduce the lane-usage inversion as obtained in both highway and urban traffic

The "*density inversion*" point is modified by the *lane-changing parameters*, P_chg, P_obs, and P_Lobs The choice P_chg = 0 4, P_obs = 0 3, P_Lobs = 0 5 for both lanes left and right, gives a good approximation to our observed data in a study performed in Dublin city to calibrate our lane-changing rules The limitations of our study was mentioned in Sec (5 4)

However, the lane-usage frequency for both lanes is not correctly modelled at very large densities, where left lane flow is higher than the right lane flow

In the last chapter we moved from deterministic cellular automata models to a completely stochastic cellular automaton models in order to model traffic in inter-urban areas with links that may exceed 5 km

The stochastic model, also, is defined on a one-dimensional array of k sites The state of each site is either empty or occupied by a car, where each car has an integer velocity between $v = 0$ and $v = v_{max}$ The model update rules, described in Sec (6 1 2) depend on the relation between the safe distance of the car velocity and its free headway distance

The model correctly reproduces the start-stop waves and the flow-density relation shows the asymmetry known from the real data obtained for highway traffic

The simulation reveals that the model can be adapted to model various road traffic conditions, by modifying its parameters

In case of an open system the model gives a good approximation to the flow-density relation obtained for highway traffic and indicates that the outflow from a jam appears to self-orgamze to maximum flow, when a high arrival rate is applied, starting from a dense traffic condition

Throughout this thesis **Microsoft Excel** was used to plot all our graphs, and a C++ code, which uses bitmaps see Appendix E **a:\ Space-time\ bc.c**, was used to plot all the space-time diagrams A bitmap is a powerful graphics object used to create, manipulate and store images as files on a disk

7.1 Future Work

- Despite the deterministic update rules of the Simple Cellular Automata Model, it was able to reproduce important features of urban traffic

  Adding the stochasticity element to the update rules might yield a more realistic behavior of the model
- Buses and Trucks represents more than 50% of the urban traffic, so future work has to be directed to incorporate long vehicles in the model (i e non-homogenous units)
- Also, future simulation has to involve networks with complex intersections (i e intersections with complex geometry), and roundabouts

- Extend the two-lane model to include a third lane, which is dictated as a bus-lane The bus-lane represents one of the important short-terms events in urban traffic
- Investigate the efficiency of the simulations in the case of non-homogenous units by looking at the bit-wise coding and also the use of parallel computing
- In case of the stochastic CA model, more investigations are required to study and scale the formation of the spontaneous traffic jams, Also, the limits of the model has to be investigated in some detail
- Use the models developed in this research to develop a High Speed Microscopic Simulation for Urban and Inter-urban Traffic (HSMSUIT) simulation package

7.2 Concluding Remarks

In this research, we have seen the importance and the capabilities of the Cellular Automata methodology in modelling traffic flow in urban and inter-urban areas Despite the complexity of the traffic dynamics, the advances we have seen in the last years are demystifying the idea that Cellular Automata are too simple to be capable of simulating highly complex systems

Bibliography

- Ardekani, S and Herman, R , 1987 Urban Network-Wide Traffic Variables and their relations Transportation Science, 21 (1), 1-16
- Allen, A , 1978 *Probability, statistics, and queueing theory* Academic press
- Adamatzky, A , 1994 *Identification of cellular automata* Taylor & Francis
- Bak, P , Tang, C , Wiesenfeld, K , 1987 Self-organized criticality Physical review, 38 (1), 365-374
- Biham, O and Middleton, A 1992 Self-organization and a dynamical transition in traffic flow models Physical Review A, 46 (10), R6124-R6127
- Brackstone, M and McDonald, M The microscopic modelling of traffic flow weakness and potential developments, Workshop on Traffic and Granular Flow, 9-11 October 1995 Julich
- Brilon, W and Ponzlet, M , Application of Traffic Flow Models, Workshop on Traffic and Granular Flow, 9-11 October 1995 Julich
- Brilon, W , 1988 *Intersections without traffic signals* London Springer
- Brilon, W , 1991 *Intersections without traffic signals* II London Springer
- Barcelo, J and Ferrer, J , 1995 A simulation study for an area of Dublin using the AIMSUN2 traffic simulator
- Binder, P , Buck, B , and Macaulay, V , 1986 Time-series Analysis of a collective variable in High-dimensional Cellular Automata Journal of Statistical Physics, 68 (5/6), 1127-1130

- Binder, P , Jensen, R , 1992 Simulating chaotic behaviour with finite-state machines Physical review A, 34(5), 4460-4463
- Bratley, P , Fox, B , and Schrage, L , 1983 *A guide to Simulation*, Springer-Verlage
- Bando, M, Hasebe, K, and Nakayama, A , 1994 Structure stability of congestion in traffic dynamics, Japan Journal of Industrial and Applied Mathematics, 11(2), 203
- Bando, M , Nakayama, A , Shibata, A , and sugiyama, Y , 1995 Dynamical model of traffic congestion and numerical simulation, Phys Rev E, 51(N2), 1035
- Cremer, M and Ludwig, J , 1986 A fast simulation model for traffic flow on the basis of Boolean operations Mathematics and Computers in Simulations, 28, 297-303
- Cohen, J and Kelly, F 1990 A paradox of congestion in a queuing networks J Appl Prob, 27, 730-734
- Catoni, S and Pallottino, S 1991 Traffic Equilibrium Paradoxes Transportation Science, 25 (3), 240-244
- Chang, M and Herman, R 1981 Trip Time Versus Stop Time and Fuel Consumption characteristics in Cities Transportation Science, 15 (3), 182-209

- Derrida, B , Domany, E , and Mukamel, D , 1993 Exact solution of 1D asymmetric exclusion model using a matrix formulation J Phys A Math Gen 26, 1493-1517
- Dutta, P and Horn, P , 1981 Low-frequency fluctuations in solids 1/f noise Review of Modern Physics, 53 (3), 497-516
- Erica, J , 1986 Global properties of cellular automata Journal of Statistical Physics 43 (1/2), 219-241
- Edie, L , 1974 Flow Theories In Traffic science Ed By D Gazis Wiley, New York
- Fukui, M and Ishibashi, Y , 1993 Evolution of traffic jam in traffic flow model J Phys Soc Japan, 62(11), 3841-3844
- Frisch, U , Hasslacher, B , and Pomeau, Y , 1986 Lattice-Gas Automata for Navier-Stockes Equation Physical Review Letters, 56 (14), 1505-1508
- Gipps, P , 1981 A behavioral car-following model for computer simulation Transpn Res B, 15, 105-111
- Gipps, P , 1986 A model for the structure of lane-changing decisions Transpn Res B, 20B (5), 403-414
- Gazis, C , Herman, R , and Rotherey, W , 1961 Nonlinear follow the leader models of traffic flow Opns Res, 9, 545-567
- Gazis, D , 1974 *Traffic Science* John Wiley
- Gabard, J , 1991, In Concise Encyclopedia of Traffic and Transportation Systems, M Papageorgiou (Ed), Pergamon Press, Oxford

- Gordon, G , 1978 *System Simulation*, 2nd ed Prentice-Hall
- Gallas, A , and Jason, C , 1994 Synchronization effect in the dynamical behaviour of elevators Hochstsleistungsrechenzentrum, Forschungszentrum Julich, D-52425, Germany
- Hall, L , Allen, L , and Gunter, A , 1986 Empirical analysis of freeway flow-density relationships Transpn Res A, 20A (3), 197-210
- Hall, L , and Montgomery, O , 1993 The investigation of an alternative interpretation of the speed-flow relationship for U K motorways Traffic Engineering and Control, 420-425
- Hammad, A , O'hEigeartaigh, M , and Ruskin, H , A cellular automata model to simulate traffic flow in urban networks Presented at the 15th IMACS World Congress, Berlin, and August 1997
- Hammad, A , Ruskin, H , and O'hEigeartaigh Urban network performance under simple CA microsimulations Modeling and Simulation Proceeding of the IASTED International Conference, 13-16 May, 1998 USA
- Herman, R , and Prigogine, I , 1979 A Two-Fluid Approach to Town Traffic Science, 204, 148-151
- Herman, R , Montroll, W , Potts, B , and Rothery, W , 1959 Traffic dynamics Analysis of stability in car following Oper Res, 76, 86
- Herman, R , and Ardekani, S , 1984 Characterizing traffic conditions in urban areas Transportation Science, 18 (2), 101-140

- Improta, G., 1987. Mathematical programming methods for urban network control. In: Flow control of congested networks, F38 of NATO ASI, Springer.
- Janowsky, S.and Lebowitz, J., 1991. Finite-size effects and shock fluctuations in the asymmetric simple-exclusion process. Physical Review A, 45 (2), 619-625.
- Kuhne, R., Macroscopic freeway model for dense traffic- stop-start waves and incident detection. Highway capacity and level of service: Proceedings of the Ninth International Symposium on Transportation and Traffic Theory, 24-27 July 1984. Karlsruhe.
- Krauß, S., Wagner, P., and Gawron, C.,. 1996. A Continuous limit of the Nagel-Schreckenberg-Model. Physical Review E 54, 3707.
- Krauß, S., 1997. The role of acceleration and deceleration in microscopic traffic flow models. Deutsche Forschungsantalt fur Luft-und Raumfahrt, Linder Hohe, 51170 Koln, Germany.
- Lighthill, J. and Whitham, B., 1955. A theory of traffic flow on long crowded roads. Proc. R. Soc. London A229, 317.
- Leutzbach, W. Some Remarks on the history of the science of traffic flow, Workshop on Traffic and Granular Flow, 9-11 October 1995. Jülich.
- Leutzbach, W., 1988. *Introduction to the Theory of Traffic flow*, Springer, Berlin.
- Mahmassani, H. and Peeta, S., 1987. Network Performance under System Optimal and user equilibrium Dynamic Assignments: Implications for

Advanced Traveller Information Systems Transportation Research Record, 83-93

- Mahamassani, H , Jayakrishnan, R , and Herman, R , 1990 Network traffic flow theory Transpn Res A, 24A(2), 149-162
- Mackett, L , 1990 Exploratory analysis of long-term travel demand and policy impacts using micro-analytical simulation In "Developments in dynamic and activity-based approaches to travel analysis" Aldershot Avebury, 384-405
- May, A , 1990 *Traffic Flow Fundamentals*, Prentice Hall, Englewood Cliffs, NJ
- Migowsky, S , Wanschura, T , and Rujan, P , 1994 Competition and Cooperation on a Toy Autobahn Model Z Phys B95, 407-414
- Montgomery, D , 1976 *Design and Analysis of Experiments* John Wiley & sons
- Minister for the environment, 1992 *Rules of the Road* Dublin Stationary office
- Muller-Krumbhaar, H , and Eerden, J , 1987 Some Properties of Simple Recursive Differential Equations Z Physics B, Condensed Matter, 67, 239-242
- Nagatani, T , 1993 Jamming transition induced by a stagnant street in a traffic flow model Physica A, 207, 574-583

- Nagatani, T , 1993 Jamming transition in the traffic flow model with two-level crossings Physical Review E, 48 (5), 3290-3294
- Nagatani, T , 1993 Traffic jam induced by a crosscut road in a traffic flow model Physica A 198, 108-116
- Nagatani, T , 1993 Clustering of cars in cellular automaton model of freeway traffic J Phys Soc Japan, 62(11), 3837-3840
- Nagatani, T , 1994 Traffic jam and shock formation in stochastic traffic flow model of two-lane roadway J Phys Soc Japan, 63(1), 52-58
- Nagatani, T , 1994 Effect of Jam-avoiding turn on jamming transition in two-dimensional Traffic Flow Model J Phys Soc Japan, 63(4), 1228-1231
- Nagatani, T , 1996 Effect of car acceleration on traffic flow in 1D stochastic CA model Physica A 223, 137-148
- Nagel, K and Schreckenberge, M , 1992 A Cellular Automaton Model for Freeway Traffic J Phys I France2, 2221
- Nagel, K and Herrmann , H, 1993 Deterministic models for traffic jams Physica A 199, 254-269
- Nagel, K , 1994 Life times of simulated traffic jams Int J Mod Phys C, 5 (3), 567-580
- Nagel, K Particle hopping vs Fluid-Dynamical Models for Traffic Flow, Workshop on Traffic and Granular Flow, 9-11 October 1995 Julich
- Nagel, K , 1995 High-speed Microsimulations of Traffic Flow, Ph D thesis, University of Cologne

- Ozaki, H Simultaneous Analysis of Signalized Intersections Proceedings of the Ninth International Symposium on transportation and traffic theory, 24-27 July 1991 Karlsruhe
- Payne, H , 1971 Models of Freeway traffic and control Simulation Council Proc 1, 51-61
- Payne, H , 1979 FREEFLO A Macroscopic Simulation of Freeway traffic 1 Transpn Res 772, 68-75
- Pen Hsu, T The problem of performance evaluation at signalized intersections with various traffic control strategies Proceedings of the Ninth International Symposium on transportation and traffic theory, 24-27 July 1991 Karlsruhe
- Paczuski, M and Nagel, K Self-organized criticality and 1/f noise in traffic, Workshop on Traffic and Granular Flow, 9-11 October 1995 Julich
- Lee, Y , Qian, S , Jones, R , Barnes, C ,Flake, K , Lee, K , Chen, H , Sun, G , Zhang, Y , Giles, C , 1990 Adaptive stochastic cellular automata theory Physica D 45, 159-180
- Qing Liu, G Congestion, flow and capacity Proceedings of the Ninth International Symposium on Transportation and Traffic Theory, 24-27 July 1991 Karlsruhe
- Rickert, M , Nagel, K , and Schreckenberg, M , 1996 Two-lane traffic simulations using cellular automata Physica A 231, 534-550
- Ross, P , 1988 Traffic Dynamics Transpn Res B, 22B (6), 421-435

- Stevens, J , Rosensweig, R , and Cerkanowicz, A , 1993 Transient and Cyclic Behavior of Cellular Automata with Null Boundary Conditions, Journal of Statistical Physics,73(1/2)
- Schadschneider, A and Schreckenberg, M , 1993 Cellular Automata Models and Traffic Flow J Phys A Math Gen 26, L679-L683
- Stauffer, D , 1991 Computer Simulation of Cellular Automata J Phys A Math Gen 24, 907-927
- Schwerdtfeger, T , DYNEMO A model for the simulation of traffic flow in motorway networks Highway capacity and level of service Proceedings of the Ninth International Symposium on transportation and traffic theory, 24-27 July 1991 Karlsruhe
- Sparmann, U , 1978 Spurwechselvorgange auf zweispurigen BAB-Richtungsfahrbahnen, Forschung Straßenbau und straßenverkehrstechnik, heft, 263
- Torok, J and Kertesz, J 1996 The Green Wave Model of two-dimensional traffic Physica A 231, 515-533
- Takayasu, M and Takayasu, H 1993 1/f noise in a traffic model World Scientific Publishing, Fractals, 1 (4),860-866
- Transportation Research Board, 1975 "Traffic Flow Theory" Special Report 165, USA Available from (http //stargate ornl gov/trb/tft html

- Yamamoto, T , 1996 self-organization between local and non-local interaction in 2-D Cellular Automata School of Environmental and Information Sciences, Charles Sturt University, Australia
- Vilar, L and de Souza, A , 1993 Cellular Automata models for general traffic conditions on a line Physica A 211, 84-92
- Vieira, M , 1992 Self-organized Criticality in a deterministic mechanical model Physical Review A, 46 (10), 6289-6293
- Wolfram, S , 1986 *Theory and Applications of Cellular Automata* World Scientific, Singapore
- Wolfram, S , 1993 Statistical mechanics of cellular automata Rev Mod Phys , 25 (3), 602-644
- Wagner, P , Nagel, K , and Wolf, D , 1997 Realistic Multi-Lane Traffic Rules for Cellular Automata Physica A, 234, 687
- Wagner, P Traffic Simulation using Cellular Automata Comparison with Reality, Workshop on Traffic and Granular Flow, 9-11 October 1995 Julich
- Williams, J , Mahmassani, H , and Herman, R , 1987 Urban Traffic Network Flow Models Transportation Research Record, 1112, 83-93
- Wiedemann, R , 1974 Simulation des straßenverkehsflüsses Schriftenreihe des Instituts fur Verkehrswesen der universitat (TH) Karlsruhe
- Whitham, G , 1974 *Linear and Nonlinear Waves* Wiley, New Yourk

- Yukawa, S , Kikuchi, M , and Tadaki, S , 1994 Dynamical phase transition in one-dimensional Traffic Flow Model with Blochage J Phys Soc Japan, 63(10), 3609-3618
- Yang, Q , 1997 A simulation laboratory for evaluation of dynamic traffic management systems, Ph D Dissertation, Massachusetts Institute of Technology

Appendices

Appendix A Statistical Analysis

In this section we use factorial analysis to study how changing the input parameters might effect the output parameters

The input parameters are length of transient period, interval length, traffic conditions, the number of network-blocked exits, and the arrival rate

In contrast our output parameters or responses are traffic density, flow rate, average velocity, number of cars input to the system, number of cars output from the system, and the queue length at each of the network entries

In the first section we study the significance for network performance of the interaction between the network size and the input parameters We examine the flow rate in each case for different arrival rates at the injection point

In section two, using different network sizes, we study the higher order interactions of the three factors, transient period, interval length, and traffic conditions, and examine their effect on the flow rate using two levels for each factor, again for various arrival rates

A.1. The relation between the network size and the input parameters

A.1.1 Network size vs traffic conditions

We have used factorial analysis to examine the realism of our simulation model, in particular to investigate the interaction between network size and traffic conditions

In the first experiment, network size and traffic conditions at intersections have levels B1 to B4 and A1 to A2 as follows

B Network size, B1 = 17 nodes, B2 = 25 nodes, B3 = 33 nodes, B4 = 41 nodes

A traffic conditions, A1 = 50% go straight through, 25% turn left, 25% turn right and A2 = 76% go straight through, 12% turn left, 12% turn right

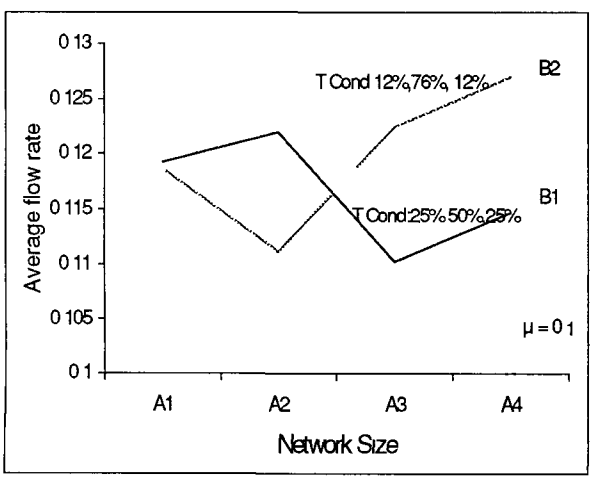

(a)

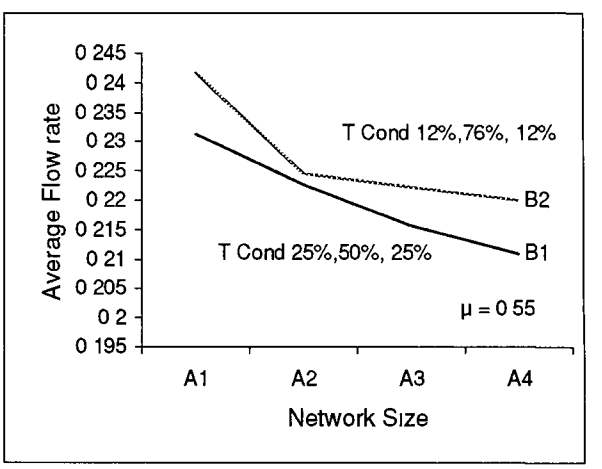

(b)

Fig (A 1)

The experiment is performed using a stochastic feeding mechanism, in which car arrivals at the injection points follow a Poisson process for different rates of arrivals (μ)

Fig (A 1) shows that, at low arrival rate $\mu = 0.1$ for free traffic conditions, a significant interaction between the traffic conditions and the network size was obtained at the $\alpha = 0.01$ level of significance Increasing the arrival rate to $\mu = 0.55$, results in a weak interaction between the two parameters

Using the higher arrival rate, Table (A 1) demonstrates that both factors have a significant effect on the flow rate

Factor	F_{calc} at $\mu = 0.1$				F_{calc} at $\mu = 0.55$			
A	10 32 (1, 312)*				14 18 (1, 312)			
B	4 28 (3, 312)	28 11 (3, 312)	4 67 (3, 232)	1 69 (3, 232)	24 65 (3, 312)	29 71 (3, 312)	50 85 (3, 232)	5 32 (3, 232)
AB	30 13 (3, 312)				1 02 (3, 312)			
C		17 16 (1, 312)				36 07 (1, 312)		
BC		6 60 (3, 312)				2 32 (3, 312)		
D			3 56 (1, 232)				314 12 (1, 232)	
DB			26 04 (3, 232)				10 94 (3, 232)	
E				0 39 (1, 232)				8 59 (1, 232)
EB				1 70 (3, 232)				0 37 (3, 232)

Table (A 1) In this table the response variable represents the flow rate for all the experiments, where A traffic conditions, B network size, C transient period, D interval length, and E network-blocked exits, and $\alpha = 0.01$

A.1.2 Network size vs length of transient period

In experiment 2 we study the effect of the transient period on the network size factor. The same levels for the network size parameter have been used as before and two levels for the transient period; C1 = 200, C2 =500.

Using the low arrival rate, the interaction between the length of transient period and network size seems to have a significant effect on the average flow rat at $\alpha = 0.01$.

Again, this is not sustained when the high arrival rate is applied to feed the network (Fig (A.2.b)). Both factors independently, however, have a significant effect on network performance, (Table (A.1)).

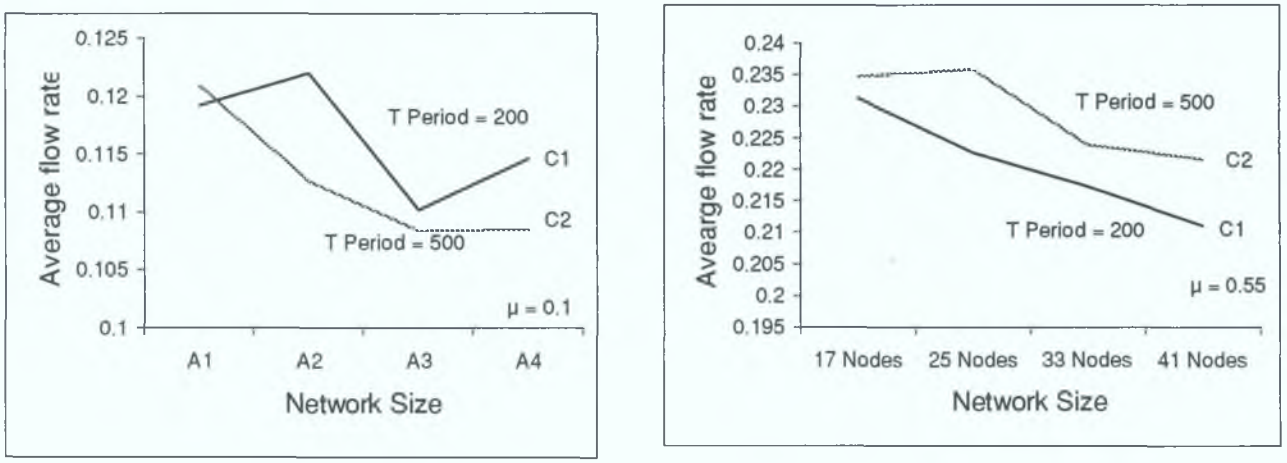

(a) (b)

Fig(A.2)

A.1.3 Network size vs interval length for calculating the output parameters

Our simulation results reveals that, as long the free flow is dominant, there are no significant changes in the traffic parameters, average flow, average density, and

average density, see Chapter 3, Sec (3 3 3) Hence, the interval length used to calculate these averages does not have much influence on their values This is not the case in the dense traffic regime period, where the interval length used to average these parameters plays a significant role (F_{calc} = 314 at α = 0 01 level of significance)

This can be observed from the statistical analysis presented in Table (A 1) with interval length having two levels, D1= 30 time step, D2 = 150 time steps

The analysis also reveals that there is a significant interaction, at α = 0 01, between network size and interval length for low arrival rate, less so for high arrival rate For high arrival rate, network size and interval length are also separately significant at the same level of significance However, for low arrival rate, interval length does not have a significant effect

A.1.4 Network size vs the number of the Network-blocked exits

When car arrivals to the network are relatively low and/or if underground parks exist inside the network, then blocking one or two of the network exits will not have a great impact on the network performance This situation is no longer true as the network becomes congested and car arrival rate increases In this case, blocking any of the network exits will strongly influence the network performance

To quantify the above performance, we have used two levels for the factor number of network-blocked exits i e E1 = 1 exit and E2 = 2 exits, and the same levels for the network size parameter (Table (A 1)) It can be seen that when free flow traffic operated through the simulated network, neither the two factors nor their interaction have a significant effect on the flow rate

By contrast, under dense traffic conditions (i e a high arrival rate) both factors (network size and number of blocked exits) have a significant role, (α = 0 01), in terms of flow performance At this level of concentration, the flow rate is not affected by interaction of the two factors

A.1.5 Network size vs arrival rate

One of the key factors in our simulation is the arrival rate To investigate how factors such as the arrival rate, network size and their combination might affect the network performance, factorial analysis was used to analysis the simulation output, where two levels, H1 = 0 1 and H2 = 0 55, have been used for the arrival rate and the same four levels as previously for the network size

Statistical analysis in Table (A 2) shows that the arrival rate has a great influence on flow performance and a significant interaction, at α = 0 01, also exists between the two factors, H and B

Factor	F_{calc}
H	738 58 (1, 232)
B	49 04 (3, 232)
HB	24 33 (3, 232)

Table (A 2) The response variable represents the flow and each order pair represents the Degrees of freedom, where H arrival rate and B network size and α = 0 01

A.2. Statistical analysis using three-input factors:

In this section we study the effect of the following factors, transient period, the interval length, and the traffic conditions on the flow rate performance using different networks size Each of these parameters has two levels as follows

A Traffic conditions, A1 = 25% turn left, 50% go straight, 25% turn right and

A2 = 12% turn left, 76% go straight, 12% turn right

B Transient Period, B1 = 200, B2 = 500

C Interval Length, C1 = 30, C2 = 150

A.2.1 Experiments using a 17 node network

Table (A 3) describes the statistical analysis performed using different arrival rates using 17-node network

Source	F_{calc} at μ=0 1	F_{calc} at μ=0 3	F_{calc} at μ=0 55
A	34 62	87 22	143 62
B	12 07	22 78	11 46
C	1 18	291 20	191 70
AB	2 08	14 78	1 076
AC	188 30	0 013	7 07
BC	11 72	14 73	7 77
ABC	13 73	10 72	0 98

Table (A 3) The table contents same as in table (A 2), but A traffic conditions, B transient period, and C interval length This was obtained for network of size 17 nodes and results obtained at α = 0 01 level of significance

From the above table it is easy to see that the interaction between the three factors does have a significant effect, at $\alpha = 0.01$, on the flow performance at low arrival rate. However, this interaction was less significant as we increase the arrival rate and was unimportant at high arrival rate of 0.55. In the case of the two-factor interactions we find a significant interaction, ($\alpha = 0.01$), between the length of transient period and the interval length at various levels of arrival rates. In contrast there is no interaction between the transient period and the traffic conditions except at a moderate arrival rate, with Poisson parameter $\mu = 0.3$.

Also a significant interaction, ($\alpha = 0.01$), between the traffic conditions and the interval length was obtained at both low and high arrival rates, whereas for μ moderate and equal to 0.3, interaction between the two factors was negligible. The statistical analysis also shows a significant effect at different arrival rates for each parameter with the exception of the interval length, where no significant effect was observed at low arrival rate as expected.

A.2.2 Experiments using 41 node network

To study further the effect of network size on traffic parameters, the simulated network was extended to include 41 nodes.

Table (A.4) shows that there is a significant interaction, $\alpha = 0.01$, between the traffic conditions and the transient period only when low arrival rate is applied whereas negligible interaction between the traffic conditions and the interval length was observed at all of arrival rates.

The individual parameters in this case have a significant effect, at the same α, on the flow performance compared to previous networks, except in the case of the interval length parameter at low arrival rate.

Factor	F_{calc} at μ=0 1	F_{calc} at μ=0 3	F_{calc} at μ=0 55
A	151 89	8 55	14 11
B	116 74	25 00	19 36
C	4 88	321 26	179 06
AB	41 15	0 01	0 003
AC	0 43	0 89	1 16
BC	4 86	10 66	6 54
ABC	5 72	0 35	0 0001

Table (A 4) the response variable represents the flow, where A traffic conditions, B transient period, and C interval length This was obtained for network of size 41 nodes and results obtained at α = 0 01 level of significance

Using Table (A 4) it is easy to see that the interval length factor and its interactions terms do not have a significant effect the flow at low arrival rate no matter what the network size However, under dense traffic conditions, the interval length as well as the other two factors are significant, (α = 0 01), in terms of influencing flow, although most of the higher order interactions become less significant as the network becomes more congested This appears to be true, irrespective of the network size (Chapter 3, Sec(3 3))

Appendix B: Summary of the simulation experiments

Experiment	Run Duration	Arrival Rate μ	Initial Density	Max Flow	Density of Max Flow	Velocity at max Flow	Queue outside the network	Total Input Cars	Total Output Cars
N17D200S30H50%L25%R25%	5000 time step	0.1	0.159274	0.14892	0.180459	0.825226	3	2744	2748
N17D200S30H50%L25%R25%	5000 time step	0.3	0.147177	0.247978	0.482386	0.514065	808	6270	5917
N17D200S30H50%L25%R25%	5000 time step	0.55	0.148185	0.250189	0.414131	0.604131	6063	6616	6215
N17D200S30H76%L12%R12%	5000 time step	0.1	0.155242	0.132537	0.15784	0.839694	6	2540	2539
N17D200S30H76%L12%R12%	5000 time step	0.3	0.145161	0.260762	0.455271	0.572761	847	6144	5781
N17D200S30H76%L12%R12%	5000 time step	0.55	0.140121	0.261315	0.453458	0.576273	6292	6810	6355
N17D200S150H50%L25%R25%	5000 time step	0.1	0.144153	0.119422	0.137413	0.869076	10	2323	2327
N17D200S150H50%L25%R25%	5000 time step	0.3	0.132056	0.249845	0.490848	0.509007	918	6217	5865
N17D200S150H50%L25%R25%	5000 time step	0.55	0.15625	0.254043	0.539544	0.470846	6270	6736	6329
N17D200S150H76%L12%R12%	5000 time step	0.1	0.138105	0.133206	0.154579	0.861731	0	2461	2452
N17D200S150H76%L12%R12%	5000 time step	0.3	0.145161	0.263661	0.509714	0.517273	997	6210	5842
N17D200S150H76%L12%R12%	5000 time step	0.55	0.144153	0.270235	0.50673	0.533292	6193	6772	6325
N17D500S30H76%L12%R12%	5000 time step	0.1	0.141129	0.141146	0.168032	0.839994	2	2683	2692
N17D500S30H76%L12%R12%	5000 time step	0.3	0.15625	0.249675	0.451186	0.553374	918	6073	5756
N17D500S30H76%L12%R12%	5000 time step	0.55	0.157258	0.247644	0.528179	0.468864	6243	6834	6410
N17D500S30H76%L12%R12%	5000 time step	0.1	0.143145	0.133296	0.154583	0.862293	3	2478	2497
N17D500S30H76%L12%R12%	5000 time step	0.3	0.137097	0.256717	0.4774	0.53774	782	6299	5932
N17D500S30H76%L12%R12%	5000 time step	0.55	0.142137	0.264442	0.504902	0.52375	5970	6721	6283
N17D500S150H50%L25%R25%	5000 time step	0.1	0.143145	0.124543	0.142374	0.874755	3	2266	2272
N17D500S150H50%L25%R25%	5000 time step	0.3	0.167339	0.249432	0.468973	0.531867	869	6064	5761
N17D500S150H50%L25%R25%	5000 time step	0.55	0.147177	0.249719	0.586972	0.425437	6370	6880	6431
N17D500S150H76%L12%R12%	5000 time step	0.1	0.153226	0.151318	0.179288	0.843993	7	2734	2714
N17D500S150H76%L12%R12%	5000 time step	0.3	0.147177	0.265604	0.463274	0.57332	914	6123	5784
N17D500S150H76%L12%R12%	5000 time step	0.55	0.149194	0.26992	0.54265	0.49741	5946	6654	6255

Table (B.1): Summary of results for a transient moment simulations for a 17 nodes network, where :D: transient period, S: interval length used to calculate averages, H: headway percentages, L: turn left percentages, R: turn right percentages

Experiment	Run Duration	Arrival Rate μ	Initial Density	Max Flow	Density of max Flow	Velocity at max Flow	Queue outside the network	Total Input Cars	Total Output Cars
N25D200S30H50%L25%R25%	5000 time step	0.1	0.157419	0.133535	0.154924	0.86194	2	2405	2467
N25D200S30H50%L25%R25%	5000 time step	0.3	0.141935	0.250938	0.42474	0.590803	995	6073	5583
N25D200S30H50%L25%R25%	5000 time step	0.55	0.152903	0.257036	0.50891	0.505071	6533	6458	5876
N25D200S30H76%L12%R12%	5000 time step	0.1	0.144516	0.122532	0.141974	0.857421	6	2376	2399
N25D200S30H76%L12%R12%	5000 time step	0.3	0.138065	0.251473	0.460259	0.546468	937	5993	5467
N25D200S30H76%L12%R12%	5000 time step	0.55	0.149032	0.255588	0.477692	0.535047	6230	6392	5794
N25D200S150H50%L25%R25%	5000 time step	0.1	0.148387	0.130982	0.145693	0.89903	4	2371	2406
N25D200S150H50%L25%R25%	5000 time step	0.3	0.155484	0.261953	0.455198	0.575471	912	6030	5532
N25D200S150H50%L25%R25%	5000 time step	0.55	0.147742	0.268279	0.516321	0.519598	6336	6452	5879
N25D200S150H76%L12%R12%	5000 time step	0.1	0.139355	0.129295	0.147715	0.8753	6	2282	2324
N25D200S150H76%L12%R12%	5000 time step	0.3	0.14	0.25995	0.46235	0.562236	838	6033	5523
N25D200S150H76%L12%R12%	5000 time step	0.55	0.150323	0.265441	0.501034	0.529786	6275	6455	5897
N25D500S30H76%L12%R12%	5000 time step	0.1	0.150323	0.125374	0.14348	0.873803	3	2338	2372
N25D500S30H76%L12%R12%	5000 time step	0.3	0.145806	0.255886	0.431914	0.592447	959	6074	5588
N25D500S30H76%L12%R12%	5000 time step	0.55	0.145161	0.261093	0.441902	0.590839	6192	6501	5859
N25D500S30H76%L12%R12%	5000 time step	0.1	0.14	0.127269	0.146585	0.868228	3	2328	2364
N25D500S30H76%L12%R12%	5000 time step	0.3	0.14129	0.254167	0.422594	0.601446	1028	6060	5566
N25D500S30H76%L12%R12%	5000 time step	0.55	0.154839	0.255759	0.42253	0.605305	6189	6479	5906
N25D500S150H50%L25%R25%	5000 time step	0.1	0.147097	0.125037	0.140622	0.88925	2	2297	2340
N25D500S150H50%L25%R25%	5000 time step	0.3	0.141935	0.263499	0.442829	0.595035	816	5973	5476
N25D500S150H50%L25%R25%	5000 time step	0.55	0.14129	0.262152	0.509705	0.514322	6502	6413	5856
N25D500S150H76%L12%R12%	5000 time step	0.1	0.151613	0.132389	0.151483	0.873958	3	2305	2364
N25D500S150H76%L12%R12%	5000 time step	0.3	0.140645	0.257569	0.459314	0.56077	952	6014	5498
N25D500S150H76%L12%R12%	5000 time step	0.55	0.149032	0.261592	0.438199	0.59697	6130	6526	5845

Table (B.2): Summary of results for a transient moment simulations for a 25 nodes network, where :D: transient period, S: interval length used to calculate averages, H: headway percentages, L: turn left percentages, R: turn right percentages

Experiment	Run Duration	Arrival Rate μ	Initial Density	Max Flow	Density of Max Flow	Velocity at Max Flow	Queue Outside the Network	Total Input Cars	Total Output Cars
N33D200S30H50%L25%R25%	5000 time step	0.1	0.145714	0.123954	0.144823	0.855896	4	2321	2369
N33D200S30H50%L25%R25%	5000 time step	0.3	0.152381	0.2334	0.419332	0.556812	739	6491	5740
N33D200S30H50%L25%R25%	5000 time step	0.55	0.16	0.236959	0.433432	0.433432	5854	6815	5989
N33D200S30H76%L12%R12%	5000 time step	0.1	0.15381	0.138539	0.163858	0.845484	4	2507	2528
N33D200S30H76%L12%R12%	5000 time step	0.3	0.143333	0.241085	0.439291	0.548804	672	6279	5467
N33D200S30H76%L12%R12%	5000 time step	0.55	0.146667	0.242875	0.458928	0.511926	5741	6751	5796
N33D200S150H50%L25%R25%	5000 time step	0.1	0.148095	0.143204	0.164671	0.869639	5	2361	2425
N33D200S150H50%L25%R25%	5000 time step	0.3	0.140952	0.242285	0.43769	0.553554	807	6263	5588
N33D200S150H50%L25%R25%	5000 time step	0.55	0.141429	0.242092	0.435438	0.555973	5776	6836	5983
N33D200S150H76%L12%R12%	5000 time step	0.1	0.152381	0.132734	0.153399	0.874409	0	2494	2552
N33D200S150H76%L12%R12%	5000 time step	0.3	0.147143	0.25041	0.481382	0.52019	791	6273	5480
N33D200S150H76%L12%R12%	5000 time step	0.55	0.152857	0.255046	0.468599	0.544273	6163	6727	5826
N33D500S30H76%L12%R12%	5000 time step	0.1	0.153333	0.119552	0.136254	0.877418	3	2377	2437
N33D500S30H76%L12%R12%	5000 time step	0.3	0.143333	0.237264	0.43985	0.539421	688	6245	5512
N33D500S30H76%L12%R12%	5000 time step	0.55	0.138095	0.23482	0.518609	0.452788	5937	6888	6030
N33D500S30H76%L12%R12%	5000 time step	0.1	0.150952	0.124745	0.148753	0.838607	8	2312	2371
N33D500S30H76%L12%R12%	5000 time step	0.3	0.144286	0.242352	0.486614	0.498037	612	6284	5523
N33D500S30H76%L12%R12%	5000 time step	0.55	0.140476	0.240965	0.508666	0.473719	6068	6790	5884
N33D500S150H50%L25%R25%	5000 time step	0.1	0.144286	0.123623	0.142087	0.870053	1	2380	2398
N33D500S150H50%L25%R25%	5000 time step	0.3	0.14381	0.241518	0.405884	0.595043	787	6230	5546
N33D500S150H50%L25%R25%	5000 time step	0.55	0.14619	0.242907	0.470925	0.515808	5882	6821	5978
N33D500S150H76%L12%R12%	5000 time step	0.1	0.144762	0.118459	0.134982	0.877589	1	2282	2309
N33D500S150H76%L12%R12%	5000 time step	0.3	0.137619	0.249781	0.400047	0.62438	615	6257	5502
N33D500S150H76%L12%R12%	5000 time step	0.55	0.145238	0.254398	0.462507	0.550043	6005	6710	5802

Table (B.3): Summary of results for a transient moment simulations for a 33 nodes network, where: D: transient period, S: interval length used to calculate averages, H: headway percentages, L: turn left percentages, R: turn right percentages

Experiment	Run Duration	Arrival Rate	Initial Density	Max Flow	Density of Max Flow	Velocity at Max Flow	Queue Outside the Network	Total Input Cars	Total Output Cars
N41D200S30H50%L25%R25%	5000 time step	0.1	0.148791	0.123815	0.143406	0.863386	3	2335	2425
N41D200S30H50%L25%R25%	5000 time step	0.3	0.150961	0.236816	0.430268	0.550393	552	6388	5351
N41D200S30H50%L25%R25%	5000 time step	0.55	0.140732	0.236763	0.494114	0.441462	5769	7385	5810
N41D200S30H76%L12%R12%	5000 time step	0.1	0.154991	0.137141	0.157631	0.86986	3	2484	2522
N41D200S30H76%L12%R12%	5000 time step	0.3	0.150961	0.245792	0.459454	0.534966	400	6514	5314
N41D200S30H76%L12%R12%	5000 time step	0.55	0.147861	0.250523	0.426943	0.586784	5700	7357	5740
N41D200S150H50%L25%R25%	5000 time step	0.1	0.150031	0.126424	0.141542	0.893192	1	2337	2412
N41D200S150H50%L25%R25%	5000 time step	0.3	0.155921	0.244922	0.365846	0.669466	629	6331	5341
N41D200S150H50%L25%R25%	5000 time step	0.55	0.151891	0.250251	0.445275	0.562015	5591	7821	6246
N41D200S150H76%L12%R12%	5000 time step	0.1	0.148411	0.140923	0.159056	0.886	5	3739	3710
N41D200S150H76%L12%R12%	5000 time step	0.3	0.147861	0.258957	0.451121	0.57403	494	6488	5250
N41D200S150H76%L12%R12%	5000 time step	0.55	0.152201	0.258452	0.433729	0.595883	5697	7295	5713
N41D500S30H76%L12%R12%	5000 time step	0.1	0.145691	0.11531	0.131372	0.877736	2	2282	2342
N41D500S30H76%L12%R12%	5000 time step	0.3	0.145071	0.235872	0.430988	0.547282	521	6353	5341
N41D500S30H76%L12%R12%	5000 time step	0.55	0.150961	0.238576	0.490861	0.486036	5476	7242	5894
N41D500S30H76%L12%R12%	5000 time step	0.1	0.144761	0.122812	0.139498	0.88039	3	2342	2414
N41D500S30H76%L12%R12%	5000 time step	0.3	0.152821	0.247386	0.455698	0.542872	492	6525	5312
N41D500S30H76%L12%R12%	5000 time step	0.55	0.156541	0.250281	0.415698	0.602073	5529	7293	5699
N41D500S150H50%L25%R25%	5000 time step	0.1	0.153131	0.132789	0.148948	0.891513	1	2327	2423
N41D500S150H50%L25%R25%	5000 time step	0.3	0.148791	0.245982	0.421425	0.58369	516	6358	5351
N41D500S150H50%L25%R25%	5000 time step	0.55	0.155921	0.247123	0.402293	0.614285	5652	7152	5765
N41D500S150H76%L12%R12%	5000 time step	0.1	0.154991	0.129713	0.145445	0.891836	4	2315	2419
N41D500S150H76%L12%R12%	5000 time step	0.3	0.146621	0.252735	0.447167	0.565193	445	6485	5279
N41D500S150H76%L12%R12%	5000 time step	0.55	0.154061	0.258279	0.441876	0.584505	5668	7266	5681

Table (B.4): Summary of results for a transient moment simulations for a 41 nodes network, where: D: transient period, S: interval length used to calculate averages, H: headway percentages, L: turn left percentages, R: turn right percentages

Experiment	Run Duration	Arrival Rate μ	Initial Density	Max Flow	Density of max Flow	Velocity at max Flow	Queue outside the network	Total Input Cars	Total Output Cars
N17D200S30B1H50%L25%R25%	5000 time step	0.1	0.147177	0.224163	0.492272	0.455363	3	2278	2202
N17D200S30B2H50%L25%R25%	5000 time step	0.1	0.133	0.2120	0.4719	0.4493	102	2868	2099
N17D200S30B1H50%L25%R25%	5000 time step	0.3	0.145161	0.236931	0.50286	0.471167	2280	5144	4551
N17D200S30B2H50%L25%R25%	5000 time step	0.3	0.135081	0.230511	0.467281	0.493303	3046	4143	3208
N17D200S30B1H50%L25%R25%	5000 time step	0.55	0.143145	0.238341	0.463133	0.514627	7450	5193	4584
N17D200S30B2H50%L25%R25%	5000 time step	0.55	0.152218	0.226313	0.508597	0.444976	8790	4279	3309
N17D200S30B1H76%L12%R12%	5000 time step	0.1	0.16129	0.217166	0.454462	0.477852	2	2486	2297
N17D200S30B2H76%L12%R12%	5000 time step	0.1	0.131048	0.21553	0.335317	0.642765	2	2291	1796
N17D200S30B1H76%L12%R12%	5000 time step	0.3	0.137097	0.244921	0.421416	0.581185	1790	5040	4404
N17D200S30B2H76%L12%R12%	5000 time step	0.3	0.145161	0.230073	0.444752	0.517306	2812	4274	3199
N17D200S30B1H76%L12%R12%	5000 time step	0.55	0.153226	0.251618	0.54804	0.459122	7427	5464	4774
N17D200S30B2H76%L12%R12%	5000 time step	0.55	0.140121	0.232449	0.476871	0.487445	8642	4268	3236
N17D200S150B1H50%L25%R25%	5000 time step	0.1	0.148185	0.236138	0.523876	0.450753	2	2407	2310
N17D200S150B2H50%L25%R25%	5000 time step	0.1	0.142137	0.210436	0.553357	0.38029	2	2437	1891
N17D200S150B1H50%L25%R25%	5000 time step	0.3	0.150202	0.23791	0.501119	0.474758	2063	4862	4294
N17D200S150B2H50%L25%R25%	5000 time step	0.3	0.140121	0.233809	0.443625	0.527042	2827	4119	3135
N17D200S150B1H50%L25%R25%	5000 time step	0.55	0.131048	0.247727	0.438452	0.565005	7464	5244	4622
N17D200S150B2H50%L25%R25%	5000 time step	0.55	0.144153	0.236659	0.389588	0.60746	8772	4191	3261
N17D200S150B1H76%L12%R12%	5000 time step	0.1	0.157258	0.216008	0.44391	0.486602	2	2485	2316
N17D200S150B2H76%L12%R12%	5000 time step	0.1	0.143145	0.209734	0.330629	0.634349	19	2401	1868
N17D200S150B1H76%L12%R12%	5000 time step	0.3	0.147177	0.2698	0.443933	0.585224	1898	5130	4473
N17D200S150B2H76%L12%R12%	5000 time step	0.3	0.139113	0.242613	0.468975	0.517326	2832	4298	3161
N17D200S150B1H76%L12%R12%	5000 time step	0.55	0.153226	0.258875	0.493992	0.526072	7584	5437	4726
N17D200S150B2H76%L12%R12%	5000 time step	0.55	0.15625	0.23615	0.502183	0.470247	8473	4252	3266
N17D500S30B1 H50%L25%R25%	5000 time step	0.1	0.154234	0.227848	0.582783	0.390966	2	2698	2497
N17D500S30B2 H50%L25%R25%	5000 time step	0.1	0.143145	0.209774	0.409535	0.512225	4	2314	1832

N17D500S30B1 H50%L25%R25%	5000 time step	0.3	0.149194	0.241441	0.502963	0.480037	2236	5055	4466
N17D500S30B2 H50%L25%R25%	5000 time step	0.3	0.140121	0.231121	0.406189	0.568998	2953	4116	3184
N17D500S30B1 H50%L25%R25%	5000 time step	0.55	0.140121	0.233647	0.510158	0.457989	7447	5370	4702
N17D500S30B2 H50%L25%R25%	5000 time step	0.55	0.149194	0.225178	0.564867	0.39864	8569	4219	3289
N17D500S30B1H76%L12%R12%	5000 time step	0.1	0.150202	0.2208	0.40343	0.547308	3	2271	2115
N17D500S30B2H76%L12%R12%	5000 time step	0.1	0.147177	0.228135	0.393391	0.579921	16	2308	1772
N17D500S30B1H76%L12%R12%	5000 time step	0.3	0.149194	0.251889	0.496906	0.506915	1964	5031	4388
N17D500S30B2H76%L12%R12%	5000 time step	0.3	0.139113	0.228963	0.451763	0.506821	2862	4128	3161
N17D500S30B1H76%L12%R12%	5000 time step	0.55	0.144153	0.252824	0.475676	0.531505	7431	5370	4723
N17D500S30B2H76%L12%R12%	5000 time step	0.55	0.141129	0.22991	0.592603	0.387966	8394	4309	3330
N17D500S150B1H50%L25%R25%	5000 time step	0.1	0.148185	0.232802	0.486852	0.478179	1	2378	2287
N17D500S150B2H50%L25%R25%	5000 time step	0.1	0.149194	0.224858	0.405369	0.554698	69	2788	2098
N17D500S150B1H50%L25%R25%	5000 time step	0.3	0.140121	0.24286	0.51085	0.475403	2388	5035	4416
N17D500S150B2H50%L25%R25%	5000 time step	0.3	0.149194	0.229888	0.484377	0.474605	3214	4083	3180
N17D500S150B1H50%L25%R25%	5000 time step	0.55	0.146169	0.246749	0.471898	0.522887	7537	5216	4601
N17D500S150B2H50%L25%R25%	5000 time step	0.55	0.154234	0.239664	0.491177	0.487938	8475	4359	3266
N17D500S150B1H76%L12%R12%	5000 time step	0.1	0.140121	0.219682	0.429647	0.511308	1	2499	2289
N17D500S150B2H76%L12%R12%	5000 time step	0.1	0.15625	0.215391	0.367112	0.586718	71	2474	1936
N17D500S150B1H76%L12%R12%	5000 time step	0.3	0.136089	0.252152	0.476765	0.52888	2030	5008	4381
N17D500S150B2H76%L12%R12%	5000 time step	0.3	0.145161	0.233687	0.536835	0.435306	2997	4074	3133
N17D500S150B1H76%L12%R12%	5000 time step	0.55	0.139113	0.255734	0.52874	0.483666	7568	5424	4749
N17D500S150B2H76%L12%R12%	5000 time step	0.55	0.141129	0.239967	0.51328	0.467516	8628	4204	3198

Table (B.5): Summary of results for a non-transient moment simulations for a 17 nodes network, where: D: transient period, S: interval length used to calculate averages, H: headway percentages, L: turn left percentages, R: turn right percentages

Experiment	Run Duration	Arrival Rate μ	Initial Density	Max Flow	Density of max Flow	Velocity at max Flow	Queue length	Total Input Cars	Total Output Cars
N41D200S30B1H50%L25%R25%	5000 time step	0.1	0.148171	0.217855	0.32573	0.668821	2	2667	2312
N41D200S30B2H50%L25%R25%	5000 time step	0.1	0.146311	0.219951	0.363491	0.605108	5	2228	1581
N41D200S30B1H50%L25%R25%	5000 time step	0.3	0.147861	0.222129	0.316262	0.702356	1018	6044	4085
N41D200S30B2H50%L25%R25%	5000 time step	0.3	0.152821	0.223269	0.360969	0.618526	1836	5314	2989
N41D200S30B1H50%L25%R25%	5000 time step	0.55	0.156851	0.233571	0.359306	0.650061	6400	6433	4395
N41D200S30B2H50%L25%R25%	5000 time step	0.55	0.147861	0.22648	0.479256	0.472567	7490	5396	3065
N41D200S30B1H76%L12%R12%	5000 time step	0.1	0.144761	0.217483	0.334089	0.650973	5	2481	2030
N41D200S30B2H76%L12%R12%	5000 time step	0.1	0.151271	0.227134	0.422467	0.537638	10	2362	1490
N41D200S30B1H76%L12%R12%	5000 time step	0.3	0.150651	0.237137	0.350863	0.6758	648	6368	4831
N41D200S30B2H76%L12%R12%	5000 time step	0.3	0.153131	0.24677	0.416134	0.593004	1946	5135	2887
N41D200S30B1H76%L12%R12%	5000 time step	0.55	0.146931	0.24966	0.431118	0.5791	6860	6950	4817
N41D200S30B2H76%L12%R12%	5000 time step	0.55	0.153131	0.246243	0.444347	0.554168	7560	5535	3119
N41D200S150B1H50%L25%R25%	5000 time step	0.1	0.147551	0.214345	0.338739	0.632774	6	2375	2085
N41D200S150B2H50%L25%R25%	5000 time step	0.1	0.152201	0.230547	0.387583	0.594834	12	2300	1611
N41D200S150B1H50%L25%R25%	5000 time step	0.3	0.149101	0.231983	0.449962	0.515561	997	5897	3981
N41D200S150B2H50%L25%R25%	5000 time step	0.3	0.140422	0.236279	0.393681	0.60018	1710	5221	2894
N41D200S150B1H50%L25%R25%	5000 time step	0.55	0.141971	0.242762	0.449484	0.540091	6573	6382	4321
N41D200S150B2H50%L25%R25%	5000 time step	0.55	0.154991	0.242762	0.449484	0.540091	7199	5438	3151
N41D200S150B1H76%L12%R12%	5000 time step	0.1	0.144761	0.224637	0.345602	0.649987	1	2335	1986
N41D200S150B2H76%L12%R12%	5000 time step	0.1	0.15902	0.231568	0.41157	0.562645	5	2274	1509
N41D200S150B1H76%L12%R12%	5000 time step	0.3	0.147241	0.247035	0.400498	0.616819	997	5925	3943
N41D200S150B2H76%L12%R12%	5000 time step	0.3	0.145691	0.25273	0.436416	0.579105	1784	5209	2887
N41D200S150B1H76%L12%R12%	5000 time step	0.55	0.151891	0.254654	0.416999	0.610683	6376	6272	4224
N41D200S150B2H76%L12%R12%	5000 time step	0.55	0.143521	0.252916	0.421461	0.600093	7207	5551	3112
N41D500S30B1H50%L25%R25%	5000 time step	0.1	0.153441	0.21754	0.403541	0.648396	4	2192	1999

N41D500S30B2 H50%L25%R25%	5000 time step	0 1	0 140112	0 205436	0 316837	0.539077	12	2404	1547
N41D500S30B1 H50%L25%R25%	5000 time step	0 3	0 146001	0 224838	0 357681	0 628598	1018	6193	4206
N41D500S30B2 H50%L25%R25%	5000 time step	0 3	0 150651	0 222188	0 437351	0 50803	2045	5257	2963
N41D500S30B1 H50%L25%R25%	5000 time step	0 55	0 148171	0 228898	0 41972	0 545359	6360	6387	4363
N41D500S30B2 H50%L25%R25%	5000 time step	0 55	0 152511	0 232706	0 393686	0 591094	7403	5508	3174
N41D500S30B1H76%L12%R12%	5000 time step	0 1	0 148791	0 221385	0 341653	0 64798	4	2405	2022
N41D500S30B2H76%L12%R12%	5000 time step	0 1	0 153441	0 224695	0 454287	0 49461	11	2608	1602
N41D500S30B1H76%L12%R12%	5000 time step	0 3	0 143831	0 2378	0 335209	0 709408	1041	5980	3978
N41D500S30B2H76%L12%R12%	5000 time step	0 3	0 146311	0 240485	0 407518	0 590121	1822	5229	2918
N41D500S30B1H76%L12%R12%	5000 time step	0 55	0 15096	0 247642	0 397962	0 622276	6511	6350	4343
N41D500S30B2H76%L12%R12%	5000 time step	0 55	0 153131	0 243118	0 424339	0 572933	7704	5343	3042
N41D500S150B1H50%L25%R25%	5000 time step	0 1	0 152821	0 218188	0 292447	0 746076	4	2330	2128
N41D500S150B2H50%L25%R25%	5000 time step	0 1	0 146621	0 221446	0 432387	0 512148	10	2305	1448
N41D500S150B1H50%L25%R25%	5000 time step	0 3	0 150031	0 235491	0 340413	0 691779	955	6016	4099
N41D500S150B2H50%L25%R25%	5000 time step	0 3	0 142901	0 233617	0 387521	0 602849	1701	5280	2989
N41D500S150B1H50%L25%R25%	5000 time step	0 55	0 154371	0 24067	0 377373	0 63775	13170	6449	4450
N41D500S150B2H50%L25%R25%	5000 time step	0 55	0 145071	0 241727	0 410919	0 588259	7009	5520	3110
N41D500S150B1H76%L12%R12%	5000 time step	0 1	0 155921	0 226911	0 353205	0 642433	5	2314	1961
N41D500S150B2H76%L12%R12%	5000 time step	0 1	0 143831	0 232345	0 437421	0 53117	12	2391	1469
N41D500S150B1H76%L12%R12%	5000 time step	0 3	0 143521	0 248775	0 416261	0 597642	1064	5859	3876
N41D500S150B2H76%L12%R12%	5000 time step	0 3	0 15902	0 250608	0 426361	0.587783	1815	5171	2892
N41D500S150B1H76%L12%R12%	5000 time step	0 55	0 153131	0 25311	0 435938	0 580609	6351	6338	4340
N41D500S150B2H76%L12%R12%	5000 time step	0 55	0 152511	0 25334	0 418776	0 604953	7273	5440	3059

Table (6) Summary of results for a non-transient moment simulations for a 41 nodes network, where D transient period, S interval length used to calculate averages, H headway percentages, L turn left percentages, R turn right percentages

Appendix C

Feeding Mechanism

For Poisson arrivals, inter-arrival time between two vehicles is randomly drawn from the negative exponential distribution, i e

$$t_{n+1} = t_n - \frac{\ln (1 - \mu)}{\mu}, \qquad \mu > 0,\ 0 < r \leq 1$$

where

t_{n+1} = inter-arrival time for next vehicle

t_n = inter-arrival time for previous vehicle

μ = arrival rate

r = random number uniformly distributed between (0, 1]

As the random number generator is fundamental in stochastic simulation, we have used the linear congruential random number generator, because of its cycle length

We compute the ith integer X_i in the pseudorandom from X_{i-1} by the recursion

$$X_i = (a X_{i-1} + c) \mod m$$

where a = 16807, c = 0, and m = 2147483647, which is widely known as the "multiplicative congruential" generator.

Appendix D

Computational Performance

Table (D 1) shows the running times for simulating two different networks at two arrival rates for two different simulation runs, 5000 and 7000 time steps

	17 nodes network				41 nodes network			
Run Duration	μ=0 1		μ=0 5		μ=0 1		μ=0 5	
	CPU time	Simulated cars	CPU time	Simulated cars	CPU time	Simulated cars	CPU time	Simulated cars
5000	39	2,635	41	12,696	49	2,309	50	11,350
7000	54	3,785	58	17,045	77	3,292	80	16,509

Table (D 1) the relation between the run duration and the computational time, in Seconds, for two different networks at two arrival rates

It can be seen from Table (D 1), that the computational time mainly depends on the network size not the number of the simulated cars Also it can be seen from the table that the complexity of the code is $O(n^2)$, being the increasing factors the network size and the run duration Also there is a slight increase in the computational time as we increase the arrival rate, Table (D 2) this increase is due to the time required to update the queues outside the simulated network

The limitation in the run duration above is due to the formation of long queues outside the network especially when a high arrival rate is used to feed the network with cars

Arrival Rate	Network size	CPU, 5000 time steps	CPU, 7000 time steps	Increasing Factor
$\mu = 0.1$	17	39	54	1.38
	41	49	77	1.57
$\mu = 0.5$	17	41	58	1.41
	41	50	80	1.60

Table (D.2) The table shows that the increasing factor in the computational time, in Seconds, depends on both the network size and the arrival rate

All computational performance measures described above is obtained on DEL PC with 400 MHZ of speed and 64 MB of RAM

Appendix E : Diskette

The list of the diskette folders and files are presented in Table (E 1)

folder	files	Brief description
Short_evt_net	model1 h	Header file, define model1 base class
	node1 h	Header file, define node1 class
	segmen1 h	Header file, define segmen1 derived class
	model1 cpp	Contains the methods of the base class model1, which create roads of the network
	node1 cpp	Contains the methods for the class node1, which initialize the network nodes and also update the network light cycles
	segmen1 cpp	Contains the methods for the derived class segmen1, which link the roads within the network and also initialize and update the road segments
	newnet cpp	The main file, see flow-chart in sec(3 2)
	nod17 dat	Contains nodes data for 17 nodes network
	nod25 dat	Contains nodes data for 25 nodes network
	nod33 dat	Contains nodes data for 33 nodes network
	nod41 dat	Contains nodes data for 41 nodes network
	seg56 dat	Contains segments data for 17 nodes network
	Seg88 dat	Contains segments data for 25 nodes network
	Seg120 dat	Contains segments data for 33 nodes network
	Seg152 dat	Contains segments data for 41 nodes network
Long_evt_net		Same as the above folder , but deals with long term events
Two_lan	2_lane_model	Simulate traffic flow using two lanes
	tlgv h	Header file contains the global variables
Stoch_model	Stoch_closed	Simulate traffic flow for inter-urban areas using closed boundary conditions
	Stoch_open	Simulate traffic flow for inter-urban areas using open boundary conditions
Space_time	bc c	Used to produce the space-time diagrams throughout the thesis

Table (E 1)